University of Stavanger

FACULTY OF SCIENCE AND TECHNOLOGY

MASTER'S THESIS

Study programme/specialisation: Master of Science: Biological Chemistry	Autumn & spring semester, 2019-2020 Open
Author: Kristin Lende	
Programme coordinator: Cathrine Lillo Supervisor(s): Emil Lindbäck	
Title of master's thesis: Tacrine hybrids as multi-target-directed ligands against Alzheimer's disease	
Credits: 60 points	
Keywords: Alzheimer disease, Tacrine analogues, Icocryptolepine, Acetylcholinesterase.	Number of pages: 74 + supplemental material/other: 40 Stavanger, 06.07/2020 date/year

UNIVERSITY OF STAVANGER

MASTER'S THESIS

Tacrine hybrids as multi-target-directed ligands against Alzheimer's disease

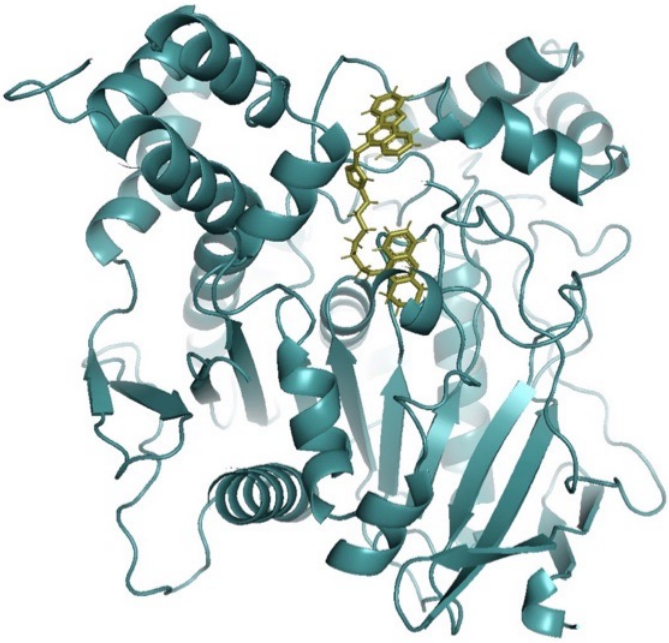

Author:

Kristin Lende

Supervisor:

Emil Lindbäck

Universitetet
i Stavanger

Abstract

World health organization estimates that nearly 9.9 million people develop dementia each year. Alzheimer disease (AD) is the most common form of dementia, and contributes to 60-70% of the cases. In addition to affecting the patient s families AD also represents substantial costs to society.

It has been discovered that deterioration of neurons in the early stages of AD is parallel to reduced levels of the neurotransmitter acetylcholine (ACh). AChE, which is responsible for regulating ACh concentration, has also been revealed to contribute to the formation Aβ aggregation, another brain change associated with AD. Aβ aggregation contributes to degradation of neurons by blocking nutrient supply. Multiple compounds have been synthesised with the purpose of preventing AChE-induced Aβ aggregation in addition to preventing hydrolyse of ACh. Among them are tacrine heterodimers.

Herein, by combining tacrine and isocryptolepine, two new tacrine heterodimers have been synthesized. The heterodimers (**1a** and **1b**) commenced from azides-alkyne click-chemistry reaction between propagylated isocryptolepine precursor and azide armed tacrine.

The evaluation of 42 tacrine analogues, suggested as potential AD treatments, are also featured. Affinity towards AChE and BChE, ability to inhibit self-induced and AChE-induced Aβ aggregation is assessed. Also, interaction with PAS is analyzed by molecular modeling studies. Compound **12** and **28** proved to give good results in all the evaluated categories.

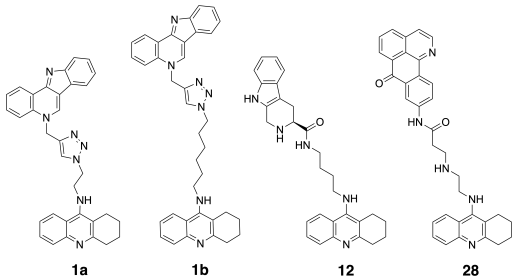

Acknowledgements

All research work conducted in this thesis was done at the University of Stavanger, Department of Chemistry, Norway, as part of my Master's Degree in Biological Chemistry. First and foremost, I would like to express my gratitude to Associate Professor Dr. Emil Lindbäck for his excellent guidance throughout this project. Thank you for always helping in the lab, assisting with NMR interpretations and your many indispensable advices during the writing process. Also, thank you for your kindness and patient.

Secondly, I would like to thank Katja Stangeland Håheim and Vebjørn Eikemo. Thank you for answering all my questions. I'm privileged to get the opportunity to work with such great minds. I would also like to thank my fellow Master's student, Geir R. Bringsjord. You made my time in the lab enjoyable. Also, I'm so grateful to Andreas Måland, Ingeborg Marie Lende and Ben David Normann for last minute proof-reading.

Finally, thank you to my friends and family for their support during my time as a Master's student. Special thanks to my mother and father for always supporting me. Soli Deo gloria.

Selected abbreviations

Aβ	Amyloid beta
ACh	Acetylcholine
AChE	Achetylcholinesterase
AD	Alzheimer disease
BChE	Butyrylcholinesterase
CAS	Aatalytic anionic site
ChE	Cholinesterase
DCM	Dichloromethane
DMSO	Dimethyl sulfoxide
Glu	Glutamic Acid
HMBC	Heteronuclear multiple bond correlation spectroscopy
HSQC	Heteronuclear single-quantum correlation spectroscopy
Hz	Hertz
His	Histidine
IC_{50}	The half maximal inhibitory concentration
h	Hour(s)
PAS	Peripheral anionic binding site
Phe	Phenylalanine
Ser	Serine
THA	Tetra Hydro Acridine
Trp	Tryptophan
Tyr	Tyrosine
WHO	World Health Organization

Contents

1 Introduction

In 2015, dementia affected approximately 5% of the world´s elderly population. World health organization (WHO) estimates that nearly 9.9 million people develop dementia each year. Thus, every third second, a person is diagnosed with dementia. In addition to affecting the patient's families, it also represents substantial costs to society. Alzheimer disease (AD) is the most common form of dementia, and contributes to 60-70% of the cases.[1]

Initial symptom of AD is a gradually worsening ability to remember new information. This memory decline occurs because the first neurons to die are usually neurons in brain regions involved with working memories. As neurons in other parts of the brain dies, individuals may experience apathy, depression, impaired communication, disorientation, confusion, poor judgment and behavior changes. Neuronal damage eventually affects parts of the brain that enable the body to carry out basic functions, such as walking and swallowing. In the final stages of the disease, the patient is bed-bound and requires around-the-clock care. AD is ultimately fatal.[2]

A healthy adult brain has about 100 billion neurons. At advanced stages of AD the patient's brain show dramatic shrinkage from cell loss and debris from dead and dying neurons. These brain changes can begin 20 or more years before symptoms appear.[2]

Why are the neurons dying? There are multiple hypotheses proposed for AD pathology, including low levels of brain cholinergic transmitter, abnormal amyloid beta (Aβ) aggregation, microtubule τ protein accumulation, metal dyshomeostasis of copper, iron and zinc, metal-induced oxidative stress, neuroinflammation and disruption of calcium homeostasis.[2–5] In this paper, emphasis will be placed on the first two in the foregoing list.

In 1921 Otto Loewi discovered the first neurotransmitter, Acetylcholine (ACh). Since then, more than 50 other neurotransmitters have been identified. Among them are glutamate, gamma-Aminobutyric acid (GABA), glycine, dopamine, norepinephrine and serotonin.[6] ACh is released by all neurons that stimulate skeletal muscles, by many neurons of the autonomic nervous system and by neurons in the central nervous system.[7,8s3–24]

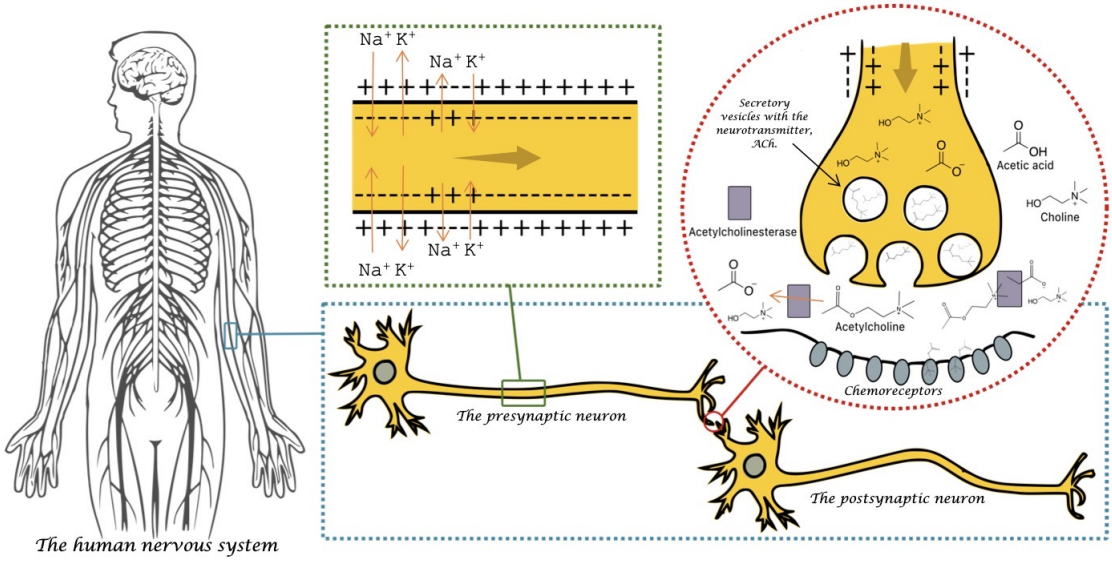

Figure 1. Graphic representation of the transmission of a nerve impulse from the presynaptic neuron to the postsynaptic neuron via the neurotransmitter ACh. AChE catalyzes hydrolysis of ACh into choline and acetic acid to terminate the activation of the postsynaptic neuron. The figure is designed with inspiration from published illustrations.[9,10]

A nerve cell is stimulated through either mechanoreceptors, chemoreceptors, thermoreceptors or photoreceptors. These receptors are linked to ion channels. Activation of the receptors will open the channel and allow potassium ions to flow out of the cell, and sodium ions to flow into the cell. The flow of ions initiated by the receptors, upon binding of a agonist may, if persistent enough, reduce the voltage over the membrane from -70 millivolt to -55 millivolt at the location. Neighboring voltage gated sodium channels will open at -55 millivolt, alowing sodium to flush into the cell and make the interior positively charged (40 millivolt). The heavy increase in positive charge acts as a domino effect, open-

ing voltage gated sodium channels further and further from the receptor. Mechanisms of the cell will quickly restore the voltage over the membrane to the resting state of -70 millivolt, ensuring the charge to travel in one direction through the nerve cell. At the synaptic cleft the nerve impulse is transferred from the pre-synaptic neuron to the trailing cell, the post-synaptic neuron. The electric impulse through the presynaptic neuron initiate exocytosis of molecules, neurotransmitters, capable of binding to a chemoreceptor on the postsynaptic neuron. The binding of neurotransmitters to chemoreceptors on the postsynaptic neuron reduces the voltage over the membrane from -70 millivolt to -55 and the nerve impulse continues its migration through the nerve system.[7,8]

Research suggests that deterioration of cholinergic neurons in the early stages of AD is parallel to reduced levels of the neurotransmitter ACh.[11,12] In vertebrates mainly acetylcholinesterase (AChE) but also butyrylcholinesterase (BChE) are responsible for regulation of acetylcholine (ACh) concentration.[13,14] The two enzymes regulate the concentration of ACh by hydrolyzing the neurotransmitter into inactive acetic acid and choline.[15]

1.1 Acethylcholinesterase

AChE has been studied for a long time and the first crystallographic structure was published in 1994 (Figure 2).[14,16] The upper part of the gorge is called *the peripheral anionic binding site* (PAS). It consists of the aminoacids Tyr-70, Asp-72, Tyr-121, Trp-279 and Tyr-334. The negative charge at the entrance attracts the positively charged quaternary ammonium group of ACh. An increased density of negative charge along the gorge drags ACh into the active site. Hydrolysis occurs at the *catalytic triad* of the *esteratic site* (figure 4).[17]

The Catalytic triad consisting of the three aminoacids, Ser-200, Glu-327 and His-440 at the bottom of a 20 Å gorge.[17] The presence of a nucleophilic serine at the catalytic site defines the enzyme as a Serine hydrolase, one of the largest enzyme classes known. Ser-

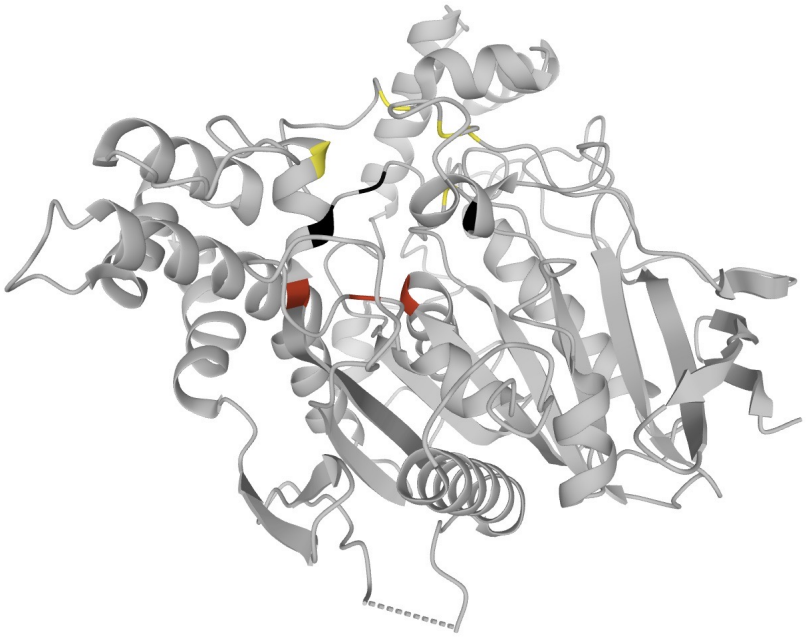

Figure 2. Crystal structure of ACh from Tetronarce californica (1ACJ).[16] The amino acids at pheripheral binding site are yellow colored. The three red colored amino acids together, make up the catalytic triad.[17]

ine initiates the formation of an acetyl-enzyme intermediate. The attachment of ACh to serine is followed by water induced release of the two ACh counterparts (Figure 3). In literature the active site is often referred to as the *catalytic anionic site* (CAS).[18–23] The ACh hydrolysis mechanisms is the same in both AChE and BChE.[13,15]

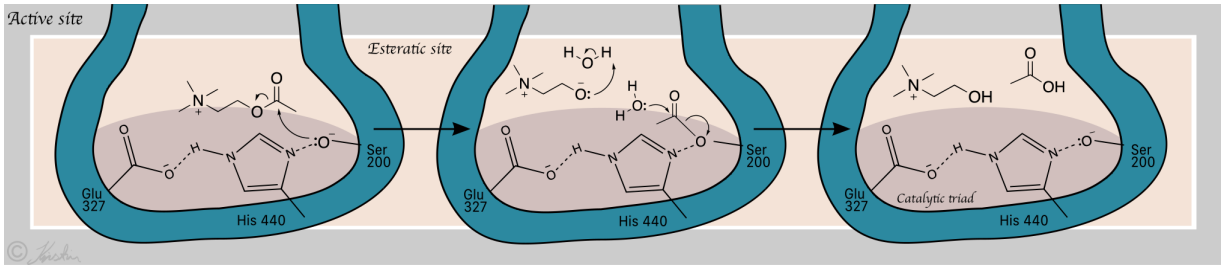

Figure 3. The mechanism in which the catalytic triad catalyzes hydrolysis of ACh.

1.2 Treatment of AD

Currently the therapeutic approaches for patients with AD is based on increasing the cholinergic neurotransmission, through AChE inhibition.[5] Earlier potential AChE inhibitors were evaluated for their selectivity towards AChE. It has later been known that as AD progresses, AChE activity decreases by up to 45%, while BChE activity increases by 40-90%. This has led to the perception that an inhibitor with the ability to bind to both AChE and BChE may be a more beneficial AD treatment.[24]

The accumulation of Aβ-protein outside neurons, also called senile plaques, is believed to interfere with the neuron-to-neuron communication at synapses and to contribute to cell death.[2,3,27] Aβ self-aggregates, but aggregation can also be triggered by molecular chaperones, one being AChE. In its missfolded state the Aβ monomers oligomerization forming fibrils and eventually Aβ aggregates. In addition, AChE is able to form stable complexes with Aβ that are more toxic than Aβ aggregates alone.[28] The conformational changes in amyloid monomers is thought to be mediated by the pheriper site of AChE.[12,28] Inhibitors occupying both PAS and CAS does not only prevent the breakdown of ACh but also prevents AChE-induced Aβ aggregation. Thus, potential treatments occupying both sites of the gorge would prevent two of the brain changes associated with AD.

1.3 Tacrine hybrids

1.3.1 Tacrine

Tacrine (THA) is an inhibitor of both AChE and BChE, and was the first drug approved for the treatment of AD.[29?] Studies have proved it to be more effective towards BChE than AChE.[19,21–23,30,31] The drug was approved for use in the United States in 1993 as therapy of mild-to-moderate dementia of the Alzheimer type. The side effects of the drug, mainly liver toxicity, led to the treatment being withdrawn from use in 2013.[29,32,33]

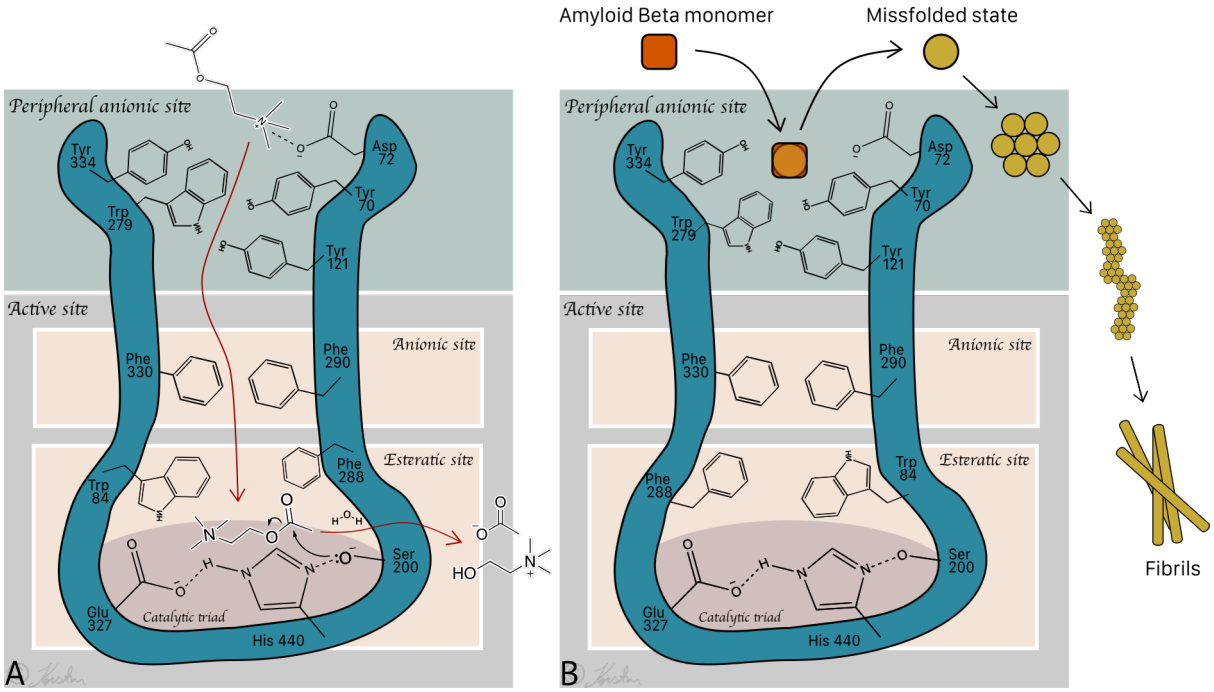

Figure 4. Illustrations of the AChE gorge. AChE catalyzes the breakdown of acetylcholine but can also promote formation of toxic fibrils known as senile plaques. [1] The figures are designed with inspiration from published illustrations. [16,25,26]

A: Catalysing the breakdown of ACh. The negatively charged entrance attracts ACh and the "anionic site" drags it into the active site before hydrolysis occurs at the "esteratic site".

B: Promoting Aβ aggregation. AChE promotes conformational changes in amyloid monomers through its peripheral anionic site which leads to the formation of senile plaques.

Since then, potential AD treatments have been synthesized by modulation of tacrine. With the goal of obtaining inhibitors with high affinity towards AChE and without being toxic to the liver. [32]

Based on Crystallographic structure analysis, Tacrine has been reported to bind to CAS (Trp84 and Phe330) through π-π-stacking interaction. Hydrogen bonding interactions between its cyclic nitrogen and His440 is also reported. The aromatic quinoline moiety

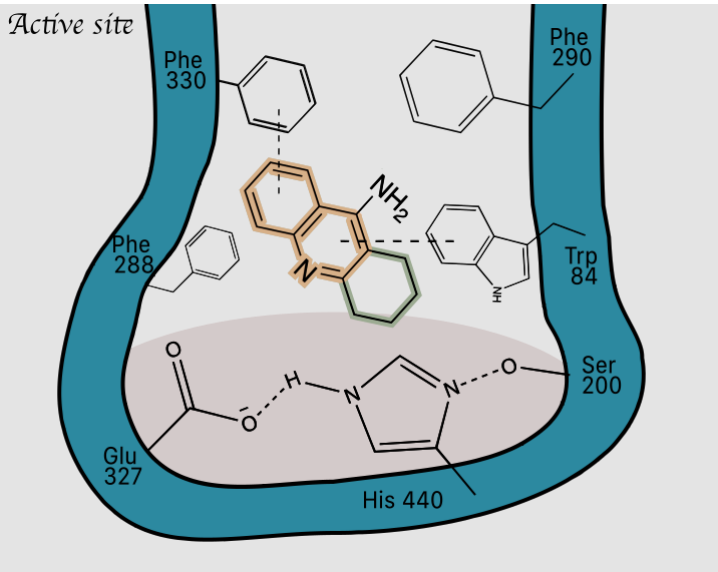

Figure 5. Tacrine is reported to bind to CAS (Trp84 and Phe330) through π-π-stacking interaction.

(orange) is largely responsible for the binding to AChE, while the cyclohexyl portion (green) is blocking ACh from approaching the active site (Figure 5).[34]

1.3.2 Opposing moiety

In search of more active and safer drugs, several tacrine analogues have been synthesized during the last years.[19,21–23,30,31] The discovery of PAS led to the synthesis of a compound consisting of two THA moieties connected with an alkylene chain spacer. Crystal structure revealed the dimer to bind simultaneously to PAS and CAS (Figure 6). The optimal space length was determined to be seven methylene groups.[24] Proving that CAS and PAS are close enough to simultaneously interact with a bis-ligand when the linker between the binding moieties is of optimal length. The majority of the later published tacrine analogues are molecules reported to span the catalytic gorge of AChE, and thus behave as dual binding site AChE inhibitors (i.e. interact simultaneously with PAS and CAS). In fact, one of the reasons why tacrine was withdrawn was because of all the new promising

tacrine hybrides.[24,29,35?]

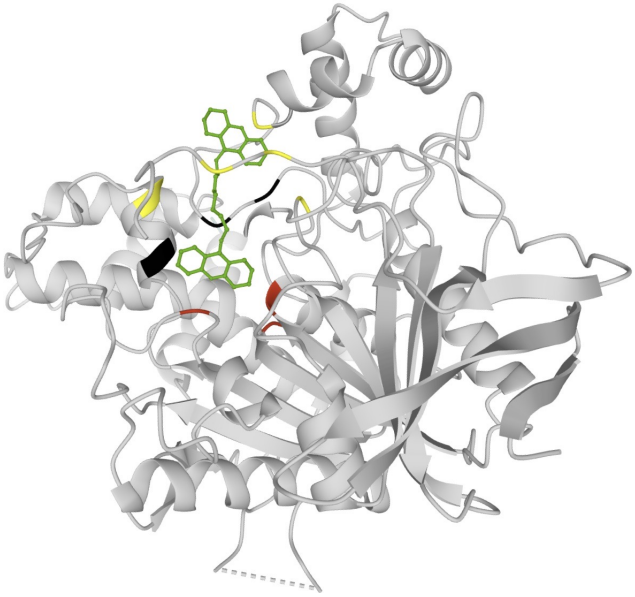

Figure 6. AChE in complex with bistacrine. The red colored amino acids are the catalytic trad in the bottom of the gorge. The amino acids colored yellow constitute the entrance of the gorge, a part of PAS.

The goal for the compound linked to tacrine[2] is to reduce its hepatotoxicity, increase its AChE affinity and interact with PAS in order to prevent AChE-induced Aβ aggregation. In addition, some literature even reports that the hybrids prevent self-induced Aβ aggregation.[21–23,30,36–38]

τ tangles and metal-induced oxidative stress are two briefly mentioned brain changes associated with AD. Tau tangles are composed of phosphorylated τ-protein and inflammation. The aggregation is believed to contribute to cell death by blocking the transport of nutrients and other essential molecules inside neurons.[2,3,27] Glycogen synthase kinase-3β (GSK-3β) is a protein associated with the formation of tau tangles. Linking a moiety to tacrine that allows the hybrid to bind to GSK-3β adds yet another mode of action to

[2]In the lack of a better word, *opposing moiety* is used as a general term when assessing the compound linked to tacrine in a tacrine heterodimer.

the potential treatment. If the opposing moiety also is a chelating agents it will remove metals and prevent oxicative stress.[32]

1.4 Target molecules

In 2017 tacrine–neocryptolepine heterodimers was synthesized (Figure 7). The compounds proved to be a highly potent human cholinesterase inhibitors. Based on molecular modeling studies, some of the heterodimers was suggested to bind simultaneously to the PAS and CAS. The optimal length was reported to be a eight methylene groups. Hydrogen-bond interactions and π-π-stacking interactions was reported between PAS and the neocryptolepine moiety. Tacrine was reported to interact with CAS through π-alkyl interactions, hydrogen-bond interactions and van der Waals interactions. Also, it was able to inhibit Aβ_{42} self-aggregation.[27]

Cryptolepine (I), Isocryptolepine(II) and neocryptolepine(III) (Figure 8) are alkaloids extracted from the West-African plant Cryptolepis sanguinolenta. The skeleton of these compounds are composed of the tetracyclic indoloquinoline ring system. They only differ with respect to the orientation and site of their indole (yellow) and quinoline (blue) ring junctures.[39,40]

Human proteins contain structural domains that are similar to some of the macromolecules targeted by natural products. Indirectly this has been known from the beginning of time vindicated by the use of medicinal plants.[40] A study published in 2012 lists the sources for new drugs between 1981 and 2010. Of the drugs approved in this period, close to half were derived from natural products or were natural products themselves.[41] Thus, the use of natural products, as the opposing moiety when designing tacrine heterodimers, has a statistically higher likelihood of providing a promising AD treatment candidate. Which for instance was observed when tacrine was armed with neocryptolepine (Figure 7).

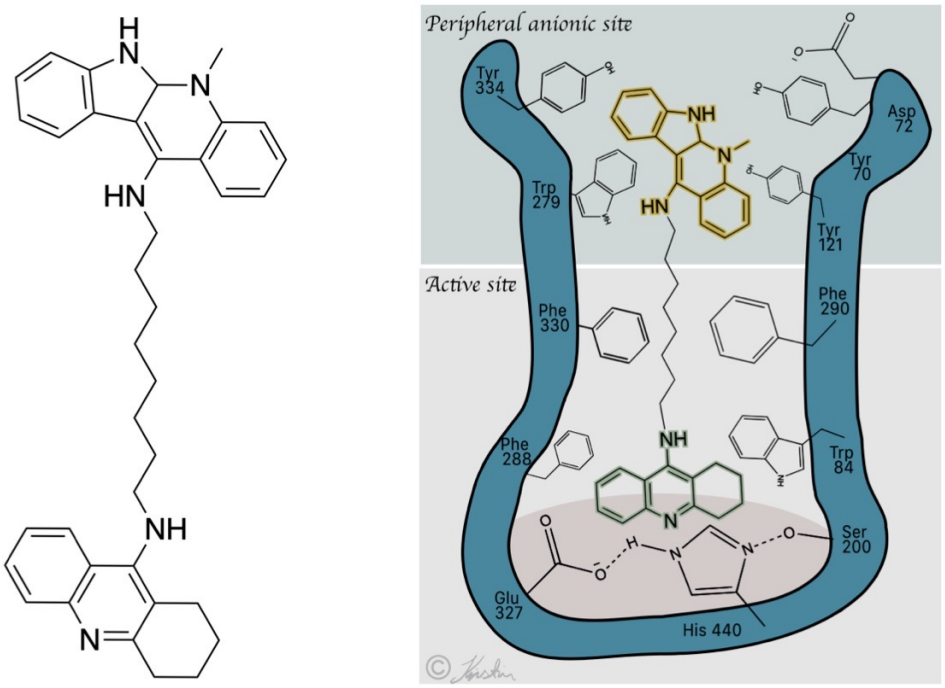

(**a**) One of the tacrine–neocryptolepine heterodimers.

(**b**) AChE in complex with the tacrine (green)–neocryptolepine(yellow) heterodimer.

Figure 7. Graphic illustration of the tacrine–neocryptolepine heterodimer with an eight carbon linker.

In this context, two tacrine-isocryptolepine heterodimers have been synthesised (Figure 9), with the hope that this would provide a potential AD treatment with the same or better potency than the tacrine–neocryptolepine heterodimers.

The first reported total synthesis of isocryptolepine was reported in 1950. Since then, several other synthetic methods have been reported for isocryptolepine.[40] For instance, Helgeland and Sydnes published a method for the synthesis of isocryptolepine, which included Suzuki–Miyaura cross coupling reaction and palladium catalyzed intramolecular C-H activation/C-N bond.[42]

Timári, Soós and Hajós descibes a synthesis where the quinoline-3-aniline is subjected to diazotization providing aryl azide, which collapses into indolquinoline, the isocryptolepine

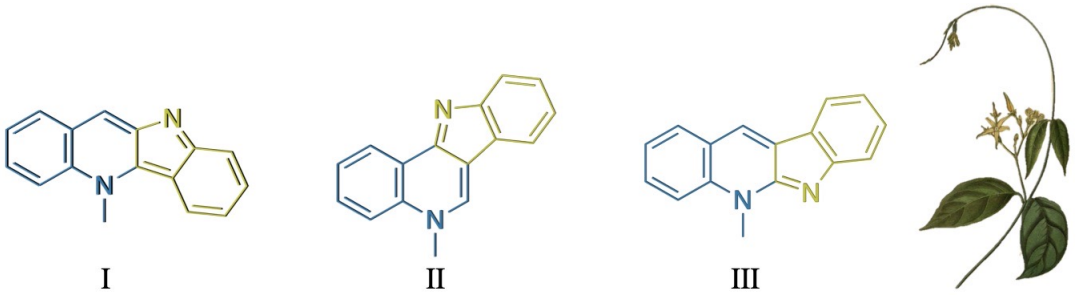

Figure 8. Cryptolepine (I), Isocryptolepine(II) and neocryptolepine(III) (Figure 8) are alkaloids extracted from the West-African plant Cryptolepis sanguinolenta.

precursor.[43] The mechanism of the ring closure is illustrated in Figure 10.[44]

Tacrine was first synthesized by Adrien Albert and Walter Gledhill in 1945. They obtained the compound by converting 5-chloroacridine into 5-aminoacridine.[45] Later published tacrine syntheses features 2-aminobenzoic acid,[12,46] 2-aminobenzonitrile,[47,48] and 4-chloroanthranilic acid[49] reacting with cyclohexanone in order to obtain the THA skeleton. The latter provides tacrine equipped with an chlorine atom on its sixth carbon.

A frequently used method for connecting biological active molecules is click chemistry. Recent research has described the use of click chemestry to obtain tacrine hybrids. In 2018; the synthesis of tacrine-valmerin hybrids,[19] in 2016 when synthesising tacrine-1,2,3-triazole hybrids[31] and the synthesis of tacrine-quinuclidinein in 2020.[49] The mentioned publication features the use of a compound with a clickable azide moiety reacting with an terminal alkyne bearing compound, cyclizing into triazole, fusing the two compounds.

1.4.1 Suzuki-Miyaura cross-coupling reaction

When synthesising natural products Suzuki-Miyaura cross-coupling reaction is a technique, frequently used.[50–52] The coupling partners are an aryl or vinylhalid and alkyl, alenyl or aryl boronic acid. Boronate ester can also be used as the latter coupling partner.

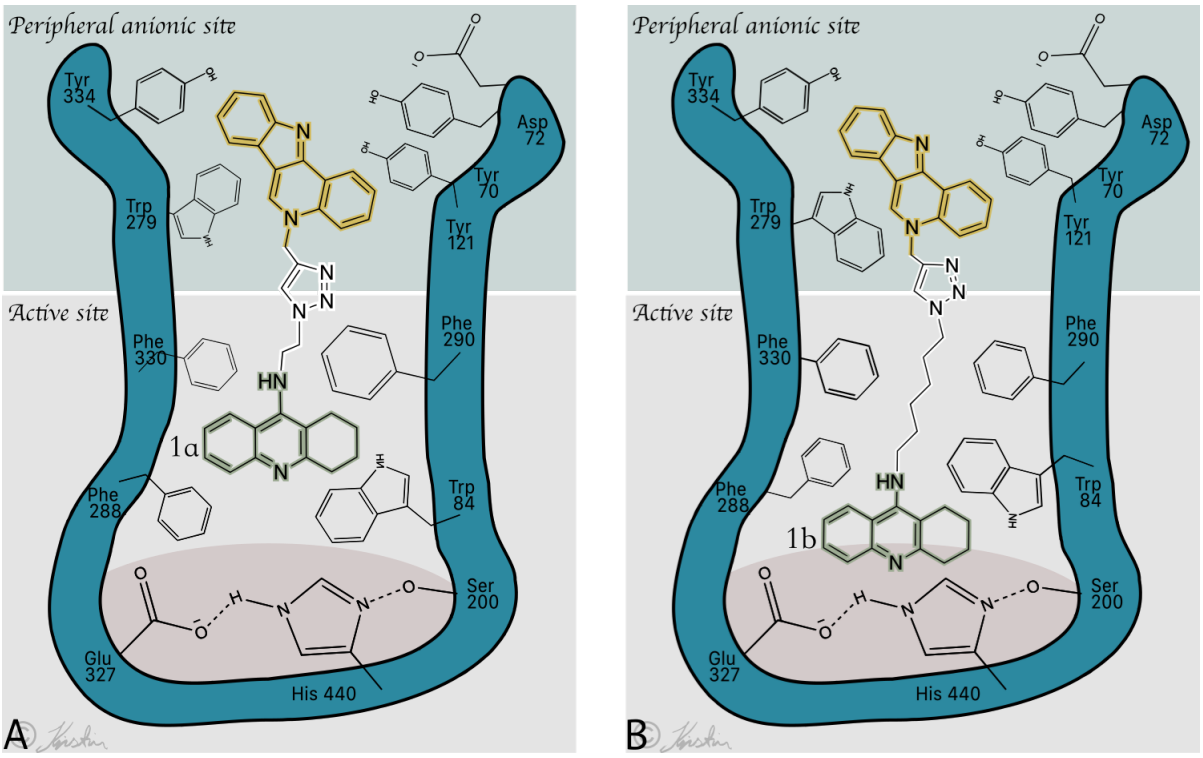

Figure 9. AChE in complex with tacrine-isocryptolepine heterodimers 1a (A) and 1b (B).

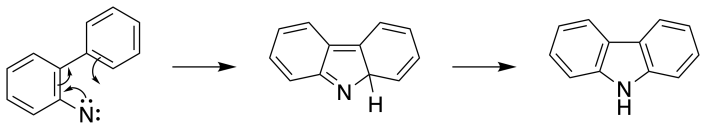

Figure 10. Electrocyclic ring closure of an aryl nitrene.[44]

The reaction is catalyzed by a palladium(0) complex.[3] The mechanism of Suzuki-Miyaura cross-coupling reaction is illustrated in figure 11.[53]

1.4.2 Diazotization

The reaction between primary amines and the nitrosonium ion creating diazonium cations is called diazotization. In acidic solutions the nitrosonium ion is formed from nitrous acid (Appendix G). The mechanism of diazotization is illustrated in figure 12.[53]

[3]Richard F. Heck, Ei-Ichi Negishi and Akira Suzuki was awarded the Nobel Prize in Chemestry (2010) for developing palladium-catalyzed coupling reactions forming new carbon-carbon bonds between carbons of aromatic rings and alkenes.[53]

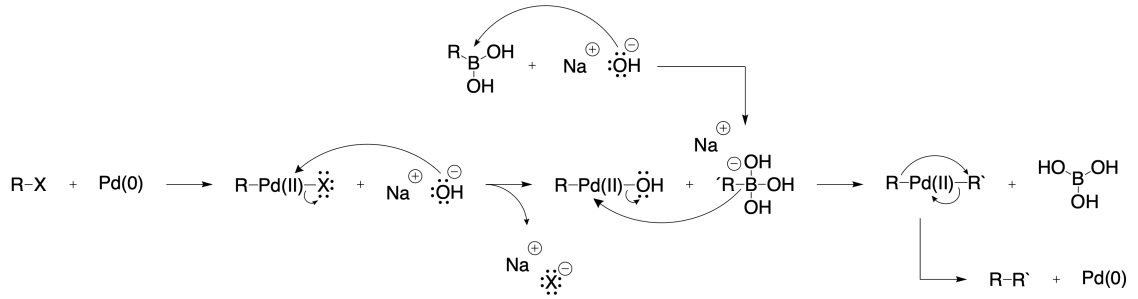

Figure 11. The reaction mechanism of Suzuki-Miyaura cross-coupling.[53]

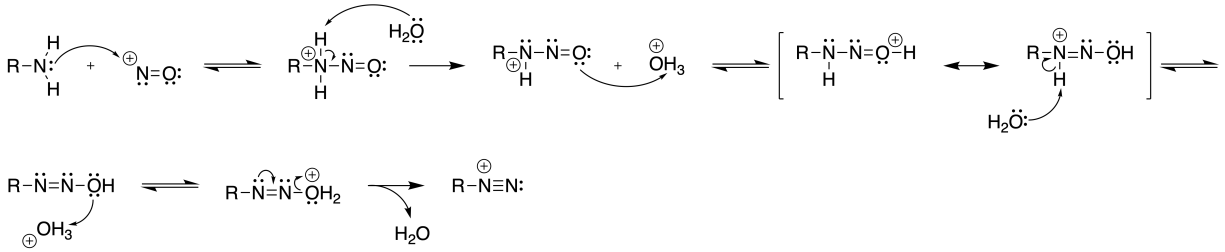

Figure 12. The diazotization reaction mechanism.[53]

1.4.3 Click Chemistry

Dr. Barry Sharples introduced the concept of click chemistry in 1999. It was described as a powerful linking reactions that are simple to perform, have high yields, require no or minimal purification and can join various structures without requiring protection steps. Among the four major classifications, cycloadditions are the most widely used. Especially the CuI-catalyzed 1,3- dipolar cycloaddition of azides and terminal alkynes to form 1,2,3-triazoles.[54]

In general, cycloadditions proceed through a concerted mechanism but the use of Cu(I) catalyzed cycloaddition of azides and terminal alkynes seem to favor a stepwise reaction pathway.[54] The mechanism is illustrated in Figure 13

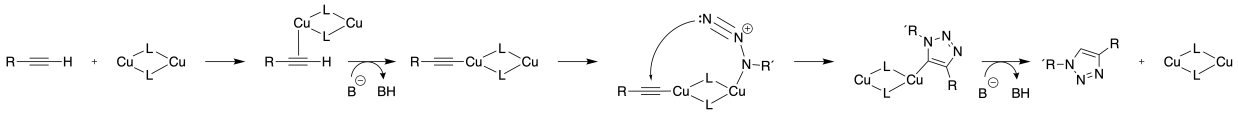

Figure 13. The mechanism of CuI-catalyzed 1,3- dipolar cycloaddition of azides and terminal alkynes to form 1,2,3-triazoles.[54]

1.5 Numerous suggested AD treatments

Databases contain a myriad of articles about potential AD treaments. Searching for "acetylcholinesterase inhibitor" in the Scifinder database provides more than 6000 references, many of which are tacrine hybrids. In order to get an overview of this group of potential pharmaceuticals, a comparison of 44 tacrine hybrids will be featured in this paper. The publications from where they was retrived is listed in Appendix A by their accession number. The molecules will be referred to by the number of the article.

The biological evaluations frequently used in these publications are Ellmas test, molecular modeling studies and the ThT method. Respectively they determine the compounds affinity towards AChE, whether it occupies PAS and its ability to prevent Aβ aggregation.

1.5.1 Ellman's method

The Ellman's method (1996) is a photometric method for determining acetylcholinesterase activity. The enzyme activity is measured by the following reactions:

$$\text{acetylthiocholine} \xrightarrow{\text{enzyme(AChE)}} \text{thiocholine} + \text{acetate}$$
$$\text{thiocholine} + \text{dithiobisnitrobenzoate} \longrightarrow \text{yellow color}$$

Thiocholine reacts rapidly with dithiobisnitrobenzoate ion and creates a yellow color, measured at 405 nm. The method is extremely sensitive and applicable to either small amounts of tissue or to low concentrations of enzyme. Sources for enzyme can be human erythrocytes, homogenates of brain, kidney, lungs, liver or muscle tissue.[19,55]

By using Ellmans method the concentration of an inhibitor needed to inhibit 50% of the enzymes (IC_{50}) can be calculated. Sometimes the inhibitor constant (K_i) is given instead of IC_{50}. For noncompetitive inhibition K_i is identical with IC_{50}. For uncompetitive or competitive inhibition IC_{50} is half of K_i. Tacrine-hybrides act as a competitive inhibitor

of AChE.[56(s234−236)]

1.6 Virtual docking

Molecular docking can be used to predict if and how the ligand will bind to a receptor.[57]

Virtual screening methods can be divided into structure-based and ligand-based algorithms. The structure-based method uses the three dimensional structure of the target protein and simulates the protein–ligand interactions. The premise is that high-resolution structural model is accessible. The ligand-based approach assesses the drug candidate by comparison to known hits and ignores the structural details of the protein target.[58]

The docking performed in this thesis is the structure-based method and the program used is 1-click docking. 1-click docking is powered by the AutoDock Vina docking algorithm.[59]

The interaction between atom type a and type b is given as a function were the interatomic distance between a and b is the variable. Interaction includes steric hindrance, van der Waals, hydrophobic, hydrogen bonding and covalent bonds. The interactions are defined relative to the surface distance.[60]

The summation of these functions is the general function of the conformation dependant part of AutoDock Vinas scoring. All of the pairs of atoms that can move relative to each other are included. Thus the summation will be the sum of intermolecular and intramolecular interactions.[60]

In addition the program uses information from the conformations preferences of the ligand complex. And if available, experimental affinity measurements is also decisive for the final score.[60]

Variables that are not included in the algorithm is change in charge distribution and protonation state of the molecule for example between their bound and unbound states. The dynamic trait of receptors is also reduced, since the algorithm only permits a chosen set of covalent bonds to rotate.[60]

Docking studies of AChE is often done using Acetyl Cholinesterase from Torpedo californica (TcAChE) also known as the Pacific electric ray. Blast search gave 57-59% indent to the human AChE (Appendix F). Despite the difference in amino acid sequence, the active site of the proteins are similar and should have identical properties.[14]

1.6.1 Interactions

Molecular modeling addresses the interactions between the ligand and the amino acids of the enzyme. Two of the frequently mentioned interactions between AChE and the ligand are π-π-stacking interaction and hydrogen bonding.[18–20,30,31,34,61,62] Programs have different requirements in order for the bond to be recognised.[63]

The software company, Schrödinger, defines π-π-stacking interaction as an interaction between two aromatic rings. The aromatic rings will interact if the angle between the ring planes is less than 30° and the distance between the center of the ring is less than 4.4 Å. Also, if the angle between the ring planes is between 60° and 120° and the distance between the center of the aromatic ring is less than 5.5 Å, interaction will be noted.[64]

Hydrogen bonding is confirmed if the distance between the hydrogen and the two electronegative atoms is maximum 2.5 Å. The angle between the electron donor and the hydrogen must be minimum 120.0 and the minimum acceptor angle is 90°.[64,65]

1.7 ThT method

The molecules ability to inhibit self aggregation of Aβ can be tested using the thioflavin T (ThT). ThT is a small molecule that gives strong fluorescence upon binding to amyloids.

The amount of amyloid fibrils can be quantitatively determined by measuring the intensity of the fluorescent signal at approximately 482 nm when excited at 450 nm. Maximal ThT fluorescence mostly depends on total ThT concentration, rather than amyloid to ThT ratio. ThT concentrations of 10–50 µM provide maximum sensitivity in the studies of aggregation kinetics. At concentration above 5 μM, in PBS, ThT becomes self-fluorescent. The amyloid fibrils involved in Alzheimer's disease is A40 and A42. Some of the Tacrine hybrids discussed in this paper are tested on one or both of these amyloid fibrils.[66]

2 Results and discussion

2.1 Chemistry

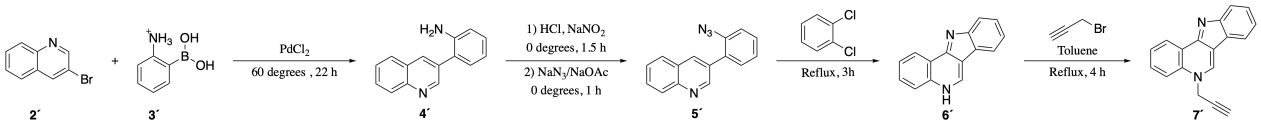

Figure 14. Synthesis of the isocryptolepine precursor **6´** and addition of alkyne.

The synthesis of compound **7´** commenced from 3-bromoquinoline (**2´**) and 2-aminoboronic acid hydrochloride (**3´**), which underwent Suzuki-Miyaura cross-coupling reaction into aniline **4´**, by following a protocol reported by Helgeland and Sydnes.[42] The successful formation of the coupling product could be identified through ^{1}H-NMR, showing 10 aromatic protons in addition to a NH_2 group appearing as a broad singlet at 3.75 ppm (Figure 15 Appendix E.4).

As described by Timári, Soós and Hajós; aniline **4´** was subjected to a diazotization reaction to provide aryl azide **5´**, which collapsed into isocryptolepine precursor **6´** at elevated temperature.[43] Treatment of isocryptolepine precursor **6´** with propagyl bromide provided the alkyne click-chemistry reaction partner **7´** (Figure 14). A two-hydrogen singlet at 4.95 ppm and a single hydrogen triplet at 2.55 ppm, on ^{1}H-NMR, confirms the presence of alkyne (Figure 16 Appendix E.6)).

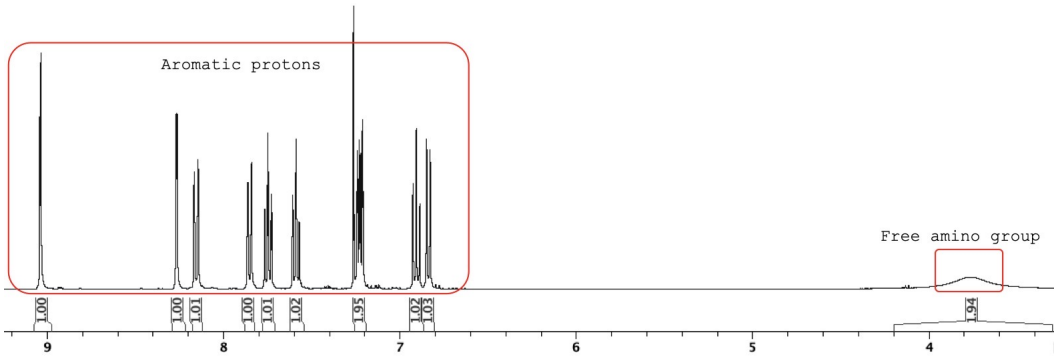

Figure 15. ^{1}H-NMR spectra of coupling product **4´**.

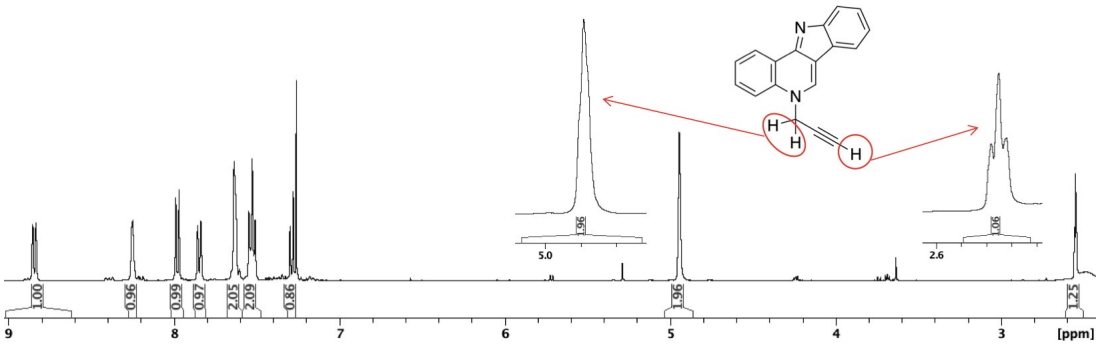

Figure 16. ^{1}H-NMR spectra of alkyne click-chemistry reaction partner **7´**.

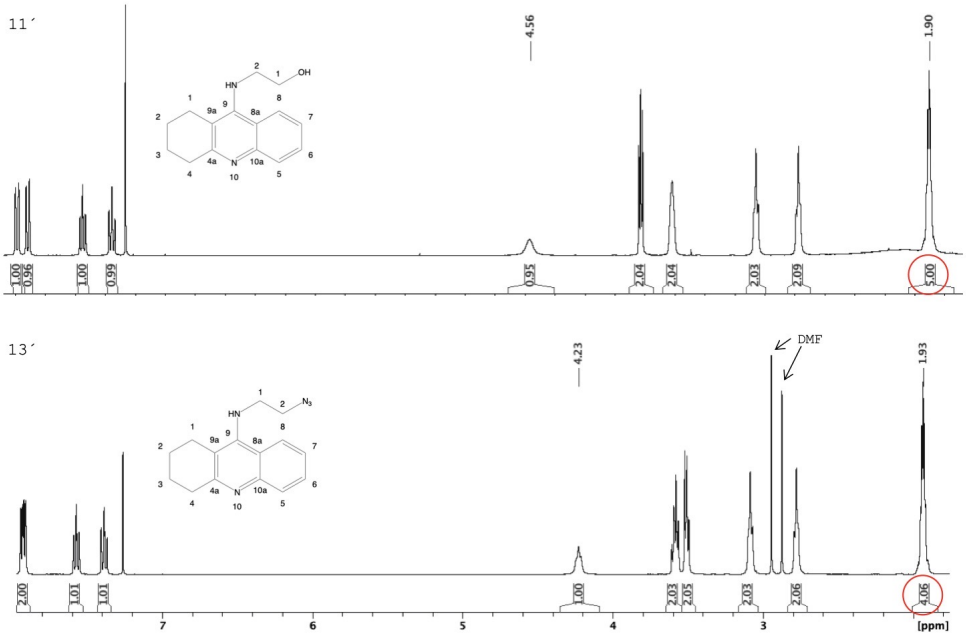

Figure 17. ^{1}H-NMR spectra of compound **11´** and compound **13´**.

The azide click-chemistry partner **13´** was obtained from anthranilic acid (**9´**) reacting with cyclohexanone (**8´**) in the presence of phosphorus(V) oxide chloride to generate compound **10´**. After which compound **10´** was subjected to a nucleophilic substitution-chlorination-azidation reaction sequence to generate azide **13´** (Figure 22).[12] The absence of the proton from the hydroxide group of compound **11´** in the ^{1}H-NMR specter of compound **13´** would indicate a successful substitution. As illustrated in figure 17 the ^{1}H-NMR spectrum of compound **13´** and compound **11´** is similar, but integration of the peak at 1.93 ppm reveal one less proton.

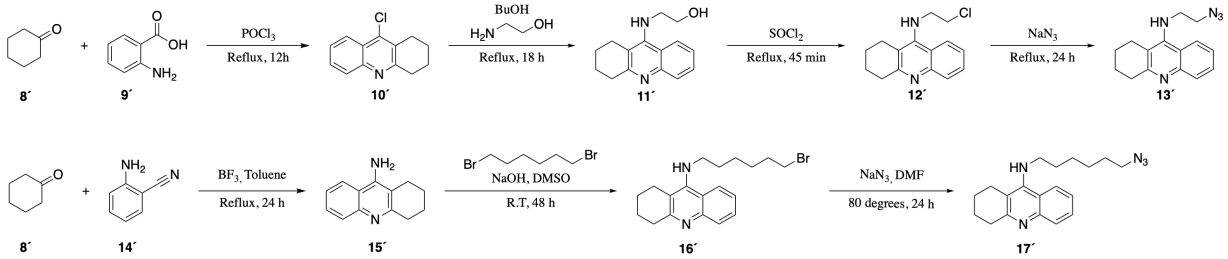

Figure 18. Synthesis of azide armed tacrine with a two carbon linker (**13´**) and azide armed tacrine with a six carbon linker (**17´**).

An azid group can be identified by the strong N≡N stretching absorption which occurs with great consistency close to 2130 cm^{-1} in the IR specrum.[67] IR of compound **13´** confirms the presence of azide (Figure 19).

Compound **14´** was reacted with ketone **8´** in the presence of a Lewis acid to provide tacrine **15´**. Tacrine was armed with a N-(6-azido)hexyl group to provide **17´** via a substitution-bromination-azidation sequence (Figure 22). To verify that the addition of the 6-carbon linker had indeed occurred, ^{1}H-NMR was used to confirm an increase of nonaromatic protons. The ^{1}H-NMR of **16´** and **17´** are close to identical (Figure 20), thus positive identification of the azide had to be assisted by IR (Figure 21.

With the azide armed tacrines **13´** and **17´** and alkyne **7´** click-chemistry reaction partners in hand, the isocryptolepine-tacrine dimers **1a** and **1b** were assembled upon treatment

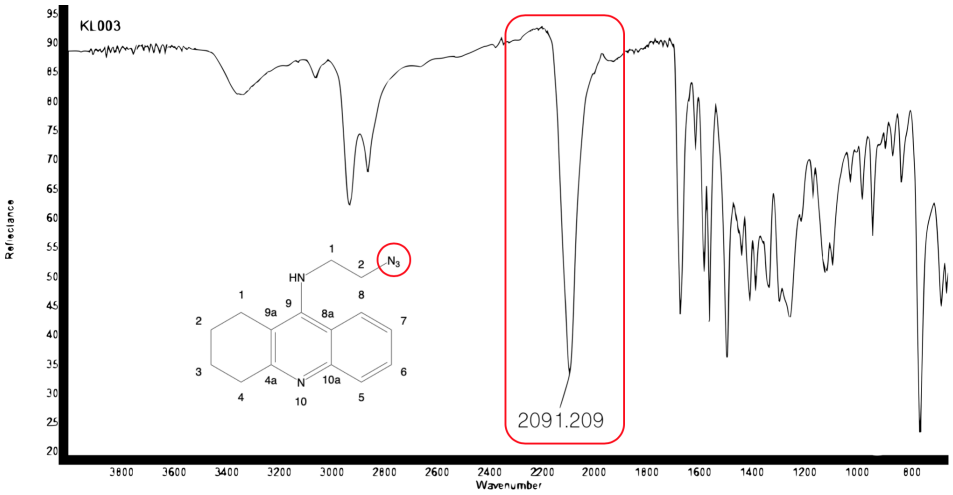

Figure 19. IR spectrum of compound **13´**.

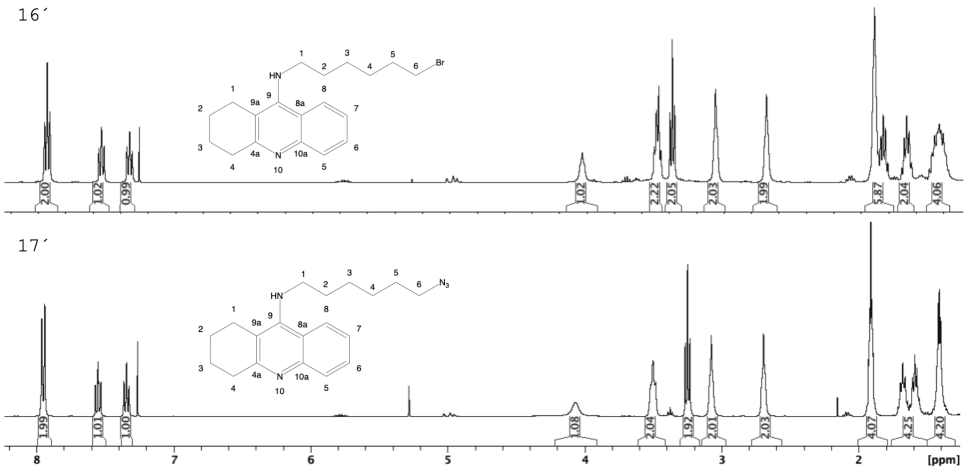

Figure 20. ^{1}H-NMR spectra of compound **16´** and compound **17´**.

with copper(II) sulfate in the presence of sodium ascorbate as an anti-oxidant (Figure 22).

When extracting **1a**, precipitation occurred. The precipitate assembled between the aqueous and organic layer, making what seemed like micelles. TLC of the pure organic phase only showed starting materials, while the mud layer between the aqueous and organic phase seemed to contain the product. Illustration of the two plates are depicted in figure 23. Thus the organic phase and the precipitate was combined, concentrated under reduced pressure and purified by silica gel column chromatography. The product was not soluble in chloroform but dissolved in methanol, though precipitate could be seen. ^{1}H-NMR and

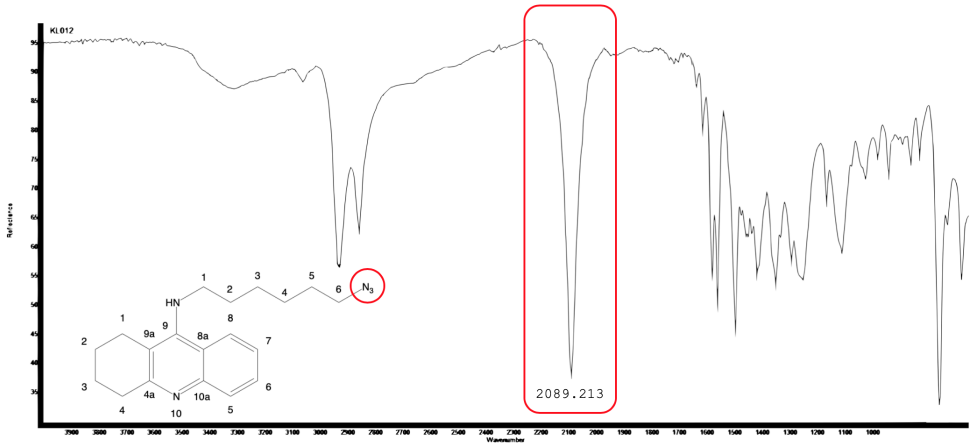

Figure 21. IR spectrum of compound **17´**.

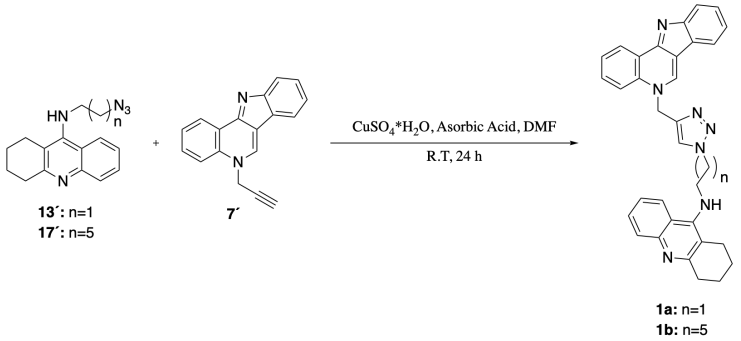

Figure 22. Click-chemistry reaction azide armed tacrines (**13´** and **17´**), and alkyne (**7´**) to obtain target molecule **1a** and **1b**.

^{1}H-^{1}H correlation (COSY) spectrum corresponded with expectations for **1a** (Figure 24). The presence of the two aromatic singlets confirms the successful formation of the triazole. The chemical shift of the triazole hydrogen is reported to be between 7 and 10 ppm.[68–70] Cosy reveals a weak coupling between 8.52 ppm singlet and its neighbouring doublet (Expanded in figure 24), indicating that the 10.22 ppm singlet is the triazole proton. Two of the non-aromatic hydrogens are missing from the spectrum, ^{1}H-^{1}H correlation spectrum revealed them to be located behind the water peak (Figure 25).

The impurities still present made a second purification necessary. The output proved to be insoluble in chloroform, methanol and dimethyl sulfoxide (DMSO). The short linker makes the structure rigid and could be the reason why its hard to dissolve.[71] Based on

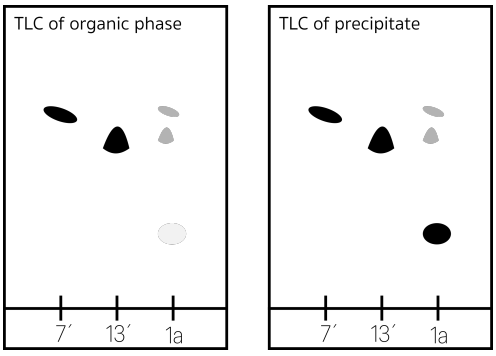

Figure 23. TLC after extraction of **1a**.

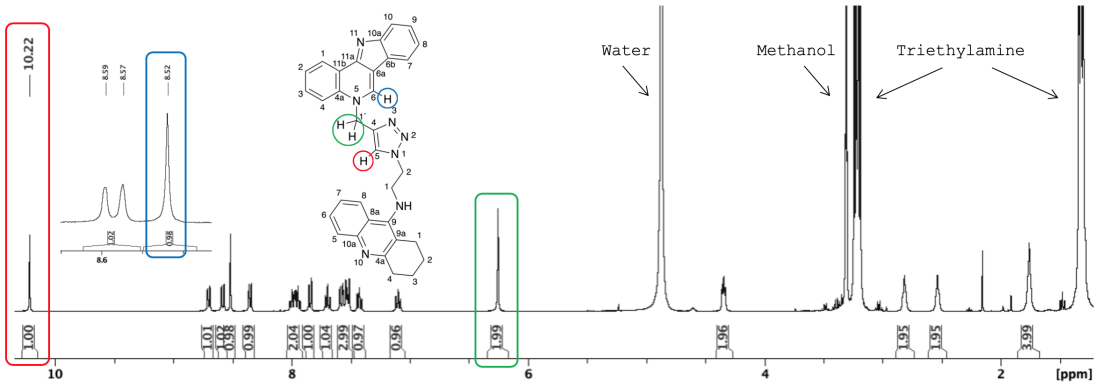

Figure 24. ^{1}H-NMR spectrum of compound **1a**.

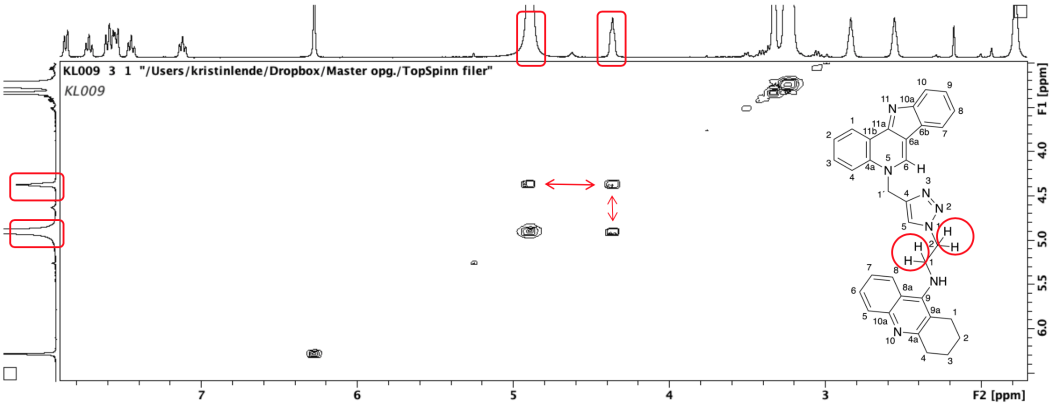

Figure 25. ^{1}H-^{1}H correlation spectrum of compound **1a**.

the evaluation of bis-tacrine[24] and tacrine-neocryptolepine[27] mentioned earlier, tacrine-isocryptolepine hybride with a longer linker would probably give a better fit to the AChE gorge. Thus, further synthesis and analysis of **1a** was not done. Because of this; IR, ^{13}C-NMR, Heteronuclear Single Quantum Correlation (HSQC), Heteronuclear Multiple Bond

Correlation (HMBC) and Nuclear Overhauser Effect Spectroscopy (NOESY) spectrum are missing and could not substantiate the successfully synthesis of **1a**.

Because of sudden termination of the lab work the purification of compound **1b** was not completed. This is also the reason why IR, HSQC, HMBC and NOESY are missing. These spectra would have substantiated the presence of **1b**. Regardless the two aromatic singlets (Figure 26) strongly indicate the successful formation of triazole. Also the number of aromatic and non-aromatic protons correlates with expectations.

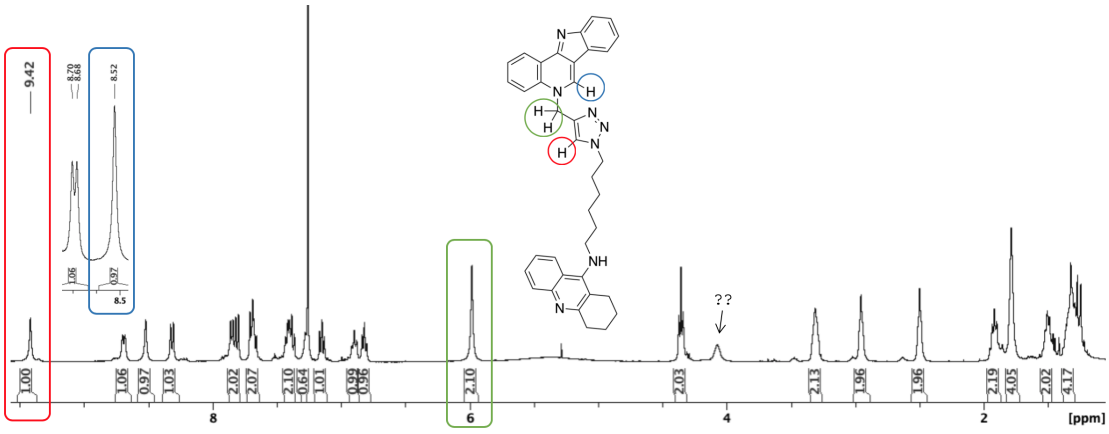

Figure 26. ^{1}H-NMR spectrum of compound 1b.

Small amount of ammonia or organic amines such as triethylamine may reduce the tailing often occurring when separating alkaloids on silica gel. Herein, ammonia and triethylamine was sometimes added to the mobile phase to separate the spots of the product from impurities on the TLC plate. Also, triethylamine was used in the mobile phase when performing silica gel column chromatography on the target molecules. When performing silica gel column chromatography, the target molecules (**1a** and **1b**) moved sluggishly through the column. Molecules are retained by the silica gel through hydrogen-bonds and dipole–dipole interactions. Polar product will thereby be retained longer in silica gel columns than nonpolar ones. The nitrogen of the target molecules, able to make hydrogen-bonds, explains the slow movement through the column. To weaken silica gel adsorption, triethylamine was added. The combination of triethylamine and methanol

in the mobile phase generates water, deactivating the silica gel and releasing the target molecule. Unfortunately impurities was also flushed out. TLC was used to optimise the concentration of MeOH, DCM and triethylamine. What seemed to be a good gradient on the TLC plate did not turn out to remove all the impurities. As already mentioned, further work on purifying the target molecule was terminated.[72]

2.2 In vitro inhibition of AChE and BChE

The AChE inhibitory activities of all the compounds, except **2**, were evaluated in vitro (Ellman´s method), with tacrine as positive control. 32 of the compounds were also evaluated for their BChE inhibitory activities. The molecules and their affinity towards AChE relative to tacrine is listed in figure 27. Appendix 12 features the extended information of the inhibitors affinity towards AChE. Table 3 features the IC_{50BChE} for the inhibitors and for tacrine.

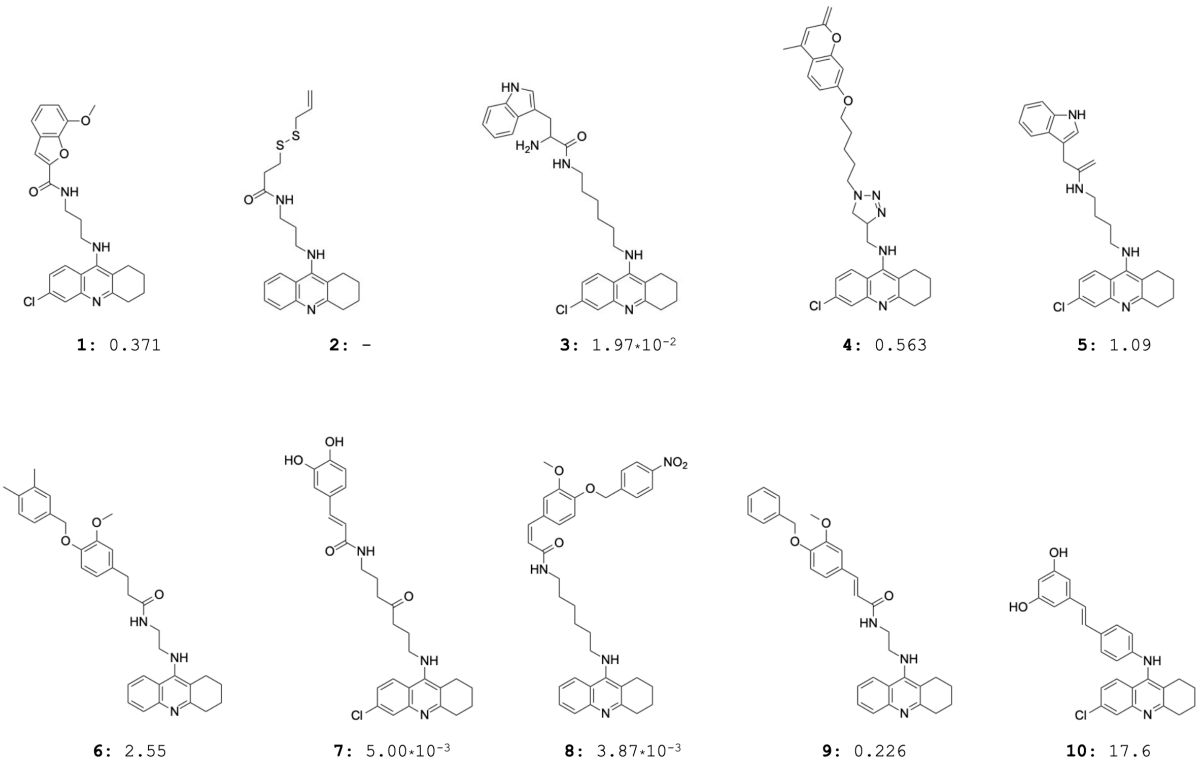

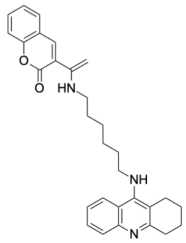

11: 0.468

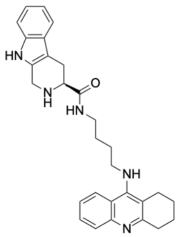

12: $8.31 \star 10^{-2}$

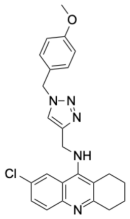

13: 10.9

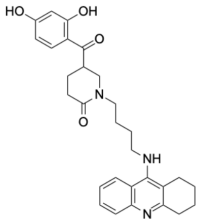

14: 1.84

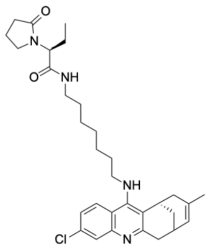

15: $1.32 \star 10^{-2}$

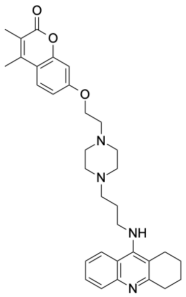

16: 0.346

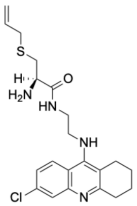

17: 1.58

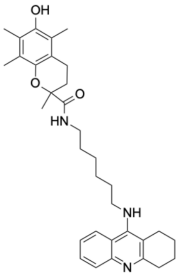

18: $8.74 \star 10^{-2}$

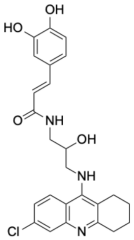

19: 1.50

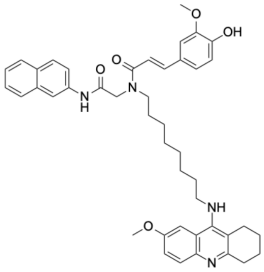

20: $5.24 \star 10^{-2}$

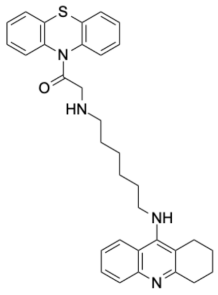

21: 0.324

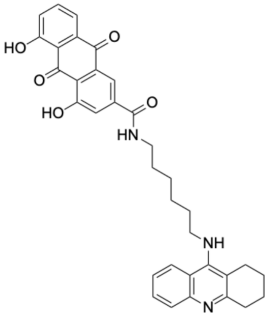

22: 0.202

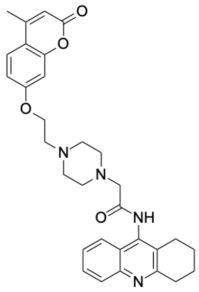

23: 0.342

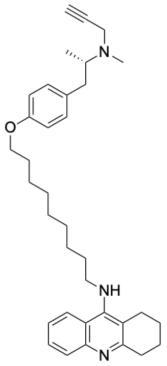

24: 0.205

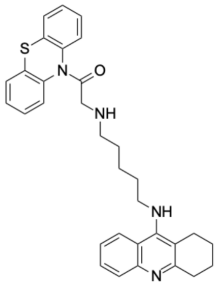

25: 0.299

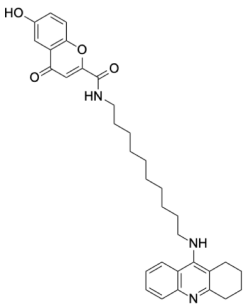

27: $2.29 \star 10^{-2}$

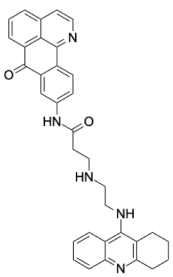

28: $3.27 \star 10^{-2}$

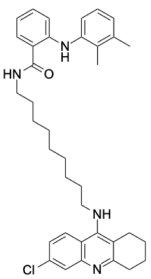

29: $9.52 \star 10^{-3}$

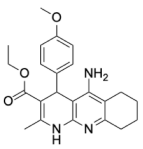

30: 0.250

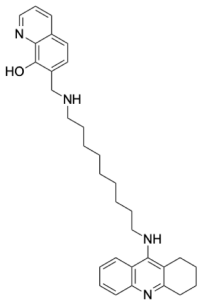

31: $1.57 \star 10^{-2}$

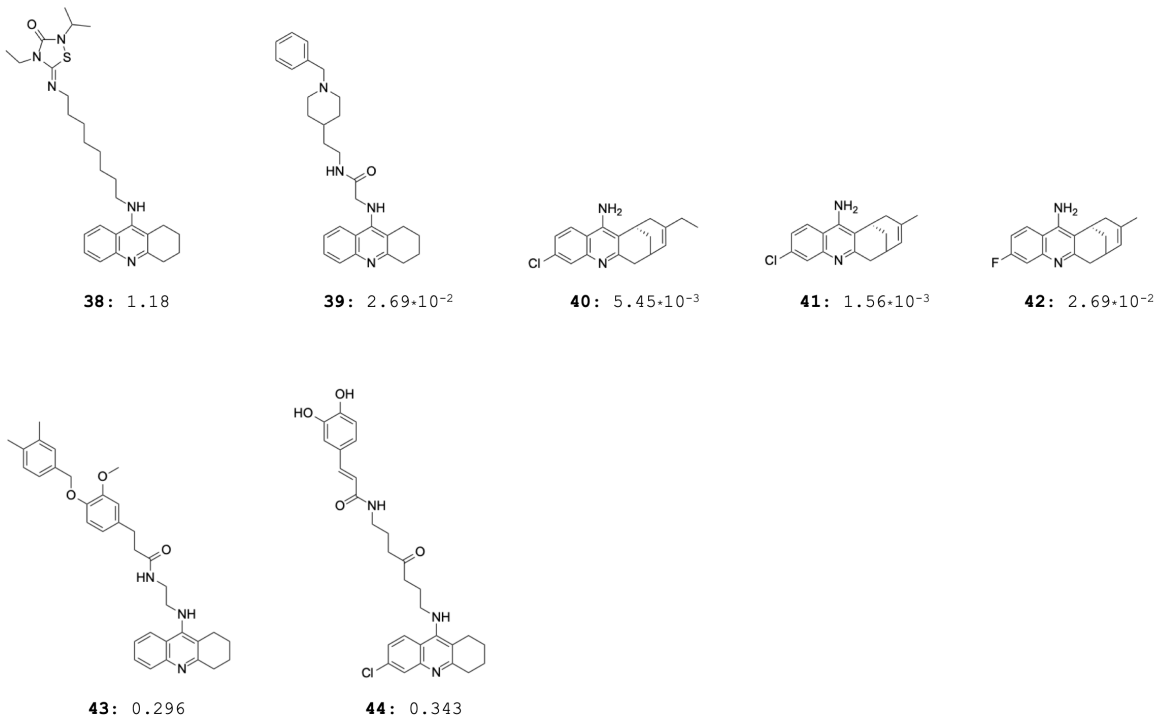

Figure 27. The molecules retrieved from the publications listed in appendix A. The affinity towards AChE relative to tacrine is given for each compound (lower number means greater relative affinity). The source of the enzyme used is listed in appendix 12.

The assay most frequently used when performing Ellman´s test of AChE, contained enzymes from eletric eel. Compound **13** stood out as the worst inhibitor relative to tacrine, compared to the other ligands tested on eeAChE. The second worst, compound **6**, showed 5 times better inhibition than compound **13**. Compound **13** is the only inhibitor having a chlorine atom on the seventh carbon of the THA ring system. This might be the reason for the low inhibition. Graphic representation of the compounds tested on eeAChE is depicted in appendix **??**. Only compound **4-6**, **13**, **14** and **19** had a relative inhibition above 0.5, which means that the rest of the compounds showed more than 50% better

inhibition than tacrine. Compound **8**, **12**, **28** and **29** showed ten times better inhibition of eeAChE than tacrine.

Ellmans test with huAChE assay revealed compound **10** as the worst inhibitor relative to tacrine. HuAChE inhibition by compound **10** proved to be 17 times less successful than the other reported compounds analyzed by huAChE assay. Appendix **??** contains a graphic representation of the inhibition of huAChE relative to tacrine. Compound **37** and compound **41** showed the best inhibition. According to Ellmans method compound **37** is extremely potent. It is 40 000 times more effective towards huAChE than tacrine. The publication reports that IC_50 for tacrine is 0.35 μM, the majority of the publications featuring Ellmans test on huAChE reports of IC_50 values between 0.30 and 0.35 μM, giving confidence to the reported values being correct.

Four compounds was tested on AChE from bovine. The average inhibition relative to tacrine was 0.38. Compound **7** showed the highest affinity, being 200 times more effective than tacrine. Ellmans test of four of the compounds was performed using AChE from rat, mouse and torpedo californica. Source of AChE used when testing compound **36** was not specified in the publication. The five latter compounds have a relative inhibition in the same range as those tested on eeAChE. Compound **39**, being 40 times more effective than tacrine, showed the best affinity.

Relative to tacrine, the inhibitors seems to have categorically higher affinity towards human AChE than AChE from eletric eel. The average relative inhibition towards eeAChE was 0.50, while the average relative inhibition towards huAChE was 0.067.[4] Too few compounds are tested on AChE from bovine, rat, mouse and torpedo californica to be able to compare the average relative inhibition.

[4]Data from compound **13** and compound **10** was removed when calculating the average of respective eeAChE and huAChE inhibition, because they differed excessively from remaining reported numbers.

The remarkable difference in average relative inhibition between inhibitors tested on eeAChE and huAChE could indicate a categorically higher affinity of tacrine hybrids towards AChE from human than from electric eel.

Elleman´s test on both eeAChE and huAChE was conducted on seven of the compounds. It did not seem to be any correlation between the IC_{50} values (Appendix C.4). Four of the compounds gave the lowest IC_{50} value when tested on huAChE, the rest gave the best result when tested on eeAChE. Only five of these publication reports IC_{50} of huAChE by tacrine. Neither the inhibition of eeAChE versus huAChE relative to tacrine showed any correlation. Too few compounds have been tested on enzymes from both eletric eel and human to discard any correlation. But the results prove, when comparing affinity of inhibitors, that an inhibitor showing highest affinity towards eeAChE does not necessarily have the highest affinity towards huAChE.

Table 3. BChE inhibition

No.	$IC_{50(I)}$(nM)	$IC_{50(Tac)}$(nM)	$IC_{50(I)}/IC_{50(Tac)}$	BChE
3	9.1	80	0.114	hu[a]
4	104	10	10.4	eq[b]
5	66	268	0.246	eq
6	101	4.5	22.4	eq
7	8.2	25	0.328	b[c]
8	6.5	10.6	0.613	eq
9	52.6	10.6	4.96	eq
10	na[a]	23	-	hu
11	8.05	4.35	1.85	hu
12	39.8	50.5	0.788	eq
13	1853	10	185	eq
15	232	24.5	9.47	hu
16	80.72	20.19	4.00	eq

Table 3. BChE inhibition

No.	$IC_{50(I)}$(nM)	$IC_{50(Tac)}$(nM)	$IC_{50(I)}/IC_{50(Tac)}$	BChE
18	22.2	35.2	0.631	eq
19	360	40	9.00	eq
20	68.2	45.8	1.49	hu
22	200	45	44.4	eq
23	234	42	5.57	eq
24	9.37	21.6	0.434	eq
27	1	10	0.100	eq
28	1.5	40	$3.75x10^{-2}$	h
29	110	21	5.24	eq
30	na	36	-	hu
31	20	40	0.500	hu
33	6.7	5.1	1.31	eq
34	9.9	5.1	1.94	eq
35	na	36	-	hu
36	$1.76x10^{-2}$	$1.16x10^{-3}$	15.2	-
37	7.8	40	0.195	hu
39	76	92	0.826	r[d]
41	247	43.9	5.63	hu
42	138	43.9	3.14	hu

[a] Human, [b] Equus caballus (horse), [c] Bovine, [d]Rat. The IC_{50} values are listed with the same number of decimals as presented in the given publication.

The assay most frequently used when performing Ellman´s test on BChE contained enzymes from equine. [5] 17 of the compounds was tested on this assay. Compound **13** was again revealed to have poor inhibition towards BChE. Compound **4**, **6** and **19** all showed

[5]Horses or other member of the horse family.

low affinity towards eqBChE, but **13** stood out, requiring 185 times higher concentration than tacrine to inhibit 50% of the enzymes. **5**, **8**, **12**, **18**, **24** and **27** were the onley compounds showing better inhibition than tacrine (appendix **??**). Compared to tacrine **27** proved to be the best inhibitor of eqBChE, having ten times higher affinity.

12 of the compounds was tested for their affinity towards huBChE. Compound **10**, **30** and **35** showed no inhibition towards the enzyme. Relative to tacrine compound **15** showed low inhibition, while compound **3**, **28** and **37** showed more than 5 times better affinity towards huBChE than tacrine. A graphic illustration of the relative affinity towards huBChE is depicted in appendix **??**. Most of the compounds tested for their huBChE inhibition did not show higher affinity than tacrine.

Elleman´s test of compound **7** and **39** was performed with BChE from respectively bovine and rat. The source for BChE used when testing compound 36 was not reported. From these three compound **7** showed the highest inhibition compared to tacrine.

In some of the publications, selective inhibiting of AChE is evaluated as more advantageous. The compound presented, by the publication, as the most promising AD treatment is included in this paper, while the others are neglected. This could lead to compounds showing great inhibition towards both AChE and BChE being neglected. The inhibitors showing highest selectivity towards AChE is compound **10**, **30** and **35**, having no affinity towards huBChE. Non of them are among the most potent AChE inhibitors.

The affinity towards eeAChE and eqBChE was tested on 16 of the compounds. Compound **5** and compound **24** showed higher affinity towards eqBChE than eeAChE. The molecules does not seem to have any evident similarity other than the tacrine moiety. Majority of the inhibitors tested on eeAChE and eqBChE has between two and five times better inhibition towards eeAChE (appendix C.3).

Seven of the compounds was tested on both AChE and BChE from human. The affinity of **11** towards huAChE and huBChE was almost identical, while **15**, **37** and **41** showed more than 50 times higher affinity towards huAChE. Regardless of the source of the enzyme the publication featuring compound **5** was the only one reporting tacrine to have higher affinity towards AChE than BChE.

Calibration mechanism, temperature change and environmental effects may effect the accuracy of an analytical balance.[73] In 16 of the publications tacrine´s IC_{50} on eeAChE and eqBChE was reported. The relationship between $IC_{50(eeAChE)}$ and $IC_{50(eqBChE)}$ ($IC_{50(eeAChE)}$ /$IC_{50(eqBChE)}$) is between 0.5 and 9 (C.5. Which means that some publications reports tacrine to have 9 times higher affinity towards BChE, while another reports it to have 50% better affinity towards AChE. Inaccuracy of the analytical balances could be the reason for the great difference in $IC_{50(eeAChE)}$ and $IC_{50(eqBChE)}$ correlation. Thus, it is possible that the difference between the compound having the highest affinity towards eeAChE and the compound having the second highest affinity is due to measurement errors.

2.3 Molecular modeling study

2.3.1 Results featured in the publications

Table 4 features the molecules from the publications were molecular modeling studies between the potential inhibitor and AChE was performed. Multiple of the compounds was also docked to BChE. BChE docking will not be discussed in this paper.

Docking of the ligand to tcAChE was featured in 14 of the publications. All reports tacrine to be oriented towards CAS due to aromatic π-π-stacking interactions with the phenyl ring of Phe 330 and the indole ring of Trp 84.[18–20,30–32,34,61,62,74–76] For some of the potential treatments a chlorine atom is bound to carbon six or seven of tetrahydro acridine (THA). The chlorine atom is reported to create hydrophobic interaction with Tyr334, Phe330, and Trp432.[31] Possibility of hydrogen bonding between the protonated

quinoline nitrogen atom of tacrine and the carbonyl oxygen of His440 is also mentioned in literature.[20,61,62]

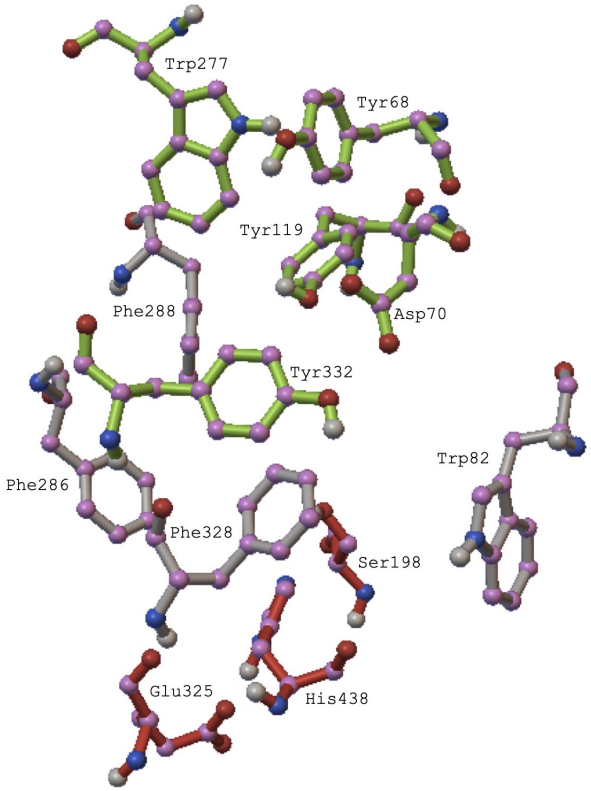

Figure 28. The aminoacids of tcAChE that are similar between species.

The moiety linked to tacrine is reported to interact with the indole ring of Trp 279 and Tyr70 of tcAChE PAS via π-π stacking interactions. H-bond interaction with Arg289 is also mentioned.[20]

10 of the publications featured docking of the ligand to huAChE. Tacrine was reported to form π-π-stacking interaction with the aromatic side chain of Trp86[21–23,38,77–80] and Tyr337.[21,22,38,77,78] Hydrogen bonding between the 1,2,3,4-tetrahydroacridin ring and Tyr337 and His447 was also reported.[21,38]

Tacrine´s opposing moiety was reported to bind to PAS of hAChE through π--stacking interaction associated with Trp286[21–23,38,77–80], Tyr72[38,77,78] and Tyr341[21,23]. The carbonyl

groups of compound **6** and compound **8** formed hydrogen-bond with respectively the the side chain of Tyr341 and the side chain of Phe295 and Arg296.[21,22]

The cumarin part of compound **11** was reported to bind to PAS through hydrogen-bond between the amide oxygen and Tyr124.[38] The tetrahydroacridin moiety of compound **9** was reported to form multiple π-π-stacking contacts with the same amino acid Tyr124, but this time reported as a part of CAS.[23] Illustration from publication 18, position the amino acid halfway down the gorge. In addition to the flexibility of the active site, this might be the reason why the residue was included in both PAS and CAS.

Docking of one of the nonhybride, compound **30**, was described in literature. Attempts to dock the compound to CAS failed while it was successfully docked to PAS. Thus the compound holds a position in which it prevents Aβ aggregation while being a non-competitive inhibitor of AChE. The reported interactions are: π--stacking interaction with Trp286 and hydrogen bonding between the NH group and the hydroxyl group of Tyr72.[81]

Table 4. Published molecular modeling results

No.	AChE	PDB entry	PAS interaction	Algorithm
1	tc	1ODC	✓	GOLD v. 5.1, ASP[a]
2	hu	4M0E	✓	Surflex
4	tc	2CKM	✓	AutoDock 4.2
5	tc	5EI5	✓	GLIDE 5.5
6	hu	4EY7	✓	CDOCKER
8	hu	4EY7	✓	CDOCKER
9	hu	4EY7	✓	CDOCKER
11	hu	1b41	✓	AutoDock 4.0
12	tc	2CKM	✓	MOE[b] 2008.10
13	tc	2CMF	✓	AutoDock 4.2
14	tc	1ODC	✓	GOLD v. 5.1, ASP

Table 4. Published molecular modeling results

No.	AChE	PDB entry	PAS interaction	Algorithm
15	hu	3LII	✓	rDock
16	hu	4EY	✓	MOE 2008.10
17	tc	1ODC	✓	GOLD v. 5.1, ASP
18	hu	4EY7	✓	MOE 2008.10
20*	hu	4EY7	✓	AutoDock 4.2
21	tc	1EVE	Not reported	MolDock
22	tc	2CKM	✓	MOE 2008.10
23	tc	2CKM	✓	MOE 2008.10
24	tc	2CMF	✓	CDOCKER
29	tc	1ACJ	✓	Autodock[c]
30[81]	hu	1ACJ	✓	rDock
39	unknown**		✓	Autodock[c]
42	tc	1VOT	Not reported	AMBER
44	tc	1ODC	✓	GOLD v. 5.1, ASP

[a]Astex Statistical Potential scoring function

[b]Molecular Operating Environment software

[c]Version not reported

*Docking of molecule 20 was performed but results from the same hybrid with one carbon longer linker is featured as a substitute.

**The source for AChE was not reported in the publication. From the numbering of the amino acids it seems to be tcAChE rather than huAChE.

2.3.2 1-click docking results

Figure 37 illustrates the docking position with the best docking score. More negative docking score indicate higher binding affinity.[59] According to autodock vina docking to tcAChE (PDB:1e3q), this is the position in which the pharmaceuticals are most likely to be oriented.

When comparing the docking results from litterature with the results presented in Appendix 37 there is one striking difference. All the reported dockings place tacrine at the catalytic anionic site while the 1-click docking results only does so in 22 of the cases. This is probably due to different approach when analyzing docking output; whether the docking score or the binding mode is emphasized.

Molecular docking gives multiple suggested binding poses and their calculated scores. The approach applied in the publications listed in table 4 is to emphasize earlier reported binding modes more than the programs docking score. The assumption is that tacrine will always bind to CAS. According to Crystal structure of AChE complexed with tacrine or tacrine hybrids, avilable at RCSB protein data bank,[82] this is likely to be true.[28,83–85] Still, it is possible that the opposing moiety have a higher attraction towards CAS than tacrine. Hydrocarbon-linked tacrine dimers co-crystallized with tcAChE, suggests that the tacrine moieties may bind to PAS through π-π-stacking interactions (Figure 6).[62] After all the main reported attractions at both PAS and CAS are π-π-stacking interactions. Thus, an aromatic moiety linked to tacrine would also have affinity towards CAS according to molecular modeling.

Neither the tacrine moiety, the THA moiety with a clorine atom at the 6th carbon or the huprine moiety is categorically oriented towards CAS. That is, when looking at the position having the highest docking score (Appendix 37).

Despite the similarity between AChE retrieved from different species, all the amino acids lining the active gorge are not identical. Another factor affecting the docking results are the ligand AChE was in complex with, when crystal structure was determined. The AChE crystal structure are sometimes picked based on the similarity between the ligand the enzyme is complexed with and the ligand used in the molecular modeling studies.[76] Docking programs use the position of the aminoacids from the given Crystal structure and allow rotation and displacement from that basis.[59] Thus the crystal structure of AChE in complex with a ligand widening the dynamic gorge of the enzyme, can give a different result than crystal structure of AChE in complex with a smaller ligand. Publication no. 44 legitimizes the use of tcAChE over huAChE because huAChE are complexed with smaller inhibitors.[76] TcAChE (PDB: 1e3q) used in this thesis is complexed with 4,4'-(3-Oxo-1,5-pentanediyl)bis(N-allyl-N,N-dimethylanilinium) dibromide. TcAChE (PDB: 5NUU) is complexed with chlorotacrine-tryptophan hybrid.[28] Using the latter AChE structure would maybe have affected the program to give the pose orienting tacrine towards CAS a higher docking score.

Compound **3** was the only molecule in which the position of the ligand in complex with ACh was determined by X-ray crystallography. The ligand is reported to bind to CAS through its 6-Cl-THA moiety. The chlorine atom exhibits a strong interaction with Trp432, and the publication underlines the increased affinity of the ligand due to this. The NH_2 moiety of the opposing unit engaged in a cation-π interaction with Trp279 and in a weak hydrogen bonding interaction with the OH of Tyr70.[28]

Since the binding mode rather than the docking score is emphasized, docking scores are rarely stated. If the docking program was perfect, the pose with the highest score would always be the most likely position in which the ligand would bind.

Docking programs can provide more than 100 compound-enzyme poses. Excluding the docking score could in some cases be the same as placing the compound manually at the

active site in the desired position. As earlier mentioned, crystal structures of AChE in complex with tacrine, places tacrine at CAS. Thus, figure 37, with almost half of the compounds oriented the opposite way, reveals the imperfection of the docking programs.

Based on the two articles; *Multifunctional iron-chelators with protective roles against neurodegenerative diseases*[86] and *Bifunctional phenolic-choline conjugates as anti-oxidants and acetylcholinesterase inhibitors*,[87] publication 14 and 17 state ASP scoring function as the one *"previously proved to give the best docking predictions for AChE inhibitors"*.[34,61] The former article states the latter as reference. "Bifunctional phenolic-choline conjugates as anti-oxidants and acetylcholinesterase inhibitors" features a comparison between the scoring functions GoldScore, ChemScore, and ASP. From these three, ASP gave the best result. These scoring functions might be implemented in some of the algorithms listed in table 4, but autodock uses its own scoring function, thus it could be as good as ASP.

The main purpose of the molecular modeling studies was to examine whether the ligands would bind to PAS in addition to CAS. Table 5 lists the higest possible scores with tacrine oriented towards CAS. If non of 1-click docking´s suggested poses placed tacrine at CAS, the score is listed as being lower than the least ideal pose suggested by the program. Compound which showed interaction with PAS is featured in figure 29.

Only a few suggested poses, the ones with the highest score, was provided by the docking program. A more expensive version of the program would have provided more possible poses.

Table 5. Docking score for the compounds when tacrine is positioned at CAS

No.	Docking score		PAS interaction
	Tacrine oriented towards CAS	Highest possible	
1*	-10.5	-10.5	X
2	-10.0	-10.5	X
3	$\leq$-10.3	-10.6	-

4	-10.5	-10.7	✓
5	-11.0	-11.0	✓
6	-10.7	-11.4	✓
7	-10.8	-10.8	X
8	≤-9.3	-9.4	-
9	-10.9	-11.5	✓
10	12.7	12.7	✓
11	≤-10.0	-10.5	-
12	-10.9	-11.6	✓
13	-10.2	-10.2	X
14	≤-10.9	-11.2	-
15	≤-9.3	-9.9	-
16	-10.4	-11.0	✓
17	≤-7.9	-8.4	-
18	≤-10.9	-12.3	-
19	-10.7	-10.7	X
20	-9.9	-9.9	✓
21	≤-10.1	-11	-
22	-11.8	-11.8	✓
23	-11.9	-11.9	✓
24	≤-7.8	-8.9	-
25	≤-10.8	-11.7	-
27	-10.5	-10.5	X
28	-12.8	-12.8	✓
29	-10.3	-10.3	✓
30	-9.1	-9.1	-[a]
31	≤-9.8	-10.4	-
33	-10.1	-10.1	X
34	-7.9	-7.9	X

35	-8.7	-8.7	-[a]
36	-9.9	-10.1	X[b]
37	≤-8.9	-10.5	-
38	only one possible pose	-8.8	-
39	-11.3	-11.3	✓
40	-10.0	-10.0	-[c]
41	-9.8	-9.8	-[c]
42	-9.8	-9.8	-[c]
43	-9.8	-9.8	-[c]
44	-10.7	-10.7	X
1a	-11.9	-12.2	✓
1b	-12.0	-11.3	✓
Tacrine	-8.1	-8.1	X

*The numbers colored green are the compounds were PAS interaction was reported, based on molecular modeling.

[a]An analogue of tacrine, not a tacrine hybrid. The pose where tacrine interacted with PAS was given the highest score by Autodock.

[b]Almost interaction with the aromatic ring of tryptophan. The angle between the ring planes is a bit off.

[c]An analogue of tacrine, not a tacrine hybrid. Autodock gives the pose were the analogue is stacked in the middle of the gorge the highest score. This pose enables Tacrine to form π-π stacking interactions with PAS (Tyr119).

Multiple of the compounds was reported to bind to PAS, based on molecular modeling, but did not show any interaction by the method used in this paper. Some of the reasons why molecular modelling may give various results have already been mentioned. In addition, interaction with the entrance and bottom of the gorge was only measured through the amino acids featured in figure 28/4. These are the amino acids of the catalytic gorge

which are similar between species. Most of the compounds probably have multiple interactions with both CAS and PAS of tcAChE, but if the amino acids they interact with are not present in huAChE the compound is useless as AD treatment.

Compound **21** and compound **42** are the only ligands were molecular docking was performed (table 4), and association with PAS not reported. 1-click-docking indicate interaction between **42** and PAS through Tyr119. No interaction between PAS and **21** was observed.

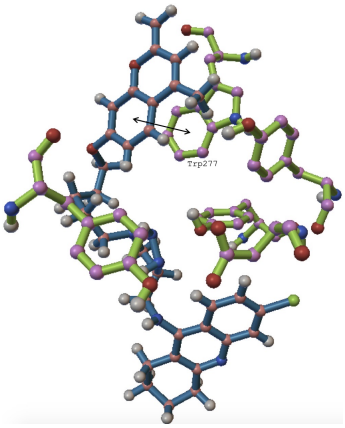

No. 4

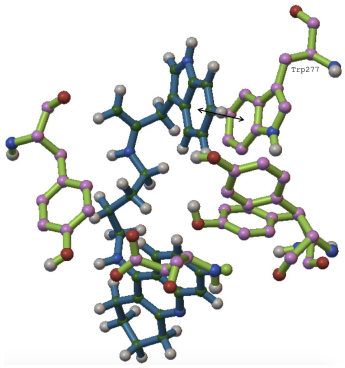

No. 5

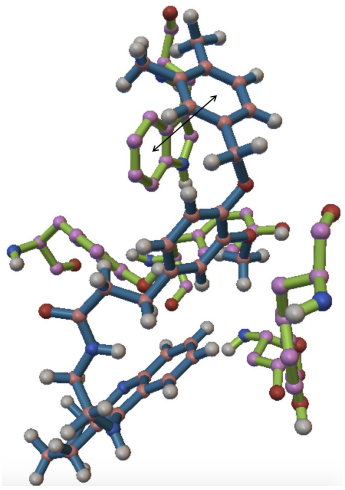

No. 6

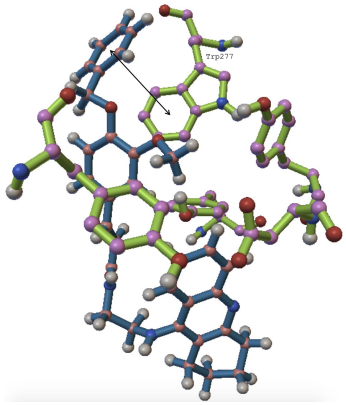

No. 9

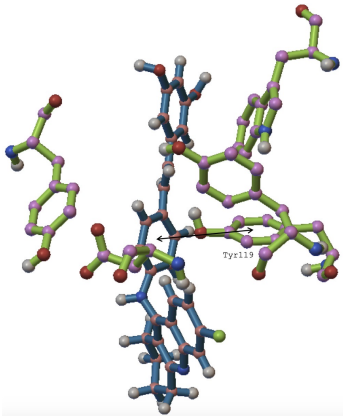

No. 10

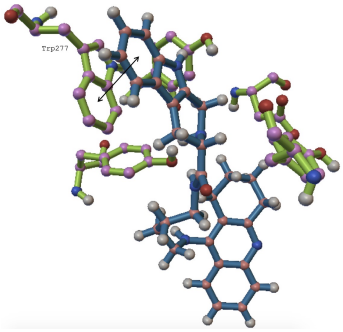

No. 12

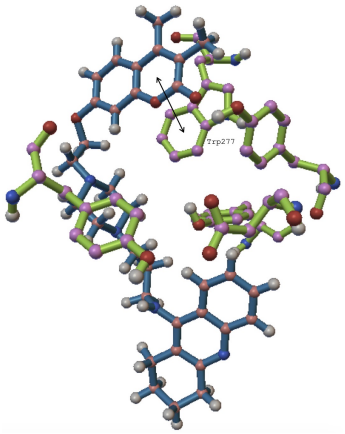

No. 16

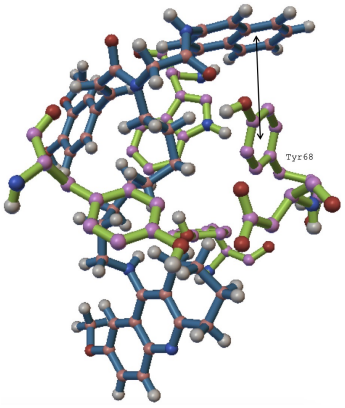

No. 20

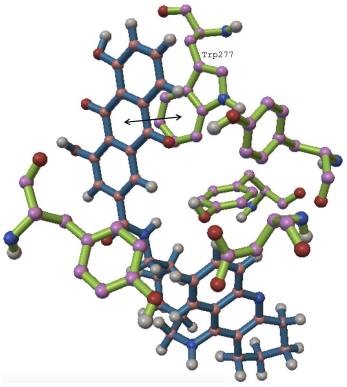

No. 22

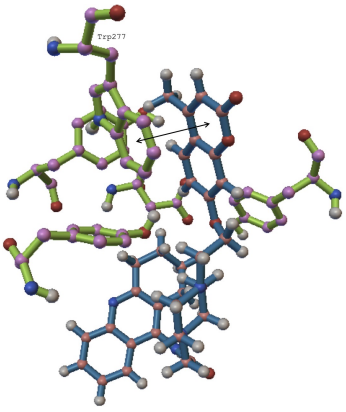

No. 23

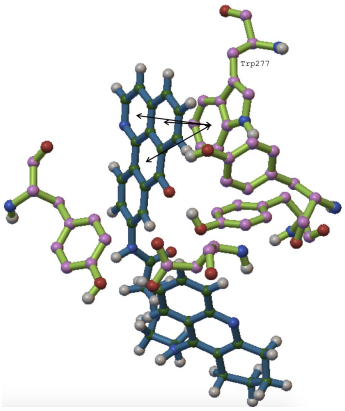

No. 28

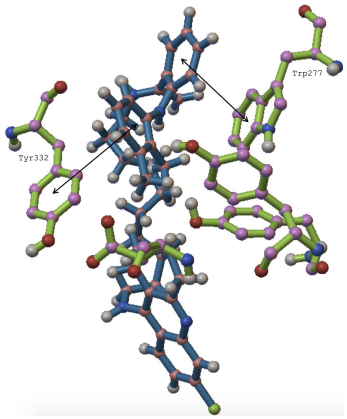

No. 29

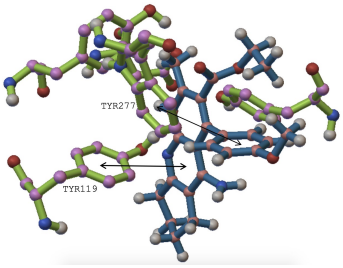

No. 30

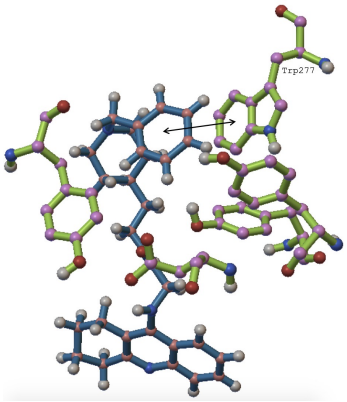

No. 39

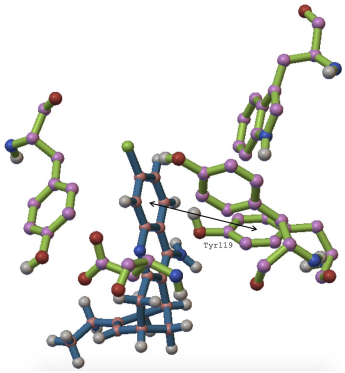

No. 40/41/42/43

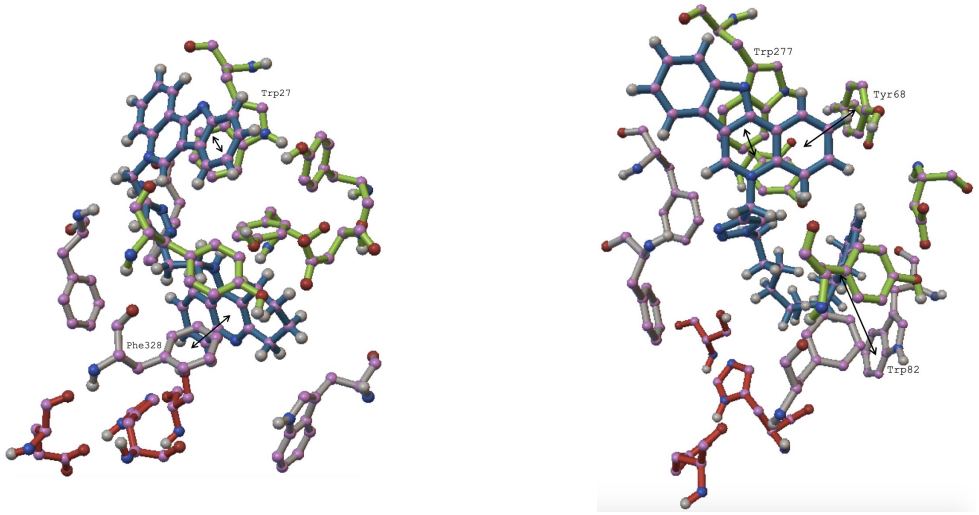

No. 1a **No. 1b**

Figure 29. The π-π-stacking interactions for compound **1a** and **1b** at both PAS (green) and CAS(grey and red) are marked. The other compounds from table 5 where π-π-stacking interactions with PAS was detected, are also featured.

When performing the molecular modeling of compound **33**, by accident, one extra carbon was added to the linker. The publication does not list the compound with 7 carbon linker as a potential inhibitor.[88] Because of the extra carbon atom, 1-click docking was unable to dock the ligand to tcAChE. If in fact the extended form of compound **33** is not compatible with tcAChE, the compound could be used as decoy ligand. A decoy molecule is a molecule designed to challenge the reliability of the docking algorithm. In that case, the incompatibility would give confidence to the program´s binding mode predictions.[89]

Autodock vina might be the best algorithm for molecular docking to AChE, but there could also be a more correct one. Also there might be a more fitting AChE crystal structure. Despite these limitations, the molecular modeling studies provided are usefull for visualizing the mode of action for the potential AD treatments. In correlation with other

methods of analysis, it can substantiate the claim of the ligands binding to PAS.

2.4 In vitro inhibition of Aβ aggregation

The purpose of comparing the compounds effect on Aβ aggregation was to ascribe one more factor substantiating the compounds ability to bind to PAS. Unfortunatly most of the publications only feature studies on self-induced Aβ aggregation, not AChE-induced Aβ aggregation. Regardless, the findings are included because the ability to prevent self-induced Aβ aggregation increases its potential as AD treatment.

2.4.1 Self-induced Aβ aggregation

Of the compounds tested with tacrine as reference **3**, **7** and **20** exhibited the strongest inhibition (Table 7). Five compounds were tested using Curcumin as referance. Of the five, compound **12**, **23** and **28** showed the best ability to inhibit self-induced Aβ aggregation (Table 8). Compound **6**, **8** and **10** were tested relative to resveratrol, revealing compound **6** to be the better inhibitor (Table 9). Publication no. 19 features the inhibition compared to congo red. Congo red inhibited 93% of the self-induced Aβ aggregation, while compound **19** inhibited 53%.

Table 7. Self-induced Aβ aggregation relative to tacrine

No.	Inhibitor	Tacrine	Relative to tacrine
1	57.8%	20.0 %	2.9
3	58.6%	<5%	>11.7
7	77.2%	<7%	>11.0
10	31.2%	<5%	>6.2
15	36.4%	<5%	>7.3
17	10.9%	<5%	>2.2
17	10.9%	<5%	>2.2
20	65.6%	<5%	>13.1

44	51%	20%	2.6

Table 8. Self-induced Aβ aggregation relative to curcumin

No.	Inhibitor	Curcumin	Relative to curcumin
9	42.2%	46.2 %	0.9
11	5%	50%	0.1
12	65.8%	42.3%	1.6
23	67.8%	42.4%	1.6
28	79.8%	41.8%	1.9

Table 9. Self-induced Aβ aggregation relative to resveratrol

No.	Inhibitor	Resveratrol	Relative to resveratrol
6	65.49%	45.72%	1.43
8	31.82%	30.36%	1.05
10	31.2%	30.0%	1.04

Both curcumin and resveratrol are considered possible anti-AD compounds due to their ability to prevent the aggregation of Aβ.[90]

2.4.2 AChE-induced Aβ aggregation

Table 10 features the three compounds tested for their ability to inhibit AChE-induced Aβ aggregation. Compound **3** and **28** proved to do so, while compound **22** did not perform better than tacrine. Does this prove that compound **3** and compound **28** bind to PAS? AChE promotes the conformational change in the Aβ monomer. This conformational

change happens regardless of AChE, but at a slower rate. Testing Aβ aggregation in the presence AChE does not necessarily mean that the inhibitor is preventing Aβ aggregation by blocking PAS. The inhibitor could act by preventing self-induced Aβ aggregation.

Compound **3**´s inhibition on self-induced Aβ aggregation was 58.6%, which in fact was higher than the AChE-induced Aβ aggregation inhibition (48.3%). The reason for this is differences in concentration and incubation time. The Aβ/inhibitor ration when testing self-induced Aβ aggregation was 1/1. When testing AChE-induced Aβ aggregation the Aβ/inhibitor ratio was 100/1. Incubation time was 24 hours[.6] The percentage of inhibition on self-induced Aβ aggregation and AChE-induced Aβ aggregation under the same analyzing condition would clarify whether the inhibitor prevents aggregation by blocking PAS.

The concentration of compound **8** used when analyzing AChE-induced Aβ aggregation is not mentioned in the experimental section. Remark below the table indicate that a concentration of 100 µM was used [7]. If so the Aβ/inhibitor ratio is approximately 1/4. The Aβ/inhibitor ratio when testing **28**´s inhibition of self-induced Aβ aggregation was 5/1. Incubation time was respectively 8 and 48 hours. Publication 28 maps the correlation between high affinity towards AChE and strong inhibition of AChE-induced Aβ aggregation. The correlation proves that the inhibitor of Aβ aggregation is achieved by inhibition of AChE.

Table 10. AChE-induced Aβ aggregation relative to tacrine

No.	Inhibitor (%)	Tacrine (%)	Relative to tacrine	
3	48.3 ± 6.3	8.1 ± 2.1	6.0	h[a]
22	6.5 ± 0.8	6.5 ± 0.8	1.0	ee[b]
28	83.3±1.2	4.5±0.7	18.5	ee

[6]Incubation temperature for AChE-induced Aβ aggregation was reported to be 30°C. Incubating temperature for self-induced Aβ aggregation was not reported.

[7]"The data (%) showed that the test compounds inhibited the co-aggregation at 100 mM." [91]

[a] Human, [b] Eletric eel

3 Experimental section

When searching for "acetylcholinesterase inhibitor tacrine hybrids alzheimer" (18.02.20) in Scifinder database, 52 references are found. Seven of the articles were listed twice, giving 45 exclusive articles. One publication featured available AD treatments (no. 26) but did not list any new tacrine hybrides. The remaning 44 articles listed potential new AChE inhibitors and the biological evaluation of the given compounds. The compound presented as the most promising Alzheimers treatment candidate from each reference were compared. If more than one compound was featured, the one with highest affinity towards AChE, according to the Ellman´s method, was chosen. The publications and their most potent inhibitor are listed from 1 to 45 (Appendix A) by their accession number. The molecules will be referred to as the number of the article. Publication 30, 32 and 45 list the same molecule as the most potent inhibitor, this molecule will be referred to as **30**. Molecules which is part of the synthesis section are numbered from **1´** to **17´**, and the target molecules are named **1a** and **1b**.

Seven of the publications do not feature a tacrine hybrid as the most potent inhibitor.[78,92–97] For some tacrine is replaced by huprine, some are not hybrids and some are neither. Regardless, they are acetylcholinesterase inhibitor and potential AD treatments. Thus, evaluation of their potency compared to the tacrine hybrid is relevant.

3.1 In vitro inhibition of AChE and BChE

The potential Alzheimer's Disease treatments from 43 of the 44 publications were evaluated using the Ellman´s method. The different sources for AChE were eletric eel, human, bovine, torpedo californica, rat and mouse. Sources for BChE were equine, human, bovine, rat. To compare the inhibition of AChE and BChE from the different sourses, the Tacrine

hybrids inhibition relative to the refference, Tacrine, was calculated. If the tacrine hybrid was tested on both human and animal AChE, the test giving the higest inhibition compared to Tacrine was selected.

To eliminate individual analyzing conditions, the ligands inhibition analyzed by Ellman´s method are evaluated compared to inhibition by tacrine.

3.2 Virtual docking

The online docking was performed using the online software, 1-click Docking, provided by Mcule. The software is equipped with autodock vina scoring function.[59]

Before deciding on using 1-click Docking, DockThor and SwissDock were tested. Using these programs requires the PDB file to be downloaded and modified. Modifications involving removal of the ligand present in the X-ray crystal structure were conducted using PyMOL. In contrast, the 1-click Docking database contain PDB files prepared for docking. When using DockThor and SwissDock, the location of the catalytic is manually marked. While the catalytic groove is pre-marked in the protein files of The 1-click Docking. Since multiple TcAChE files were available in their database 1-click Docking proved to be the most efficient software. The X-ray crystal structure of (TcAChE), with the PDB ID: 1e3q, was used.[98]

There are some limitations to the versions of 1-click Docking used in this paper. Docking output only provides a few possible poses. Nevertheless, these are the poses the program ranks as the most likely.

The amino acid sequence of 1e3q present in the 1-click Docking database is numbered from 1 to 533.[98] Amino acids lining the catalytic grove mentioned in literature[83,98–106] do not always have the same numbering. The numbers of these amino acids were modified by comparing the sequences of the X-ray crystal structure files with the amino acid sequence

of 1e3q from the 1-click Docking database.

The 1-click Docking output files were modified using MGL Autodock tools. Most of the amino acids were removed, leaving only the residues lining the catalytic gorge that are similar between organisms. The interactions with binding pocket residues at PAS and CAS were visually inspected in comparison to reported dockings. MGL measuring tools were used to measure the distances and angles between the ligands and the residues at PAS.[107]

3.3 Chemistry

3.3.1 General

Solvents and reagents

All chemicals were obtained from Merck, VWR or Sigma Aldrich. No further purification was done.

Spectroscopic and spectrometric analysis

Nuclear magnetic resonance (NMR) spectra were recorded on a Bruker AscendTM 400 series, operating at 400 MHz for ^{1}H and 100 MHz for ^{1}3C. The chemical shifts (δ) are expressed in ppm. The spectra are calibrated relative to chloroform-d (^{1}H: 7.26 ppm, ^{1}3C: 77.16 ppm) and methanol-d_4 (^{1}H: 3.31 ppm, ^{1}3C: 49.00 ppm). Coupling constants (J) are given in Hertz (Hz) and the multiplicity is reported as: singlet (s), broad singlet (br s) doublet (d), double doublets (dd), double triplets (dt), double quartets (dq), triplet (t), double triplets (dt) and multiplet (m). Conformation of compounds was was assisted by two dimensional NMR spectra (COSY, HSQC, HMBC and NOSEY) in addition to ^{1}H and ^{1}3C NMR.

Infrared (IR) spectra were recorded on an Agilent Cary 630 FTIR spectrophotometer. Samples were analyzed by placing the sample directly onto the crystal of an attenuated

total reflectance module.

Melting points were determined on a Stuart melting point apparatus (SMP20).

Chromatography

Flash chromatography was carried out with silica gel (particle size 40-60 µm), with solvent gradients as indicated in the experimental procedures. Thin-layer chromatography (TLC) was carried out using aluminum backed 0.2 mm thick silica gel plates from Merck (type: 60 F_{254}). Ultraviolet light was used to detect the spots (excitation at $\lambda = 254$ nm).

3.3.2 Methods

9-chloro-1,2,3,4-tetrahydroacridine 10‘

Compound **10‘** was obtained by partly following a reported procedure.[12] A solution Cyclohexanone **8‘** (3.60 ml, 35.0 mmol) and 2-aminobenzoic acid **9‘** at 0 ^{o}C under an N_2-atmosphere was added slowly $POCl_3$ (10.0 ml, 292 mmol). After addition, the mixture was kept stirring at reflux for 12 h. After this time, the mixture was cooled down to 0 ^{o}C and neutralized upon the slow addition of aqueous saturated Na_2CO_3. The aqueous layer was extracted with Et_2O (3x15 ml). The combined organic fractions were dried over $MgSO_4$, filtered and concentrated under reduced pressure to give a crude product, which was purified by recrystallization from acetone to afford compound **10‘** (4.17g, 66%) as a light brown solid. Melting point: 75-77 ^{o}C. R_f: 0.44 (19/1 DCM/MeOH). ^{1}H-NMR (400 MHz, CDCl3) δ_H: 8.16 (d, 8.3 Hz, 1H), 7.97 (d, 8.5 Hz, 1H), 7.66 (t, 6.9 Hz, 1H), 7.53 (t, 7.2 Hz, 1H), 3.12 (t, 6.0 Hz, 2H), 3.01 (t, $J = 5.6$ Hz, 2H), 1.94 (m, 4H). ^{13}C-NMR (100 MHz, $CDCl_3$) δ_C: 159.64, 146.82, 141.56, 129.37, 128.99, 128.77, 126.60, 125.52, 123.81, 34.34, 27.64, 22.80, 22.76.

2-((1,2,3,4-tetrahydroacridin-9-yl)amino)ethan-1-ol 11‘

Compound **11‘** was obtained by partly following a reported procedure.[12] A solution of 9-

chloro-1,2,3,4-tetrahydroacridine **10'** (2.00 g, 9.19 mmol) in butanol (10.0 ml) was added 2-aminoethanol (1.65 ml, 27.6 mmol). The mixture was refluxed for 18 h, cooled to room temperature and diluted in EtOAc.[8] Brine and DCM were added to the mixture and the aqueous layer was extracted with DCM (x4). The combined organic fractions were concentrated under reduced pressure. The residue was purified by silica gel column chromatography (9/1 DCM/MeOH, 8.5/1.5/0.01 DCM/MeOH/NH_4OH) to afford compound **11'** (1.66 g, 75%) as a pale yellow solid. Melting point: 173-178 ^{o}C. R_f: 0.34 (17/3/ DCM/MeOH, NH_4OH 1 drop/ml). ^{1}H-NMR (400 MHz, CDCl3) δ_H: 7.98 (d, 8.7 Hz, 1H), 7.91 (d, 8.4 Hz, 1H), 7.55 (dq, 1.3 Hz 6.9 Hz, 1H), 7.35 (dq, 1.1 Hz 6.8 Hz, 1H), 4.56 (s, 1H), 3.82 (t, 5.0 Hz, 2H), 3.61(br s, 2H), 3.06 (t, 6.2 Hz, 2H), 2.77 (t, 6.2 Hz, 2H), 1.90 (m, 5H). ^{1}3C-NMR (100 MHz, CDCl3) δ_C: 158.70, 150.74, 147.35, 128.70, 128.56, 124.10, 122.87, 120.75, 117.46, 62.26, 51.08, 34.05, 24.81, 23.12, 22.89.

N-(2-azidoethyl)-1,2,3,4-tetrahydroacridin-9-amine 13'

Compound **13'** was obtained by partly following a reported procedure.[12] A solution of 2-((1,2,3,4-tetrahydroacridin-9-yl)amino)ethan-1-ol **11'** (1.56 g, 6.44 mmol) in $SOCl_2$ (9.88 ml, 136 mmol) was refluxed for 45 min. The mixture was basified with 1 M aqueous NaOH before extracted with EtOAc (x2). The organic phase was washed with brine, dried over $MgSO_4$ and concentrated under reduced pressure. The concentrate was dissolved in DMF (20 ml) and added NaN_3 (1.66 g, 25.6 mmol). The mixture was heated at 80 ^{o}C for 24 h. After cooling the mixture to room temperature, 200 ml water was added followed by extraction with EtOAc (x2). The combined organic fractions were concentrated under reduced pressure. The residue was purified by silica gel column chromatography (19.5/0.5 DCM/MeOH 19/1 DCM/MeOH) to afford compound **13'** (1.42 g, 82%) as a dark brown oil. NMR showed remnants of DMF in the product (1/0.25) which reduces the yield to 77%. Rf: 0.46 (17/3/0.02 DCM/MeOH/NH4OH). ^{1}H-NMR (400 MHz, CDCl3) δ_H: 7.92 (m, 2H), 7.57 (dq, 1.3 Hz 6.8 Hz, 1H), 7.38 (dq, 1.2 Hz 6.8 Hz, 1H), 4.23 (t, 5.8 Hz,

[8]When EtOAc was added to the reaction mixture precipitation happened. NMR of the precipitate showed impurities.

1H), 3.58 (m, 2H), 3.50 (m, 2H), 3.08 (t, 6.4 Hz, 2H), 2.78 (t, 6.4 Hz, 2H), 1.93 (m, 4H). ^{1}3C-NMR (100 MHz, $CDCl_3$) δ_C: 159.02, 149.54, 147.50, 129.10, 128.59, 124.45, 122.44, 120.97, 118.32, 52.26, 47.96, 34.19, 24.89, 23.12, 22.91.

2-(quinolin-3-yl)aniline 4'

A solution of 3-bromoquinoline (0.330 ml, 2.43 mmol), 2-aminoboronic acid hydrochloride (500 mg, 2.92 mmol) and 10 ml ethanol was mixed with K_2CO_3 (1.01, 7.29 mmol), $PdCl_2$(dppf)xDCM (99.6 mg, 0.122 mmol) and dH_2O (2.00 ml). The mixture was heated at 60 ^{o}C under inert atmosphere for 22 h and concentrated under reduced pressure. The residue was purified by silica gel column chromatography (95/5 and 45/55 PE/EtOAc). The fractions were concentrated under reduced pressure to give **4'** (0.447g, 84%) as a dark brown solid. Melting point: 130-132 ^{o}C. R_f: (7/3 PE/EtOAc). ^{1}H-NMR (400 MHz, $CDCl_3$) δ_H: 9.03 (d, 2.3 Hz, 1H), 8.26 (d, 1.8, 1H), 8.15 (d, 8.5 Hz, 1H), 7.85 (dd, 1.3 Hz 8.2 Hz, 1H), 7.74 (dq, 1.5 Hz 6.9 Hz, 1H), 7.59 (dq, 1.1 Hz, 6.9 Hz, 1H), 7.23 (m, 2H), 6.90 (dt, 1.1 Hz 7.4 Hz, 1H), 6.84 (dd, 0.8 Hz, 8.0 Hz, 1H), 3.75 (br s, 2H). ^{13}C-NMR (100 MHz, $CDCl_3$) δ_C: 151.65, 147.28, 144.13, 135.60, 132.59, 130.98, 129.67, 129.57, 129.40, 128.08, 127.96, 127.15, 123.89, 119.22, 116.11.

5H-indolo[3,2-c]quinoline 6'

2-(quinolin-3-yl)aniline **4'** (423 mg, 1.92 mmol) was dissolved in 37% HCl (13.0 ml) and cooled to 0 ^{o}C. Ice cold $NaNO_2$ (358 mg, 5.18 mmol) was added dropwise and the solution was stirred for 1 h at 0 ^{o}C. Into the mixture, ice cold NaN_3 (262 mg, 4.03 mmol) in NaOAc (20.0 ml, 26.89 mmol) was added dropwise, followed by stirring the solution for 1 h at 0 ^{o}C. The reaction was quenched by dropwise adding aqueous $NaCO_3$ (30 ml). The aqueous layer was extracted with EtOAc (5x30ml). The combined organic fractions were dried with $MgSO_4$, filtered and concentrated under reduced pressure to give **5'** without further purifications. 1,2-dichlorobenzene (13.0 ml, 0.115 mmol) was added to **5'** and the mixture was stirred at 180 ^{o}C, under inert atmosphere, for 3 h. Unreacted 1,2-dichlorobenzene was removed under reduced pressure. The residue was purified by silica gel column chro-

matography (7/3 and 3/7 PE/EtOAc)[9] to afford **6'** (361mg, 86%) as a light brown solid. Decomposes at temperature above 340 ^{o}C. Rf: 0.56 (7/1 DCM/MeOH). 1H-NMR (400 MHz, CDCl3) δ_H: 13.53 (s, 1H), 10.41 (s, 1H), 9.33 (dd, 8.0 Hz, 1,5 Hz, 1H), 9.13 (d, 7.8 Hz, 1H), 8.95 (d, 8.1 Hz, 1H), 8.54 (m, 3H), 8.31 (t, 7.6 Hz, 1H), 8.16 (t, 7.5 Hz, 1H).

5-(prop-2-yn-1-yl)-5H-indolo[3,2-c]quinoline 7'

5H-indolo[3,2-c]quinoline **6'** (50.0 mg, 0.229 mmol), propargyl bromide 80% in toluene (0.254 ml, 2.29 mmol) and toluene (1.7 ml) were added to a vacuum tube. The solution was stirred at 130 ^{o}C for 4 h. Propargyl bromide was removed under reduced pressure. DCM (10 ml) and saturated $NaCO_3$ (10 ml) were added and the solution was stirred for 30 min, extracted with DCM (2x10 ml) and concentrated under reduced pressure. No further purification was done. 1H-NMR (400 MHz, CDCl3) δ_H: 8.84 (d, 7.8 Hz, 1H), 8.25 (s, 1H), 7.98 (d, 8.0 Hz, 1H), 7.85 (d, 7.7 Hz, 1H), 7.63 (m, 2H), 7.53 (m, 2H), 4.95 (s, 2H), 2.55 (t, 2.5 Hz, 1H). 13C-NMR (100 MHz, CDCl3) δ_C: 154.83, 153.76, 134.34, 133.83, 129.46, 126.76, 125.34, 125.29, 125.11, 121.21, 120.96, 119.26, 119.05, 117.77, 116.05, 76.95, 75.83, 44.11.

N-(4-((5H-indolo[3,2-c]quinolin-5-yl)methyl)-1H-1,2,3-triazol-1-yl)-1,2,3,4-tetrahydroacridin-9-amine (1a)

A mixture of 5-(prop-2-yn-1-yl)-5H-indolo[3,2-c]quinoline **7'** (59.0 mg, 0.229 mmol), N-(2-azidoethyl)-1,2,3,4-tetrahydroacridin-9-amine **13'** (55.0 mg, 0.206 mmol), CuSO4x5H2O (17.0 mg, 0.0686 mmol), (+)-Sodium L-ascorbate (27.0 mg, 0.137 mmol) and DMF (1.35 ml) were stirred at room temperature for 24 h. DMF was removed under reduced pressure. Water (10 ml) and DCM (10 ml) were added to the crude before extracting the aqueous layer with DCM (3x3 ml).[10] The combined organic fractions were concentrated under reduced pressure. To take away any remains of water, toluene was added and removed under reduced pressure (x2). The residue was purified by silica gel column chromatography (19/1/0.4 and 18/2/0.4 DCM/MeOH/Et_3N) to give **1a'** as a pale yellow solid. Decom-

[9] This is probably not the best eluent, as it took many hours to get the product out of the column.

[10] The mud layer between the organic and aqueous layer was included in the organic phase.

poses at temperature above 200 ^{o}C. Rf: 0.19 (18/2/0.4 DCM/MeOH/Et3N). ^{1}H-NMR (400 MHz, CDCl3) δ_H: 10.22 (s, 1H), 8.70 (dd, 7.8 Hz, 1.51 Hz, 1H), 8.58 (d, 8.7 Hz, 1H), 8.52 (s, 1H), 8.35 (d, 8.0 Hz, 1H), 7.98 (m, 2H), 7.84 (d, 8.0 HZ, 1H), 7.70 (t, 7.7 Hz, 1H), 7.55 (m, 3H), 7.43 (t, 7.7 Hz, 1H), 7.10 (dt, 7.0 Hz, 1.3 Hz, 1H), 6.26 (s, 2H), 4.91 (2H[11]) 4.35 (t, 5.5 Hz, 2H), 2.82 (br s, 2H), 2.54 (br s, 2H), 1.76 (m, 4H).

1,2,3,4-tetrahydroacridin-9-amine 15'

Compound **15'** was obtained by following a reported procedure.[47] To a solution of Cyclohexanone **8'** (4.91 ml, 47.4 mmol), 2-aminobenzonitrile **14'** (5.00 g, 42.3 mmol) in sodium-dried toluene (110 ml) boron trifluoride etherate (6.22 ml, 50.4 mmol) was added dropwise. The mixture was refluxed for 24 h under argon atmosphere, cooled to room temperature. Toluene was removed by decantation. NaOH (120 ml, 2M) was added to the precipitate and the mixture was heated at reflux for 24 h, cooled and extracted with $CHCl_3$ (x3). The combined organic layers were dried with $MgSO_4$ and concentrated under reduced pressure to give compound **15'** (7.76 g, 93%) as a pale yellow solid. Melting point: 176 - 179 ^{o}C. R_f: 0.23 (195/5/2 DCM/MeOH/Et_3N). ^{1}H-NMR (400 MHz, CDCl3) δ_H: 7.89 (d, 8.6 Hz, 1H), 7.68 (d, 8.3 Hz, 1H), 7.56 (t, 7.0 Hz, 1H), 7.35 (t, 7.2 Hz, 1H), 4.64 (s, 2H), 3.02 (t, 6.2 Hz, 1H), 2.61 (t, 6.1 Hz, 1H), 1.93 (m, 4H). ^{13}C-NMR (100 MHz, $CDCl_3$) δ_C: 158.59, 146.59, 146.25, 128.90, 128.37, 123.81, 119.51, 117.13, 110.40, 34.14, 23.73, 22.85, 22.76.

N-(6-bromohexyl)-1,2,3,4-tetrahydroacridin-9-amine 16'

To a solution of 1,2,3,4-tetrahydroacridin-9-amine **15'** (1 g, 5.05 mmol) in DMSO (10 ml), NaOH (0.606 g, 15.1 mmol) was added and the mixture was stirred for 1 h. 1,6-dibromohexane was added and the mixture was stirred for 48 h. The aqueous layer was extracted with DCM (3x50 ml). The combined organic layers were extracted with brine (5x20 ml) to remove DMSO, dried with $MgSO_4$ and concentrated under reduced pres-

[11] These protons are hidden behind the water peak. The shift are derived from ^{1}H-^{1}H correlation spectrum.

sure. The residue was purified by silica gel column chromatography (9/1 DCM/MeOH, 9/1/0.2 DCM/MeOH/Et_3N) to afford compound 4 (0.847 g, 46%) as an orange oil. R_f: 0.70 (9/1/0.2 DCM/MeOH/Et3N). ^{1}H-NMR (400 MHz, $CDCl_3$) δ_H: 7.92 (t, 9.1 Hz, 2H), 7.53 (t, 7.5 Hz, 1H), 7.32 (t, 7.5 Hz, 1H), 3.99 (br s, 1H), 3.46 (m, 2H), 3.36 (t, 6.5 Hz, 2H), 3.05 (s, 2H), 2.68 (s, 2H), 1.89 (s, 4H), 1.82 (m, 2H), 1.65 (m, 2H), 1.41 (m, 4H). ^{1}3C-NMR (100 MHz, CDCl3) δ_C: 158.14, 150.69, 147.09, 128.39, 128.27, 123.57, 122.70, 120.03, 115.77, 49.16, 33.77, 33.56, 32.42, 31.45, 27.74, 25.97, 24.67, 22.90, 22.62.

N-(6-azidohexyl)-1,2,3,4-tetrahydroacridin-9-amine 17'

To a solution of N-(6-bromohexyl)-1,2,3,4-tetrahydroacridin-9-amine **16'** (0.843 g, 2.34 mmol) in DMF (10 ml), NaN_3 (0.610 g, 9.38 mmol) was added. The mixture was stirred at reflux (80 ^{o}C) for 24 h, under Argon atmosphere and cooled to R.T. Water (10 ml) was added and aqueous layer was extracted with EtOAc (x2). The combined organic fractions were dried with $MgSO_4$, filtrated and concentrated under reduced pressure. The residue was purified by silica gel column chromatography (19/1, 17/3 DCM/MeOH) to afford compound **17'** (0.56 g, 74%) as a dark brown oil. R_f: 0.36 (9/1/0.2 DCM/MeOH/Et_3N). ^{1}H-NMR (400 MHz, CDCl3) δ_H: 7.95 (d, 8.8 Hz, 2H), 7.55 (dq, 1.2 Hz 6.8 Hz, 1H), 7.34 (dq, 1.1 Hz 6.9 Hz, 1H), 3.50 (m, 2H), 3.25 (t, 7.0 Hz, 2H), 3.07 (m, 2H), 2.69 (m, 2H), 1.91 (m, 4H), 1.68 (m, 2H), 1.58 (m, 2H), 1.41 (m, 4H). ^{1}3C-NMR (100 MHz, CDCl3) δ_C: 157.95, 150.93, 146.82, 128.51, 128.20, 123.71, 122.79, 119.91, 115.62, 51.24, 49.23, 33.61, 31.55, 28.68, 26.45 (2C), 24.68, 22.92, 22.59.

N-(6-(4-((5H-indolo[3,2-c]quinolin-5-yl)methyl)-1H-1,2,3-triazol-1-yl)hexyl)-1,2,3,4-tetrahydroacridin-9-amine (1b)

A mixture of 5-(prop-2-yn-1-yl)-5H-indolo[3,2-c]quinoline **7'** (164 mg, 0.639 mmol), N-(6-azidohexyl)-1,2,3,4-tetrahydroacridin-9-amine **17'** (207 mg, 0.639 mmol), CuSO4x5H2O (47.9 mg, 0.192 mmol), (+)-Sodium L-ascorbate (75.9 mg, 0.383 mmol) and DMF (3.50 ml) was stirred at room temperature, covered with aluminum foil, for 24 h. DMF was removed under reduced pressure. The residue was purified by silica gel column chromatog-

raphy (87/13/1.5 DCM/MeOH/Et_3N) to give **1b‘** as a brown solid. Rf: 0.26 (15/5/0.5 DCM/MeOH/Et3N).^{1}H-NMR (400 MHz, CDCl3) δ_H: 9.36 (s, 1H), 8.63 (d, 7.8 Hz,1H), 8.46 (s, 1H), 8.26 (d, 8.9 Hz, 1H), 7.79 (d, 7.8 Hz, 1H), 7.75 (d, 7.8 Hz, 1H), 7.63 (m, 2H), 7.34 (m, 2H), 7.22 (-, 1H) 7.09 (t, 7.7 Hz, 1H), 6.84 (t, 7.3 Hz, 1H), 6.76 (t, 7.3 Hz, 1H), 5.92 (s, 2H), 4.30 (t, 6.7 Hz, 1H), 4.02 (s, 1H), 3.26 (br s, 2H), 2.90 (br s, 2H), 2.44 (br s, 2H), 1.86 (m, 2H), 1.73 (br s, 4H), 1.45 (m, 2H), 1.26 (m, 4H). ^{1}3C-NMR (100 MHz, CDCl3) δ_C: 157.55, 151.09, 146.21, 141.26, 139.38, 135.01, 131.36, 128.75, 127.57, 127.12, 126.85, 125.99, 125.07, 123.82, 122.99, 122.50, 122.35, 120.30, 119.58, 118.00, 115.34, 115.18, 114.83, 51.15, 50.62, 48.93, 33.39, 31.39, 30.06, 26.30, 26.25, 24.74, 22.94, 22.55.

4 Concluding remarks

4.0.1 Synthesis of compound 1a´ and 1b´

The two Isocryptole-tacrine heterodimers (**1a** and **1b**) commenced from azides-alkyne click-chemistry reaction between propagylated isocryptolepine precursor and azidated tacrine.

The isocryptolepine precursor was gained in three steps starting with Suzuki-Miyaura cross-coupling reaction between 3-bromoquinoline and 2-aminoboronic acid hydrochloride. Followed by a diazotization reaction to provide aryl azide which collapsed into isocryptolepine precursor. The overall yield was 72%.

Over four steps, the tacrine with a two-alkyne linker was obtained. Reaction between anthranilic acid and cyclohexanone was followed by a nucleophilic substitution-chlorination-azidation reaction sequence to generate the azide linker. The overall yield was 38%.

Tacrine was synthesised by reaction between ketone and in the presence of a Lewis acid. It was armed with a N-(6-azido)hexyl group by a substitution-bromination-azidation sequence, to give the six-linker tacrine with the azide group in three steps. The overall yield

was 32%.

H-NMR strongly indicate the succsessfull formation of the two Isocryptole-tacrine heterodimers (**1a** and **1b**).

4.0.2 Evaluation of published tacrine-hybrids

The compounds have been evaluated for their ability to bind to PAS, affinity towards AChE and BChE and their ability to prevent self-induced Aβ aggregation.

Compound **7**, **8**, **12**, **28** and **37** showed high affinity towards AChE and BChE compared to the other inhibitors tested on enzymes from the same species. Based on molecular modeling compound **8** and **12** were reported to bind to PAS. In addition to have high affinity towards AChE and BChE, compound **7**, **12** and **28** also proved to be among the ones having the greatest inhibition of self-induced Aβ aggregation. Molecular modeling revealed both **12** and **28** to interact with PAS through π-π-stacking interactions. The ability of compound **28** to bind to PAS was further substantiated by the inhibition of AChE-induced Aβ.

Among the ones with high ability to prevent self-induced Aβ, interaction with PAS through π-π-stacking by **6**, **20** and **23** was observed. Reported molecular modeling results substantiate interaction with PAS.

Molecular modeling revealed **1a**, **1b**, **5**, **29**, **39** and **41** to interact with PAS through π-π-stacking interactions. In addition **29** and **41** were among the ones showing highest affinity towards AChE. **5** and **39** were among the ones showing highest affinity towards BChE. Molecular modeling results from the publications report compound **5**, **29** and **39** to interact with PAS.

Compound **3** was also among the ones having high affinity towards BChE. The potential treatment was also among the ones with high ability to prevent self-induced Aβ aggregation. The ability to prevent AChE-induced Aβ aggregation indicates its ability to bind to PAS, although the molecular modeling results did not reveale π-π-stacking interactions with PAS.

Compound **12** and **28** proved to give good results in all the evaluated categories. Because some of the compounds are only tested for affinity towards AChE and by the molecular modeling in this paper, they might not stand out as the AD treatments with the greatest potential. Regardless of **12** and **28** seeming to have the greatest potential; **3**, **5**-**8**, **20**, **23**, **29**, **37**, **39** and **41** also revealed good results in two or more of the evaluated categories.

5 Future work

Ellmans test of compound **1b** and test on inhibition of AChE-induced Aβ aggregation and self-induced Aβ aggregation would have made it possible to evaluate whether the suggested drug candidate is among the most promising AD treatments. In order to perform these, further purification of the compound is needed.

The molecule modeling study was perforemed because it provides comparison of multiple distinctive compounds analyzed under the same conditions. Challenging the 1-click docking program with decoys and testing different AChE crystal structure would increase the credibility of the docking results. Investigation of all the ligands interaction with CAS and more thorough investigation of interaction between the ligands and PAS would perhaps indicate more of the compound as dual inhibitors. In this case, time and limitation in the programs limited further studies.

Morris water maze, an invivo drug test was performed on multiple of the compounds.[19,21–23,28,31] The ability to repel the effect of Scopolamine hydrobromide on rats are tested. Scopo-

lamine is used to induce cognitive impairment in rats, mimicking AD.[28] Comparison of the results would add another factor in the evaluation of which AD treatment is more promising.

References

[1] Organisation, W. H. Global action plan on the public health response to dementia 2017 - 2025. *Geneva: World Health Organization* **2017**, 52.

[2] Association, A. 2015 Alzheimer's disease facts and figures. *Alzheimer's and Dementia* **2015**, *11*, 332–384.

[3] Ma, K. G.; Qian, Y. H. Alpha 7 nicotinic acetylcholine receptor and its effects on Alzheimer's disease. *Neuropeptides* **2019**, *73*, 96–106.

[4] Simunkova, M.; Alwasel, S. H.; Alhazza, I. M.; Jomova, K.; Kollar, V.; Rusko, M.; Valko, M. Management of oxidative stress and other pathologies in Alzheimer's disease. *Archives of Toxicology* **2019**, *93*, 2491–2513.

[5] Jalili-Baleh, L.; Babaei, E.; Abdpour, S.; Nasir Abbas Bukhari, S.; Foroumadi, A.; Ramazani, A.; Sharifzadeh, M.; Abdollahi, M.; Khoobi, M. A review on flavonoid-based scaffolds as multi-target-directed ligands (MTDLs) for Alzheimer's disease. *European Journal of Medicinal Chemistry* **2018**, *152*, 570–589.

[6] Sheffler, Z. M.; Reddy, V.; Pillarisetty, L. S. Physiology , Neurotransmitters. 20894.

[7] Marieb, E. N.; Hoehn, K. In *Human Anatomy & Physiology*, 10th ed.; Beauparlent, S., Ed.; Pearson, 2016.

[8] Perry, E.; Ashton, H.; Young, A.; Greenfield, S. In *Neurochemistry of Consciousness*; Perry, E., Ashton, H., Young, A., Eds.; JohnBenjamins Publishing Company, 2002; p 356.

[9] Donato, A. Peripheral nervous system. https://qbi.uq.edu.au/brain/brain-anatomy/peripheral-nervous-system.

[10] Khan Academy, The synapse.

[11] Więckowska, A. et al. Novel multi-target-directed ligands for Alzheimer's disease: Combining cholinesterase inhibitors and 5-HT6 receptor antagonists. Design, synthesis and biological evaluation. *European Journal of Medicinal Chemistry* **2016**, *124*, 63–81.

[12] Oukoloff, K. et al. Design, biological evaluation and X-ray crystallography of nanomolar multifunctional ligands targeting simultaneously acetylcholinesterase and glycogen synthase kinase-3. *European Journal of Medicinal Chemistry* **2019**, *168*, 58–77.

[13] Jbilo, O.; L'hermite, Y.; Talesa, V.; Toutant, J. Chatonnet, A. Acetylcholinesterase and Butyrylcholinesterase Expression in Adult Rabbit Tissues and During Development. *European Journal of Biochemistry* **1994**, *225*, 115–124.

[14] Wiesner, J.; Kříz, Z.; Kuca, K.; Jun, D.; Koca, J. Acetylcholinesterases - The structural similarities and differences. *Journal of Enzyme Inhibition and Medicinal Chemistry* **2007**, *22*, 417–424.

[15] Long, J. Z.; Cravatt, B. F. The metabolic serine hydrolases and their functions in mammalian physiology and disease. *Chemical Reviews* **2011**, *111*, 6022–6063.

[16] Harel, M.; Schalk, I.; Ehret-Sabatier, L.; Bouet, F.; Goeldner, M.; Hirth, C.; Axelsen, P. H.; Silman, I.; Sussman, J. L. Quaternary ligand binding to aromatic residues in the active-site gorge of acetylcholinesterase. *Proceedings of the National Academy of Sciences* **1993**, *90*, 9031–9035.

[17] Stoddard, S. V.; Hamann, M. T.; Wadkins, R. M. Insights and ideas garnered from marine metabolites for development of dual-function acetylcholinesterase and amyloid-β aggregation inhibitors. *Marine Drugs* **2014**, *12*, 2114–2131.

[18] Orlandini, E.; Silva, D. F. Novel tacrine – benzofuran hybrids as potential multitarget drug candidates for the treatment of Alzheimer ' s Disease. **2020**, 211–226.

[19] Najafi, Z.; Mahdavi, M.; Saeedi, M.; Karimpour-Razkenari, E.; Edraki, N.; Sharifzadeh, M.; Khanavi, M.; Akbarzadeh, T. Novel tacrine-coumarin hybrids linked to 1,2,3-triazole as anti-Alzheimer's compounds: In vitro and in vivo biological evaluation and docking study. *Bioorganic Chemistry* **2019**, *83*, 303–316.

[20] Cheng, Z. Q.; Zhu, K. K.; Zhang, J.; Song, J. L.; Muehlmann, L. A.; Jiang, C. S.; Liu, C. L.; Zhang, H. Molecular-docking-guided design and synthesis of new IAA-tacrine hybrids as multifunctional AChE/BChE inhibitors. *Bioorganic Chemistry* **2019**, *83*, 277–288.

[21] Zhu, J.; Yang, H.; Chen, Y.; Lin, H.; Li, Q.; Mo, J.; Bian, Y.; Pei, Y.; Sun, H. Synthesis, pharmacology and molecular docking on multifunctional tacrine-ferulic acid hybrids as cholinesterase inhibitors against Alzheimer's disease. *Journal of Enzyme Inhibition and Medicinal Chemistry* **2018**, *33*, 496–506.

[22] Chen, Y.; Zhu, J.; Mo, J.; Yang, H.; Jiang, X.; Lin, H.; Gu, K.; Pei, Y.; Wu, L.; Tan, R.; Hou, J.; Chen, J.; Lv, Y.; Bian, Y.; Sun, H. Synthesis and bioevaluation of new tacrine-cinnamic acid hybrids as cholinesterase inhibitors against Alzheimer's disease. *Journal of Enzyme Inhibition and Medicinal Chemistry* **2018**, *33*, 290–302.

[23] Chen, Y.; Lin, H.; Zhu, J.; Gu, K.; Li, Q.; He, S.; Lu, X.; Tan, R.; Pei, Y.; Wu, L.; Bian, Y.; Sun, H. Design, synthesis,: In vitro and in vivo evaluation of tacrine-cinnamic acid hybrids as multi-target acetyl- and butyrylcholinesterase inhibitors against Alzheimer's disease. *RSC Advances* **2017**, *7*, 33851–33867.

[24] Rampa, A.; Belluti, F.; Gobbi, S.; Bisi, A. Hybrid-Based Multi-Target Ligands for the Treatment of Alzheimer ' s Disease. **2011**, 2716–2730.

[25] Dvir, H.; Silman, I.; Harel, M.; Rosenberry, T. L.; Sussman, J. L. Acetylcholinesterase: From 3D structure to function. *Chemico-Biological Interactions* **2010**, *187*, 10–22.

[26] Carvajal, F. J.; Inestrosa, N. C. Interactions of AChE with A? Aggregates in Alzheimer?s Brain: Therapeutic Relevance of IDN 5706. *Frontiers in Molecular Neuroscience* **2011**, *4*, 2009–2010.

[27] Li Wang, Ignacio Moraleda, Isabel Iriepa, Alejandro Romero, Francisco López-Munoz, Mourad Chioua, Tsutomu Inokuchi, Manuela Bartolini, J. M.-C. 5-Methyl-N-(8-(5,6,7,8-tetrahydroacridin-9- ylamino)octyl)-5H-indoloij2,3-b]quinolin-11-amine: a highly potent human cholinesterase inhibitor †‡. *MedChemComm* **2017**, *8*, 1307–1317.

[28] Chalupova, K. et al. Novel tacrine-tryptophan hybrids: Multi-target directed ligands as potential treatment for Alzheimer's disease. *European Journal of Medicinal Chemistry* **2019**, *168*, 491–514.

[29] Ramsay, R. R.; Giovanni, G. D. *Structure-Based Drug Design for Diagnosis and Treatment of Neurological Diseases*; 2017.

[30] Lan, J. S.; Xie, S. S.; Li, S. Y.; Pan, L. F.; Wang, X. B.; Kong, L. Y. Design, synthesis and evaluation of novel tacrine-(β-carboline) hybrids as multifunctional agents for the treatment of Alzheimer's disease. *Bioorganic and Medicinal Chemistry* **2014**, *22*, 6089–6104.

[31] Najafi, Z.; Mahdavi, M.; Saeedi, M.; Karimpour-Razkenari, E.; Asatouri, R.; Vafadarnejad, F.; Moghadam, F. H.; Khanavi, M.; Sharifzadeh, M.; Akbarzadeh, T. Novel tacrine-1,2,3-triazole hybrids: In vitro, in vivo biological evaluation and docking study of cholinesterase inhibitors. *European Journal of Medicinal Chemistry* **2017**, *125*, 1200–1212.

[32] Li, S. Y.; Jiang, N.; Xie, S. S.; Wang, K. D.; Wang, X. B.; Kong, L. Y. Design, synthesis and evaluation of novel tacrine-rhein hybrids as multifunctional agents for the treatment of Alzheimer's disease. *Organic and Biomolecular Chemistry* **2014**, *12*, 801–814.

[33] Lou, Y. H.; Wang, J. S.; Dong, G.; Guo, P. P.; Wei, D. D.; Xie, S. S.; Yang, M. H.; Kong, L. Y. The acute hepatotoxicity of tacrine explained by 1H NMR based metabolomic profiling. *Toxicology Research* **2015**, *4*, 1465–1478.

[34] Chand, K.; Alsoghier, H. M.; Chaves, S.; Santos, M. A. Tacrine-(hydroxybenzoyl-pyridone) hybrids as potential multifunctional anti-Alzheimer's agents: AChE inhibition, antioxidant activity and metal chelating capacity. *Journal of Inorganic Biochemistry* **2016**, *163*, 266–277.

[35] Muñoz-Torrero, D. Acetylcholinesterase Inhibitors as Disease-Modifying Therapies for Alzheimer's Disease. *Frontiers in Medicinal Chemistry* **2015**, 34–86.

[36] TIANJUN, L.; GUOLIANG, L.; GE, H. Preparation method and application of tacrine-sinapic acid heterozygote. 2018.

[37] Jeřábek, J.; Uliassi, E.; Guidotti, L.; Korábečný, J.; Soukup, O.; Sepsova, V.; Hrabinova, M.; Kuča, K.; Bartolini, M.; Peña-Altamira, L. E.; Petralla, S.; Monti, B.; Roberti, M.; Bolognesi, M. L. Tacrine-resveratrol fused hybrids as multi-target-directed ligands against Alzheimer's disease. *European Journal of Medicinal Chemistry* **2017**, *127*, 250–262.

[38] Sun, Q.; Peng, D. Y.; Yang, S. G.; Zhu, X. L.; Yang, W. C.; Yang, G. F. Syntheses of coumarin-tacrine hybrids as dual-site acetylcholinesterase inhibitors and their activity against butylcholinesterase, Aβ aggregation, and β-secretase. *Bioorganic and Medicinal Chemistry* **2014**, *22*, 4784–4791.

[39] Wang, N.; Marta, Ś.; Hossain, I. Search for Articles : Structural Modifications of Nature-Inspired Indoloquinolines : A Mini Review of Their Potential Antiproliferative Activity by. **2020**,

[40] Thobokholt, E. N.; Larghi, E. L.; Bracca, A. B.; Kaufman, T. S. Isolation and synthesis of cryptosanguinolentine (isocryptolepine), a naturally-occurring bioactive indoloquinoline alkaloid. *RSC Advances* **2020**, *10*, 18978–19002.

[41] Newman, D. J.; Cragg, G. M. Natural products as sources of new drugs over the 30 years from 1981 to 2010. *Journal of Natural Products* **2012**, *75*, 311–335.

[42] Helgeland, I.; Sydnes, M. A Concise Synthesis of Isocryptolepine by C–C Cross-Coupling Followed by a Tandem C–H Activation and C–N Bond Formation. *Syn-Open* **2017**, *01*, 0041–0044.

[43] Timári, G.; Soós, T.; György, H. A Convenient Synthesis of Two New Indoloquinoline Alkaloids. **1997**, *3*, 54–67.

[44] Shankar Singh, M. Reactive Intermediates in Organic Chemistry. **2014**,

[45] Chemie, F.; Stahl, J.; Weigel, C.; Weigmann, P.; Wilhelm, H. Tacrine. **2017**, 1–13.

[46] Szymański, P.; Markowicz, M.; Mikiciuk-Olasik, E. Synthesis and biological activity of derivatives of tetrahydroacridine as acetylcholinesterase inhibitors. *Bioorganic Chemistry* **2011**, *39*, 138–142.

[47] Xie, S. S.; Wang, X. B.; Li, J. Y.; Yang, L.; Kong, L. Y. Design, synthesis and evaluation of novel tacrine-coumarin hybrids as multifunctional cholinesterase inhibitors against Alzheimer's disease. *European Journal of Medicinal Chemistry* **2013**, *64*, 540–553.

[48] Proctor, G.; Harvey, A. Synthesis of Tacrine Analogues and Their Structure-Activity Relationships. *Current Medicinal Chemistry* **2012**, *7*, 295–302.

[49] Cieslikiewicz-Bouet, M.; Naldi, M.; Bartolini, M.; Pérez, B.; Servent, D.; Jean, L.; Aráoz, R.; Renard, P.-Y. Functional characterization of multifunctional ligands targeting acetylcholinesterase and alpha 7 nicotinic acetylcholine receptor. *Biochemical Pharmacology* **2020**, 114010.

[50] Singh, D. K.; Kim, I. Convergent synthesis of diptoindonesin G. *Tetrahedron Letters* **2019**, *60*, 300–301.

[51] Zhang, W.; Xiao, D.; Wang, B. A concise total synthesis of cochlearoid B. *Organic and Biomolecular Chemistry* **2018**, *16*, 3358–3361.

[52] García-Pindado, J.; Royo, S.; Teixidó, M.; Giralt, E. Bike peptides: a ride through the membrane. *Journal of Peptide Science* **2017**, *23*, 294–302.

[53] Leroy G. Wade, J.; Simek, J. W. In *Organic Chemistry*, ninth ed.; Zalesky, J., Terry Haugen,, Eds.; 2017.

[54] Hein, C. D.; Liu, X. M.; Wang, D. Click chemistry, a powerful tool for pharmaceutical sciences. *Pharmaceutical Research* **2008**, *25*, 2216–2230.

[55] Ellman, G. L.; Courtney, K. D.; Andres, V.; Featherstone, R. M. A new and rapid colorimetric determination of acetylcholinesterase activity. *Biochemical Pharmacology* **1961**, *7*, 88–95.

[56] Berg, J. M.; Tymoczko, J. L.; Gatto Jr, G. J.; Stryer, L. In *Biochemistry*, eighth ed.; Showers, D., Redd, S., Eds.; Parker, Kate Ahr, 2015; p 1056.

[57] Meng, X.-Y.; Zhang, H.-X.; Mezei, M.; Cui, M. Molecular Docking: A Powerful Approach for Structure-Based Drug Discovery. *Current Computer Aided-Drug Design* **2012**, *7*, 146–157.

[58] Du, H.; Brender, J. R.; Zhang, J.; Zhang, Y. Protein structure prediction provides comparable performance to crystallographic structures in docking-based virtual screening. *Methods* **2015**, *71*, 77–84.

[59] Kiss, R.; Sándor, M.; Szalai, Z.; Szalai, F.; Havancsák, L. Mcule. 2019; https://mcule.com/dashboard/.

[60] Trott, O.; Olson, A. J. AutoDock Vina: Improving the speed and accuracy of docking with a new scoring function, efficient optimization, and multithreading. *Journal of Computational Chemistry* **2009**, NA–NA.

[61] Keri, R. S.; Quintanova, C.; Chaves, S.; Silva, D. F.; Cardoso, S. M.; Santos, M. A. New Tacrine Hybrids with Natural-Based Cysteine Derivatives as Multitargeted Drugs for Potential Treatment of Alzheimer's Disease. *Chemical Biology and Drug Design* **2016**, *87*, 101–111.

[62] Bornstein, J. J.; Eckroat, T. J.; Houghton, J. L.; Jones, C. K.; Green, K. D.; Garneau-Tsodikova, S. Tacrine-mefenamic acid hybrids for inhibition of acetylcholinesterase. *MedChemComm* **2011**, *2*, 406–412.

[63] Raschka, S.; Wolf, A. J.; Bemister-Buffington, J.; Kuhn, L. A. Protein–ligand interfaces are polarized: discovery of a strong trend for intermolecular hydrogen bonds to favor donors on the protein side with implications for predicting and designing ligand complexes. *Journal of Computer-Aided Molecular Design* **2018**, *32*, 511–528.

[64] Zhu, K.; Borrelli, K.; Greenwood, J.; Day, T.; Abel, R.; Farid, R.; Harder, E. Docking covalent inhibitors: A parameter free approach to pose prediction and scoring. **2014**,

[65] Jeong, E.; Kim, H.; Lee, S. W.; Han, K. Discovering the interaction propensities of amino acids and nucleotides from protein-RNA complexes. *Molecules and Cells* **2003**, *16*, 161–167.

[66] Xue, C.; Lin, T. Y.; Chang, D.; Guo, Z. Thioflavin T as an amyloid dye: Fibril quantification, optimal concentration and effect on aggregation. *Royal Society Open Science* **2017**, *4*.

[67] Lieber, E.; Rao, C. N.; Hoffman, C. W.; Chao, T. S. Infrared Spectra of Organic Azides. *Analytical Chemistry* **1957**, *29*, 916–918.

[68] Nkrumah-Agyeefi, S.; Scholz, C. Chemical modification of functionalized polyhydroxyalkanoates via "Click" chemistry: A proof of concept. *International Journal of Biological Macromolecules* **2017**, *95*, 796–808.

[69] Lang, C.; Kiefer, C.; Lejeune, E.; Goldmann, A. S.; Breher, F.; Roesky, P. W.; Barner-Kowollik, C. Palladium-containing polymers via a combination of RAFT and triazole chemistry. *Polymer Chemistry* **2012**, *3*, 2413–2420.

[70] Aiken, K.; Bunn, J.; Sutton, S.; Christianson, M.; Winder, D.; Freeman, C.; Padgett, C.; McMillen, C.; Ghosh, D.; Landge, S. Nuclear Magnetic Resonance Spectroscopy Investigations of Naphthalene-Based 1,2,3-Triazole Systems for Anion Sensing. *Magnetochemistry* **2018**, *4*, 15.

[71] Nile, S. H.; Keum, Y. S.; Nile, A. S.; Jalde, S. S.; Patel, R. V. Antioxidant, anti-inflammatory, and enzyme inhibitory activity of natural plant flavonoids and their synthesized derivatives. *Journal of Biochemical and Molecular Toxicology* **2018**, *32*, 3099067.

[72] Zhang, Q. W.; Lin, L. G.; Ye, W. C. Techniques for extraction and isolation of natural products: A comprehensive review. *Chinese Medicine (United Kingdom)* **2018**, *13*.

[73] González, A. G.; Herrador, M. Á. The assessment of electronic balances for accuracy of mass measurements in the analytical laboratory. *Accreditation and Quality Assurance* **2007**, *12*, 21–29.

[74] Xie, S. S.; Wang, X. B.; Li, J. Y.; Yang, L.; Kong, L. Y. Design, synthesis and evaluation of novel tacrine-coumarin hybrids as multifunctional cholinesterase inhibitors against Alzheimer's disease. *European Journal of Medicinal Chemistry* **2013**, *64*, 540–553.

[75] Lu, C.; Zhou, Q.; Yan, J.; Du, Z.; Huang, L.; Li, X. A novel series of tacrine-selegiline hybrids with cholinesterase and monoamine oxidase inhibition activities for the treatment of Alzheimer's disease. *European Journal of Medicinal Chemistry* **2013**, *62*, 745–753.

[76] Fancellu, G.; Chand, K.; Tomás, D.; Orlandini, E.; Piemontese, L.; Silva, D. F.; Cardoso, S. M.; Chaves, S.; Santos, M. A. Novel tacrine–benzofuran hybrids as

potential multi-target drug candidates for the treatment of Alzheimer's Disease. *Journal of Enzyme Inhibition and Medicinal Chemistry* **2020**, *35*, 211–226.

[77] Cheng, X. J.; Gu, J. X.; Pang, Y. P.; Liu, J.; Xu, T.; Li, X. R.; Hua, Y. Z.; Newell, K. A.; Huang, X. F.; Yu, Y.; Liu, Y. Tacrine-Hydrogen Sulfide Donor Hybrid Ameliorates Cognitive Impairment in the Aluminum Chloride Mouse Model of Alzheimer's Disease. *ACS Chemical Neuroscience* **2019**, *10*, 3500–3509.

[78] Sola, I.; Aso, E.; Frattini, D.; López-González, I.; Espargaró, A.; Sabaté, R.; Di Pietro, O.; Luque, F. J.; Clos, M. V.; Ferrer, I.; Muñoz-Torrero, D. Novel Levetiracetam Derivatives That Are Effective against the Alzheimer-like Phenotype in Mice: Synthesis, in Vitro, ex Vivo, and in Vivo Efficacy Studies. *Journal of Medicinal Chemistry* **2015**, *58*, 6018–6032.

[79] Xie, S. S.; Wang, X.; Jiang, N.; Yu, W.; Wang, K. D.; Lan, J. S.; Li, Z. R.; Kong, L. Y. Multi-target tacrine-coumarin hybrids: Cholinesterase and monoamine oxidase B inhibition properties against Alzheimer's disease. *European Journal of Medicinal Chemistry* **2015**, *95*, 153–165.

[80] Xie, S. S.; Lan, J. S.; Wang, X. B.; Jiang, N.; Dong, G.; Li, Z. R.; Wang, K. D.; Guo, P. P.; Kong, L. Y. Multifunctional tacrine-trolox hybrids for the treatment of Alzheimer's disease with cholinergic, antioxidant, neuroprotective and hepatoprotective properties. *European Journal of Medicinal Chemistry* **2015**, *93*, 42–50.

[81] León, R.; de los Ríos, C.; Marco-Contelles, J.; Huertas, O.; Barril, X.; Javier Luque, F.; López, M. G.; García, A. G.; Villarroya, M. New tacrine-dihydropyridine hybrids that inhibit acetylcholinesterase, calcium entry, and exhibit neuroprotection properties. *Bioorganic and Medicinal Chemistry* **2008**, *16*, 7759–7769.

[82] Berman, H.; Westbrook, J.; Feng, Z.; Gilliland, G.; Bhat, T.; Weissig, H.; Shindyalov, I.; Bourne, P. RCSB PDB. 2000.

[83] Rydberg, E. H.; Brumshtein, B.; Greenblatt, H. M.; Wong, D. M.; Shaya, D.; Williams, L. D.; Carlier, P. R.; Pang, Y.-P.; Silman, I.; Sussman, J. L. Complexes

of Alkylene-Linked Tacrine Dimers with Torpedo c alifornica Acetylcholinesterase: Binding of Bis(5)-tacrine Produces a Dramatic Rearrangement in the Active-Site Gorge. *Journal of Medicinal Chemistry* **2006**, *49*, 5491–5500.

[84] Zha, X. et al. Novel Tacrine–Benzofuran Hybrids as Potent Multitarget-Directed Ligands for the Treatment of Alzheimer's Disease: Design, Synthesis, Biological Evaluation, and X-ray Crystallography. *Journal of Medicinal Chemistry* **2016**, *59*, 114–131.

[85] Haviv, H.; Wong, D. M.; Greenblatt, H. M.; Carlier, P. R.; Pang, Y.-P.; Silman, I.; Sussman, J. L. Crystal Packing Mediates Enantioselective Ligand Recognition at the Peripheral Site of Acetylcholinesterase. *Journal of the American Chemical Society* **2005**, *127*, 11029–11036.

[86] Cardoso, S. M.; Santos, M. A. Dalton Transactions. **2013**, 6058–6073.

[87] Šebestík, J.; Marques, S. M.; Falé, P. L.; Santos, S.; Arduíno, D. M.; Cardoso, S. M.; Oliveira, C. R.; Serralheiro, M. L. M.; Santos, M. A. Bifunctional phenolic-choline conjugates as anti-oxidants and acetylcholinesterase inhibitors. *Journal of Enzyme Inhibition and Medicinal Chemistry* **2011**, *26*, 485–497.

[88] Fang, L.; Kraus, B.; Lehmann, J.; Heilmann, J.; Zhang, Y.; Decker, M. Design and synthesis of tacrine-ferulic acid hybrids as multi-potent anti-Alzheimer drug candidates. *Bioorganic and Medicinal Chemistry Letters* **2008**, *18*, 2905–2909.

[89] Huang, N.; Shoichet, B. K.; Irwin, J. J. Benchmarking sets for molecular docking. *Journal of Medicinal Chemistry* **2006**, *49*, 6789–6801.

[90] Villaflores, O. B.; Chen, Y. J.; Chen, C. P.; Yeh, J. M.; Wu, T. Y. Curcuminoids and resveratrol as anti-Alzheimer agents. *Taiwanese Journal of Obstetrics and Gynecology* **2012**, *51*, 515–525.

[91] Tang, H.; Zhao, L. Z.; Zhao, H. T.; Huang, S. L.; Zhong, S. M.; Qin, J. K.; Chen, Z. F.; Huang, Z. S.; Liang, H. Hybrids of oxoisoaporphine-tacrine congeners:

Novel acetylcholinesterase and acetylcholinesterase-induced β-amyloid aggregation inhibitors. *European Journal of Medicinal Chemistry* **2011**, *46*, 4970–4979.

[92] Leon, R.; Marco-Contelles, J. A Step Further Towards Multitarget Drugs for Alzheimer and Neuronal Vascular Diseases: Targeting the Cholinergic System, Amyloid-β Aggregation and Ca2++ Dyshomeostasis. *Current Medicinal Chemistry* **2011**, *18*, 552–576.

[93] Marco-Contelles, J.; León, R.; De Los Ríos, C.; Guglietta, A.; Terencio, J.; Lòpez, M. G.; Garcìa, A. G.; Villarroya, M. Novel multipotent tacrine-dihydropyridine hybrids with improved acetylcholinesterase inhibitory and neuroprotective activities as potential drugs for the treatment of Alzheimer's disease. *Journal of Medicinal Chemistry* **2006**, *49*, 7607–7610.

[94] Camps, P.; Munoz-Torrero, D. Tacrine-Huperzine A Hybrids (Huprines) A New Class of Highly Potent and Selective Acetylcholinesterase Inhibitors of Interest for the Treatment of Alzheimer Disease. *Mini-Reviews in Medicinal Chemistry* **2005**, *1*, 163–174.

[95] Camps, P.; El Achab, R.; Morral, J.; Munoz-Torrero, D.; Badia, A.; Eladi Banos, J.; Vivas, N. M.; Barril, X.; Orozco, M.; Javier Luque, F. New tacrine-huperzine A hybrids (huprines): Highly potent tight-binding acetylcholinesterase inhibitors of interest for the treatment of Alzheimer's Disease. *Journal of Medicinal Chemistry* **2000**, *43*, 4657–4666.

[96] Camps, P.; El Achab, R.; Görbig, D. M.; Morral, J.; Muñoz-Torrero, D.; Badia, A.; Baños, J. E.; Vivas, N. M.; Barril, X.; Orozco, M.; Luque, F. J. Synthesis, in vitro pharmacology, and molecular modeling of very potent tacrine-huperzine A hybrids as acetylcholinesterase inhibitors of potential interest for the treatment of Alzheimer's disease. *Journal of Medicinal Chemistry* **1999**, *42*, 3227–3242.

[97] Badia, A.; Baños, J. E.; Camps, P.; Contreras, J.; Görbig, D. M.; Muñoz-Torrero, D.; Simón, M.; Vivas, N. M. Synthesis and evaluation of tacrine-huperzine a hybrids as

acetylcholinesterase inhibitors of potential interest for the treatment of Alzheimer's disease. *Bioorganic and Medicinal Chemistry* **1998**, *6*, 427–440.

[98] Felder, C. E.; Harel, M.; Silman, I.; Sussman, J. L. Structure of a complex of the potent and specific inhibitor BW284C51 with Torpedo californica acetylcholinesterase. *Acta Crystallographica Section D Biological Crystallography* **2002**, *58*, 1765–1771.

[99] Dvir, H.; Silman, I.; Harel, M.; Rosenberry, T. L.; Sussman, J. L. Acetylcholinesterase: From 3D structure to function. *Chemico-Biological Interactions* **2010**, *187*, 10–22.

[100] Legler, P. M.; Soojhawon, I.; Millard, C. B. A conformational change in the peripheral anionic site of Torpedo californica acetylcholinesterase induced by a bis-imidazolium oxime. *Acta Crystallographica Section D Biological Crystallography* **2015**, *71*, 1788–1798.

[101] Dvir, H.; Wong, D. M.; Harel, M.; Barril, X.; Orozco, M.; Luque, F. J.; Muñoz-Torrero, D.; Camps, P.; Rosenberry, T. L.; Silman, I.; Sussman, J. L. 3D Structure of Torpedo californica Acetylcholinesterase Complexed with Huprine X at 2.1 Å Resolution: Kinetic and Molecular Dynamic Correlates † , ‡. *Biochemistry* **2002**, *41*, 2970–2981.

[102] Bartolucci, C.; Stojan, J.; Yu, Q.-s.; Greig, N. H.; Lamba, D. Kinetics of Torpedo californica acetylcholinesterase inhibition by bisnorcymserine and crystal structure of the complex with its leaving group. *Biochemical Journal* **2012**, *444*, 269–277.

[103] Bartolucci, C.; Haller, L. A.; Jordis, U.; Fels, G.; Lamba, D. Probing Torpedo californica Acetylcholinesterase Catalytic Gorge with Two Novel Bis-functional Galanthamine Derivatives. *Journal of Medicinal Chemistry* **2010**, *53*, 745–751.

[104] Bartolucci, C.; Haller, L. A.; Jordis, U.; Fels, G.; Lamba, D. Probing Torpedo californica Acetylcholinesterase Catalytic Gorge with Two Novel Bis-functional Galanthamine Derivatives. *Journal of Medicinal Chemistry* **2010**, *53*, 745–751.

[105] Greenblatt, H. M.; Guillou, C.; Guénard, D.; Argaman, A.; Botti, S.; Badet, B.; Thal, C.; Silman, I.; Sussman, J. L. The Complex of a Bivalent Derivative of Galanthamine with Torpedo Acetylcholinesterase Displays Drastic Deformation of the Active-Site Gorge: Implications for Structure-Based Drug Design. *Journal of the American Chemical Society* **2004**, *126*, 15405–15411.

[106] Millard, C. B.; Kryger, G.; Ordentlich, A.; Greenblatt, H. M.; Harel, M.; Raves, M. L.; Segall, Y.; Barak, D.; Shafferman, A.; Silman, I.; Sussman, J. L. Crystal Structures of Aged Phosphonylated Acetylcholinesterase: Nerve Agent Reaction Products at the Atomic Level. *Biochemistry* **1999**, *38*, 7032–7039.

[107] Sanner., M. F. MGL tools. http://mgltools.scripps.edu.

[108] Digiacomo, M.; Chen, Z.; Wang, S.; Lapucci, A.; Macchia, M.; Yang, X.; Chu, J.; Han, Y.; Pi, R.; Rapposelli, S. Synthesis and pharmacological evaluation of multifunctional tacrine derivatives against several disease pathways of AD. *Bioorganic and Medicinal Chemistry Letters* **2015**, *25*, 807–810.

[109] Benchekroun, M. et al. Novel tacrine-grafted ugi adducts as multipotent anti-alzheimer drugs: A synthetic renewal in tacrine-ferulic acid hybrids. *ChemMedChem* **2015**, *10*, 523–539.

[110] Hui, A. L.; Chen, Y.; Zhu, S. J.; Gan, C. S.; Pan, J.; Zhou, A. Design and synthesis of tacrine-phenothiazine hybrids as multitarget drugs for Alzheimer's disease. *Medicinal Chemistry Research* **2014**, *23*, 3546–3557.

[111] AILING, H.; JIAN, P.; GAN, C. Tacrine-phenothiazine isodiad compound and preparation method thereof. **2013**, 17.

[112] Fernández-Bachiller, M. I.; Pérez, C.; Monjas, L.; Rademann, J.; Rodríguez-Franco, M. I. New tacrine-4-oxo-4H-chromene hybrids as multifunctional agents for the treatment of Alzheimer's disease, with cholinergic, antioxidant, and β-amyloid-reducing properties. *Journal of Medicinal Chemistry* **2012**, *55*, 1303–1317.

[113] Fernández-Bachiller, M. I.; Pérez, C.; González-Muñoz, G. C.; Conde, S.; López, M. G.; Villarroya, M.; García, A. G.; Rodríguez-Franco, M. I. Novel tacrine-8-hydroxyquinoline hybrids as multifunctional agents for the treatment of Alzheimers disease, with neuroprotective, cholinergic, antioxidant, and copper-complexing properties. *Journal of Medicinal Chemistry* **2010**, *53*, 4927–4937.

[114] Drug, H. A.-a.; Fang, L.; Appenroth, D.; Decker, M.; Kiehntopf, M.; Roegler, C.; Deufel, T. Synthesis and Biological Evaluation of NO-Donor-Tacrine Hybrids as. *Society* **2008**, 713–716.

[115] Szymański, P.; Zurek, E.; Mikiciuk-Olasik, E. New tacrine-hydrazinonicotinamide hybrids as acetylcholinesterase inhibitors of potential interest for the early diagnostics of Alzheimer's disease. *Pharmazie* **2006**, *61*, 269–273.

[116] Rodríguez-Franco, M. I.; Fernández-Bachiller, M. I.; Pérez, C.; Hernández-Ledesma, B.; Bartolomé, B. Novel tacrine-melatonin hybrids as dual-acting drugs for alzheimer disease, with improved acetylcholinesterase inhibitory and antioxidant properties. *Journal of Medicinal Chemistry* **2006**, *49*, 459–462.

[117] Dorronsoro, I.; Alonso, D.; Castro, A.; Del Monte, M.; García-Palomero, E.; Martínez, A. Synthesis and biological evaluation of tacrine-thiadiazolidinone hybrids as dual acetylcholinesterase inhibitors. *Archiv der Pharmazie* **2005**, *338*, 18–23.

[118] Shao, D.; Zou, C.; Luo, C.; Tang, X.; Li, Y. Synthesis and evaluation of tacrine-E2020 hybrids as acetylcholinesterase inhibitors for the treatment of Alzheimer's disease. *Bioorganic and Medicinal Chemistry Letters* **2004**, *14*, 4639–4642.

[119] Marco-Contelles, J.; León, R.; De Los Ríos, C.; Guglietta, A.; Terencio, J.; Lòpez, M. G.; Garcìa, A. G.; Villarroya, M. Novel multipotent tacrine-dihydropyridine hybrids with improved acetylcholinesterase inhibitory and neuroprotective activities as potential drugs for the treatment of Alzheimer's disease. *Journal of Medicinal Chemistry* **2006**, *49*, 7607–7610.

A Publication list

Table 11. List of the articles and patents from which the discussed molecules are retrived.

No.	Article or patent	Compound name
1	*Novel tacrine–benzofuran hybrids as potential multitarget drug candidates for the treatment of Alzheimer's Disease*[18]	19
2	*Tacrine-Hydrogen Sulfide Donor Hybrid Ameliorates Cognitive Impairment in the Aluminum Chloride Mouse Model of Alzheimer's Disease*[77]	THS
3	*Novel tacrine-tryptophan hybrids: Multi-target directed ligands as potential treatment for Alzheimer's disease*[28]	S-K1035
4	*Novel tacrine-coumarin hybrids linked to 1,2,3-triazole as anti-Alzheimer's compounds: In vitro and in vivo biological evaluation and docking study*[19]	8e
5	*Molecular-docking-guided design and synthesis of new IAA-tacrine hybrids as multifunctional AChE/BChE inhibitors*[20]	5e
6	*Synthesis, pharmacology and molecular docking on multifunctional tacrine-ferulic acid hybrids as cholinesterase inhibitors against Alzheimer's disease*[21]	10g
7	*Preparation method and application of tacrine-sinapic acid heterozygote*[36]	4
8	*Synthesis and bioevaluation of new tacrine-cinnamic acid hybrids as cholinesterase inhibitors against Alzheimer's disease*[22]	19
9	*Design, synthesis, in vitro and in vivo evaluation of tacrine–cinnamic acid hybrids as multitarget acetyl- and butyrylcholinesterase inhibitors against Alzheimer's disease*[23]	36
10	*Tacrine-resveratrol fused hybrids as multi-target-directed ligands against Alzheimer's disease*[37]	12

11	*Syntheses of coumarin–tacrine hybrids as dual-site acetylcholinesterase inhibitors and their activity against butylcholinesterase, Aβ aggregation, and b-secretase*[38]	1g
12	*Design, synthesis and evaluation of novel tacrine-(b-carboline) hybrids as multifunctional agents for the treatment of Alzheimer's disease*[30]	11l
13	*Novel tacrine-1,2,3-triazole hybrids: In vitro, in vivo biological evaluation and docking study of cholinesterase inhibitors*[31]	5l
14	*Tacrine-(hydroxybenzoyl-pyridone) hybrids as potential multifunctional anti-Alzheimer's agents: AChE inhibition, antioxidant activity and metal chelating capacity*[34]	17
15	*Novel Levetiracetam Derivatives That Are Effective against the Alzheimer-like Phenotype in Mice: Synthesis, in Vitro, ex Vivo, and in Vivo Efficacy Studies*[78]	10
16	*Multi-target tacrine-coumarin hybrids: Cholinesterase and monoamine oxidase B inhibition properties against Alzheimer's disease*[79]	14c
17	*New Tacrine Hybrids with Natural-Based Cysteine Derivatives as Multi-targeted Drugs for Potential Treatment of Alzheimer's Disease*[61]	9d
18	*Multifunctional tacrineetrolox hybrids for the treatment of Alzheimer's disease with cholinergic, antioxidant, neuroprotective and hepatoprotective properties*[80]	6d
19	*Synthesis and pharmacological evaluation of multifunctional tacrine derivatives against several disease pathways of AD*[108]	1b
20	*Novel Tacrine-Grafted Ugi Adducts as Multipotent Anti- Alzheimer Drugs: A Synthetic Renewal in Tacrine–Ferulic Acid Hybrids*[109]	10n
21	*Design and synthesis of tacrine-phenothiazine hybrids as multitarget drugs for Alzheimer's disease*[110]	T5
22	*Design, synthesis and evaluation of novel tacrine–rhein hybrids as multifunctional agents for the treatment of Alzheimer's disease*[32]	10b

23	*Design, synthesis and evaluation of novel tacrineecoumarin hybrids as multifunctional cholinesterase inhibitors against Alzheimer's disease*[74]	8f
24	*A novel series of tacrineeselegiline hybrids with cholinesterase and monoamine oxidase inhibition activities for the treatment of Alzheimer's disease*[75]	8g
25	*Tacrine-phenothiazine isodiad compound and preparation method thereof*[111]	I-1
26	*Hybrid-Based Multi-Target Ligands for the Treatment of Alzheimer's Disease*[24]	-
27	*New Tacrine4-Oxo-4H-chromene Hybrids as Multifunctional Agents for the Treatment of Alzheimer's Disease, with Cholinergic, Antioxidant, and -Amyloid-Reducing Properties*[112]	19
28	*Hybrids of oxoisoaporphine-tacrine congeners: Novel acetylcholinesterase and acetylcholinesterase-induced b-amyloid aggregation inhibitors*[91]	7f
29	*Tacrine-mefenamic acid hybrids for inhibition of acetylcholinesterase*[62]	11e
30	*A Step Further Towards Multitarget Drugs for Alzheimer and Neuronal Vascular Diseases: Targeting the Cholinergic System, Amyloid-β Aggregation and Ca^{2+} Dyshomeostasis*[92]	104
31	*Novel Tacrine-8-Hydroxyquinoline Hybrids as Multifunctional Agents for the Treatment of Alzheimer's Disease, with Neuroprotective, Cholinergic, Antioxidant, and Copper-Complexing Properties*[113]	6
32	*New tacrine-dihydropyridine hybrids that inhibit acetylcholinesterase, calcium entry, and exhibit neuroprotection properties*[81]	4
33	*Design and synthesis of tacrine–ferulic acid hybrids as multi-potent anti-Alzheimer drug candidates*[88]	6d
34	*Synthesis and Biological Evaluation of NO-Donor-Tacrine Hybrids as Hepatoprotective Anti-Alzheimer Drug Candidates*[114]	9

35	*Novel Multipotent Tacrine-Dihydropyridine Hybrids with Improved Acetylcholinesterase Inhibitory and Neuroprotective Activities as Potential Drugs for the Treatment of Alzheimer's Disease*[93]	10
36	*New Tacrine-Hydrazinonicotinamide Hybrids as Acetylcholinesterase Inhibitors of Potential Interest for the Early Diagnostics of Alzheimer's Disease*[115]	6d
37	*Novel Tacrine-Melatonin Hybrids as Dual-Acting Drugs for Alzheimer Disease, with Improved Acetylcholinesterase Inhibitory and Antioxidant Properties*[116]	6b
38	*Synthesis and Biological Evaluation of Tacrine-Thiadiazolidinone Hybrids as Dual Acetyl- cholinesterase Inhibitors*[117]	8
39	*Synthesis and evaluation of tacrine–E2020 hybrids as acetylcholinesterase inhibitors for the treatment of AlzheimerÕs disease*[118]	3
40	*TacrineHuperzine A Hybrids (Huprines): A New Class of Highly Potent and Selective Acetylcholinesterase Inhibitors of Interest for the Treatment of Alzheimer's Disease*[94]	64
41	*New Tacrine-Huperzine A Hybrids (Huprines): Highly Potent Tight-Binding Acetylcholinesterase Inhibitors of Interest for the Treatment of Alzheimer´s Disease*[95]	(-)-20
42	*Synthesis, in Vitro Pharmacology, and Molecular Modeling Very Highly Potent Tacrine-Huperzine A Hybrids as Acetylcholinesterase Inhibitors of Potential Interest for the Treatment of Alzheimer´s Disease*[96]	(-)-28
43	*Synthesis and Evaluation of Tacrine±Huperzine A Hybrids as Acetylcholinesterase Inhibitors of Potential Interest for the Treatment of Alzheimer's Disease*[97]	7ey
44	*Novel tacrine–benzofuran hybrids as potential multi-target drug candidates for the treatment of Alzheimer's Disease*[76]	15

45	*Novel Multipotent Tacrine-Dihydropyridine Hybrids with Improved Acetylcholinesterase Inhibitory and Neuroprotective Activities as Potential Drugs for the Treatment of Alzheimer's Disease*[119]	11

B Molecular structures

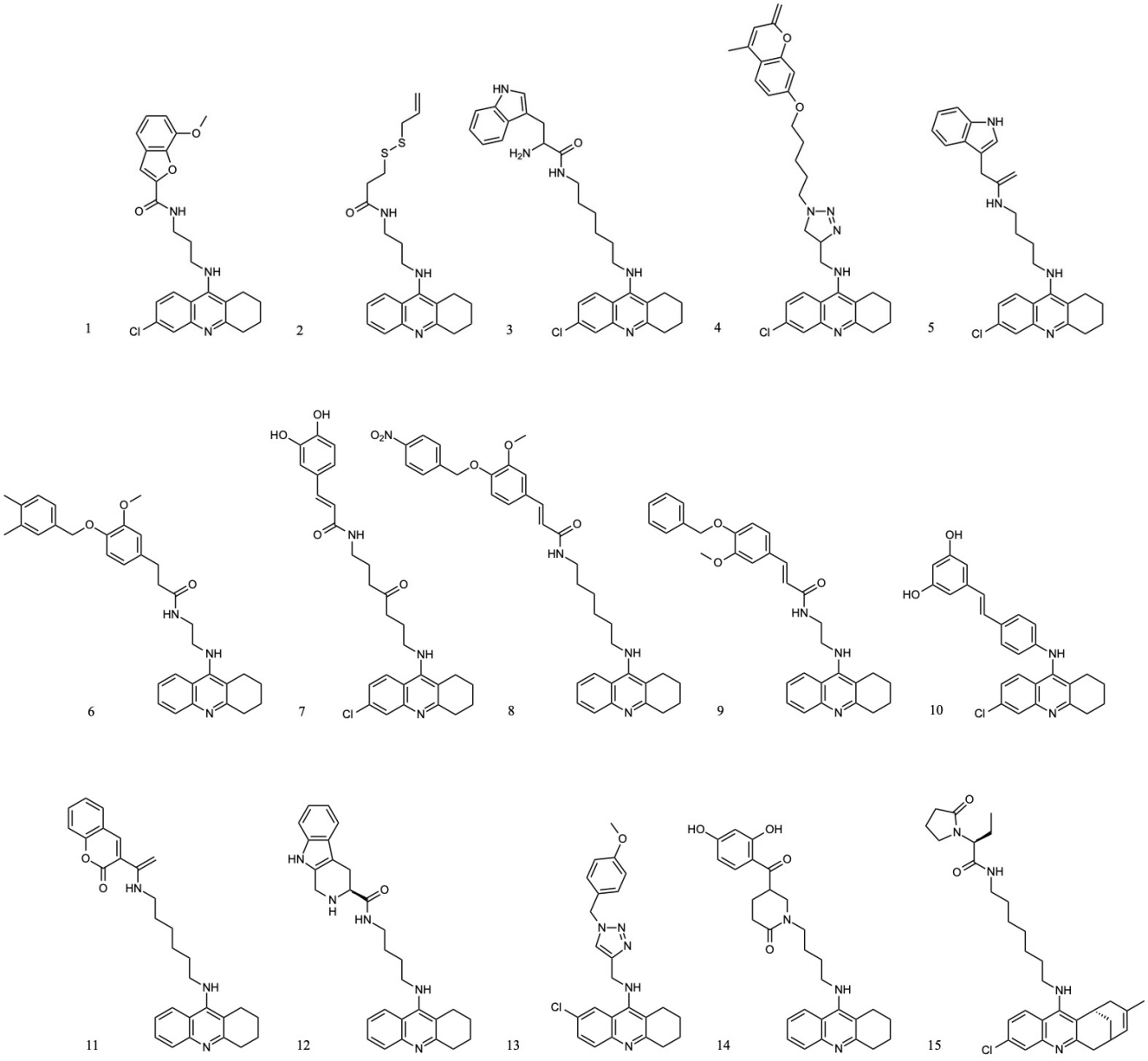

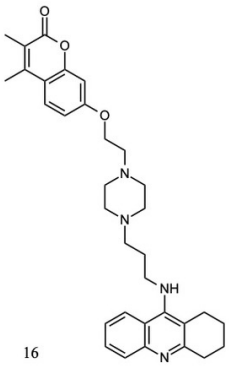
16

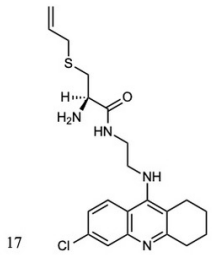
17

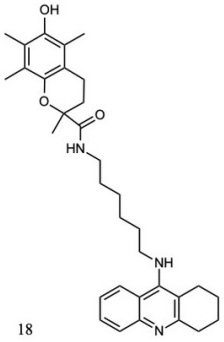
18

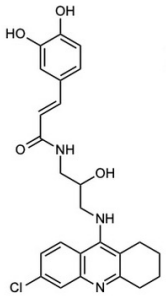
19

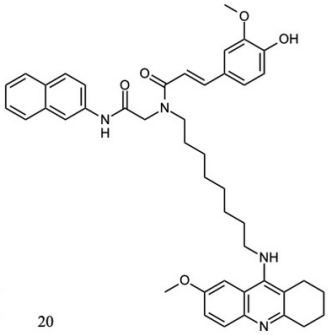
20

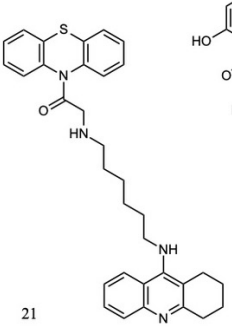
21

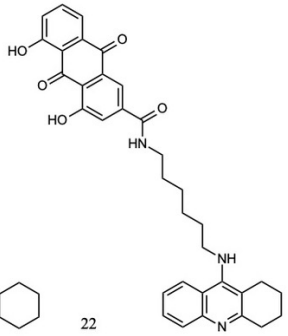
22

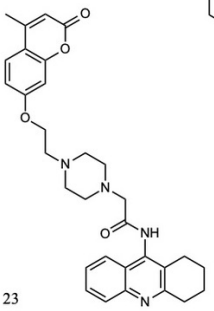
23

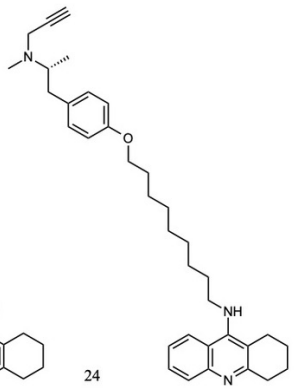
24

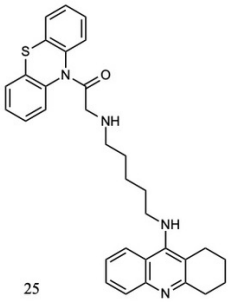
25

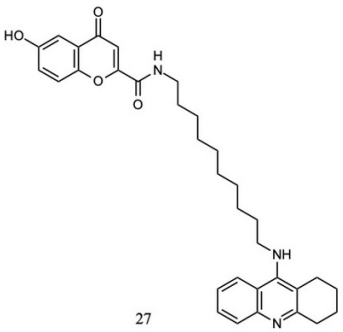
27

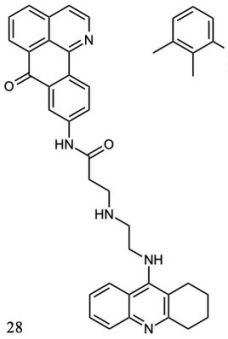
28

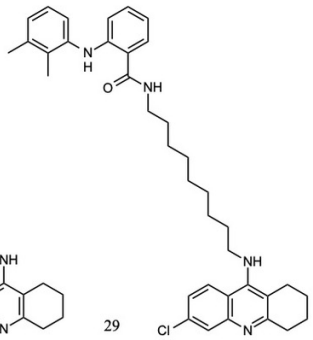
29

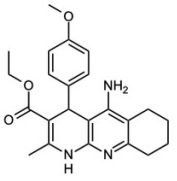
30

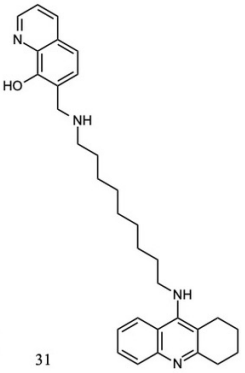
31

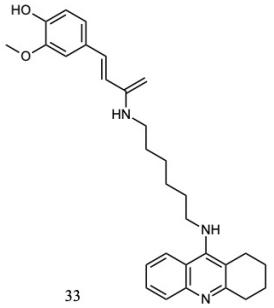
33

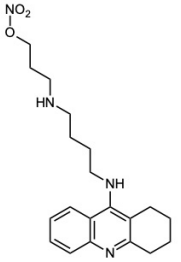
34

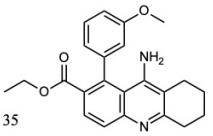
35

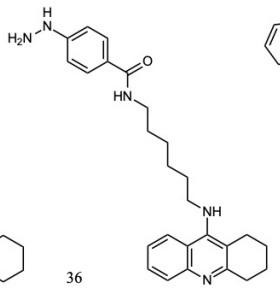
36

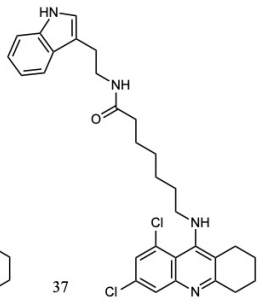
37

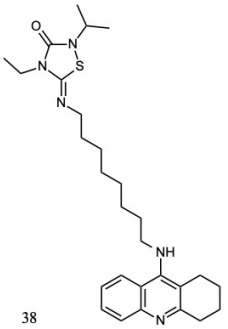

38

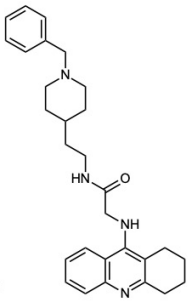

39

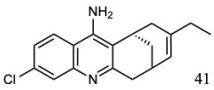

40

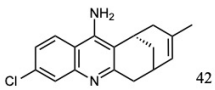

41

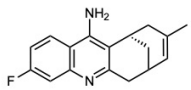

42

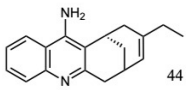

43

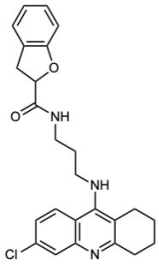

44

C Ellman´s test

C.1 Affinity towards AChE

Table 12. Compounds tested for their AChE affinity by Elmans test.

No.	$IC_{50(I)}$(nM)	$IC_{50(Tac)}$(nM)	$IC_{50(I)}/IC_{50(Tac)}$	AChE
1	130	350	0.371	ee[a]
2	-	-	-	-
3	6.3	320	1.97 x 10^{-2}	hu[b]
4	27	48	0.563	ee
5	173	158	1.09	ee
6	37	14,5	2.55	ee
7	0.2	40	5.00 x 10^{-3}	b[c]
8	2.7	69.8	3.87 x 10^{-2}	ee
9	15.8	69.8	0.226	ee
10	8800	500	17.6	hu
11	8.35	17.85	0.468	hu
12	21.6	260	8.31 x 10^{-2}	ee
13	521	48	10.9	ee
14	570	310	1.84	ee
15	4.2	317	1.32 x 10^{-2}	hu
16	33.63	97.3	0.346	ee
17	300	190	1.58	tc[d]
18	9.8	112.1	8.74 x 10^{-2}	ee
19	150	100	1.50	ee
20	22.2	424	5.24 x 10^{-2}	hu
21	89	275	0.324	r[e]
22	27.3	135	0.202	ee
23	92	269	0.342	ee

Table 12. Compounds tested for their AChE affinity by Elmans test.

No.	$IC_{50(I)}$(nM)	$IC_{50(Tac)}$(nM)	$IC_{50(I)}/IC_{50(Tac)}$	AChE
24	22.6	110	0.205	ee
25	83	278	0.299	m[f]
27	8	350	2.29 x 10^{-2}	hu
28	3.4	104	3.27 x 10^{-2}	ee
29	0.495	52	9.52 x 10^{-3}	ee
30	45	180	0.250	ee
31	5.5	350	1.57 x 10^{-2}	hu
33	4.4	45.1	9.76 x 10^{-2}	ee
34	5.6	45.1	0.124	ee
35	61	180	0.339	ee
36	2.65 x 10^{-3}	2.38 x 10^{-2}	0.111	-
37	8 x 10^{-3}	350	2.286 x 10^{-5}	h
38	200	170	1.18	b
39	6	223	2.69 x 10^{-2}	r
40	0.75	137.7	5.45 x 10^{-3}	hu
41	0.32	205	1.56 x 10^{-3}	hu
42	3.49	130	2.68 x 10^{-2}	b
43	38.5	130	0.296	b
44	120	350	0.343	ee

[a] Eletric eel, [b] Human, [c] Bovine, [d] Torpedo californica (Pacific electric ray), [e] Rat, [f] Mouse. The IC_{50} values are listed with the same number of decimals as presented in the given publication.

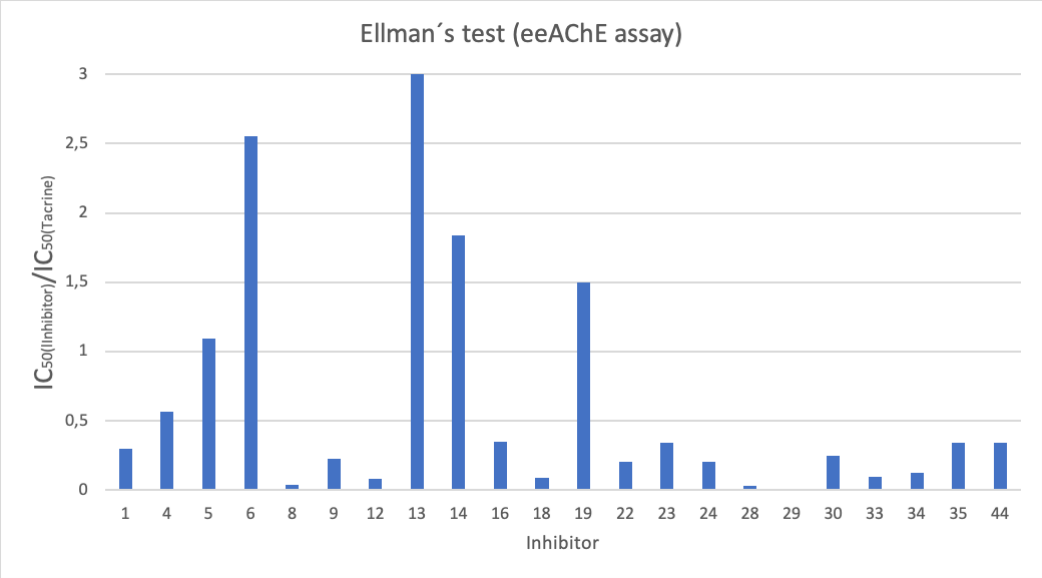

Figure 30. Graphic representation of $IC_{50(inhibitor)}/IC_{50(tacrine)}$ for the compounds tested on eeAChE.

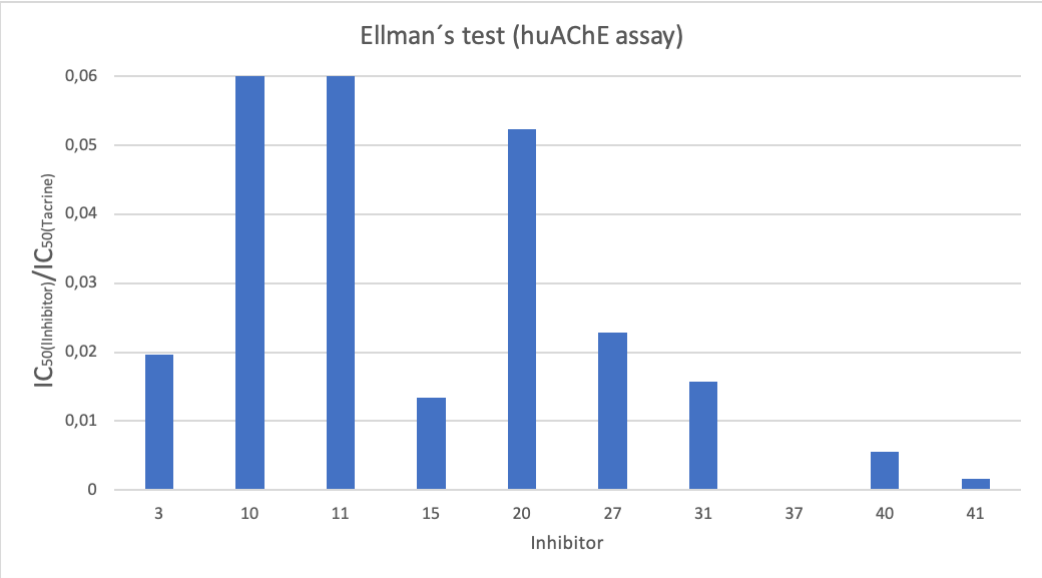

Figure 31. Graphic representation of $IC_{50(inhibitor)}/IC_{50(tacrine)}$ for the compounds tested on huAChE.

C.2 Affinity towards BChE

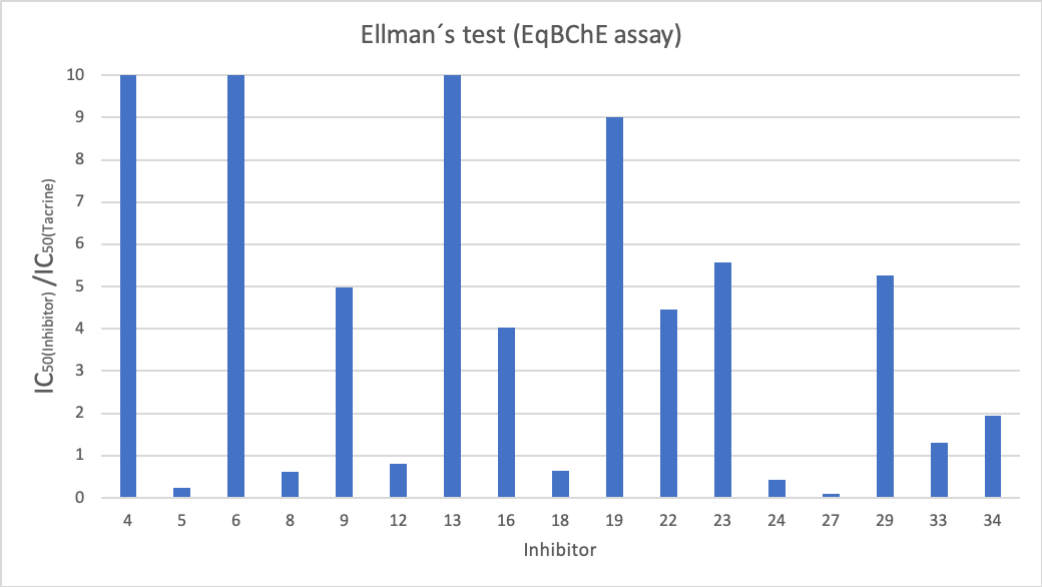

Figure 32. Graphic representation of $IC_{50(inhibitor)}/IC_{50(tacrine)}$ for the compounds tested on eqBChE.

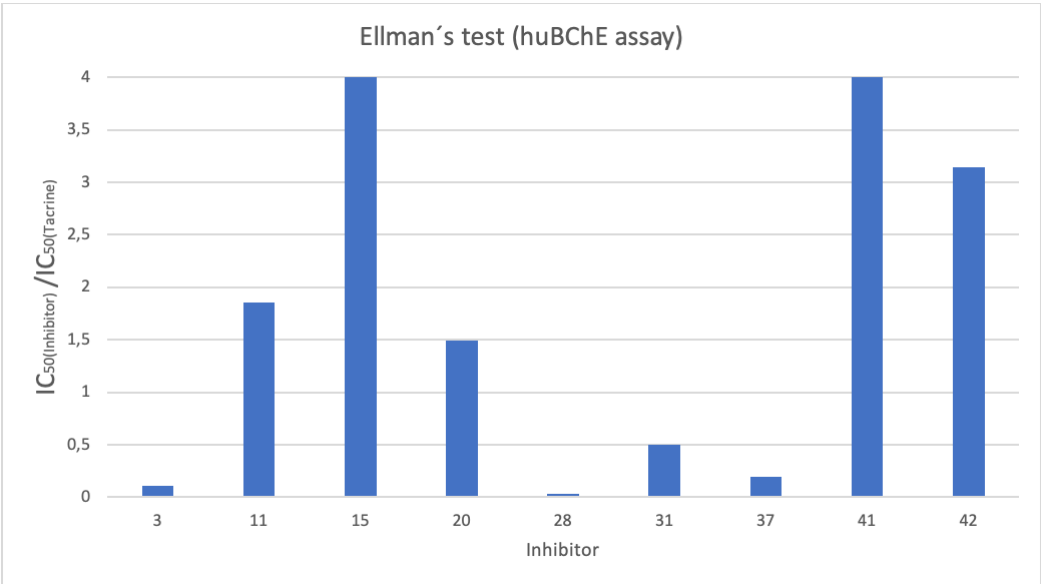

Figure 33. Graphic representation of $IC_{50(inhibitor)}/IC_{50(tacrine)}$ for the compounds tested on huBChE.

C.3 Selectivity towards AChE

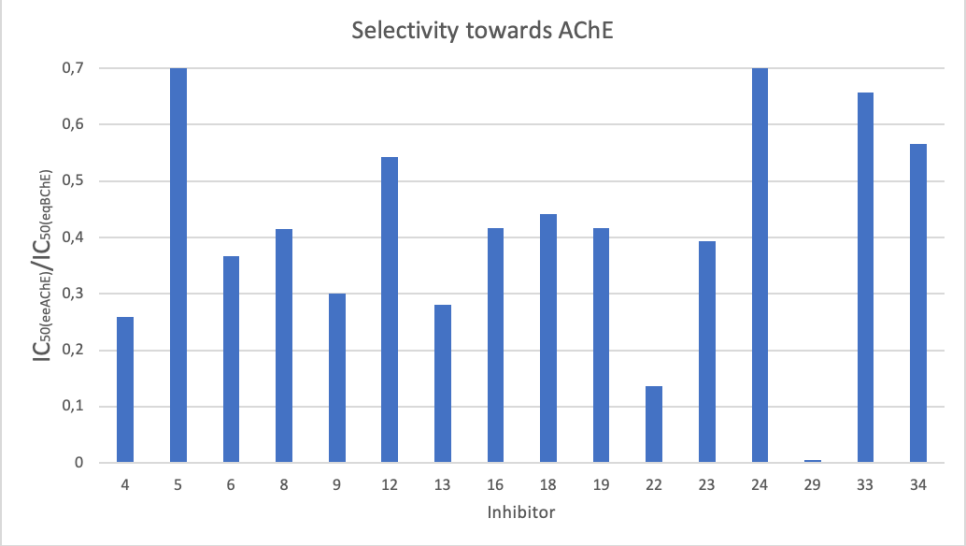

Figure 34. Majority of the inhibitors tested on eeAChE and eqBChE has between two and five times better inhibition towards eeAChE

C.4 $IC_{50(eeAChE)}$ vs $IC_{50(huAChE)}$

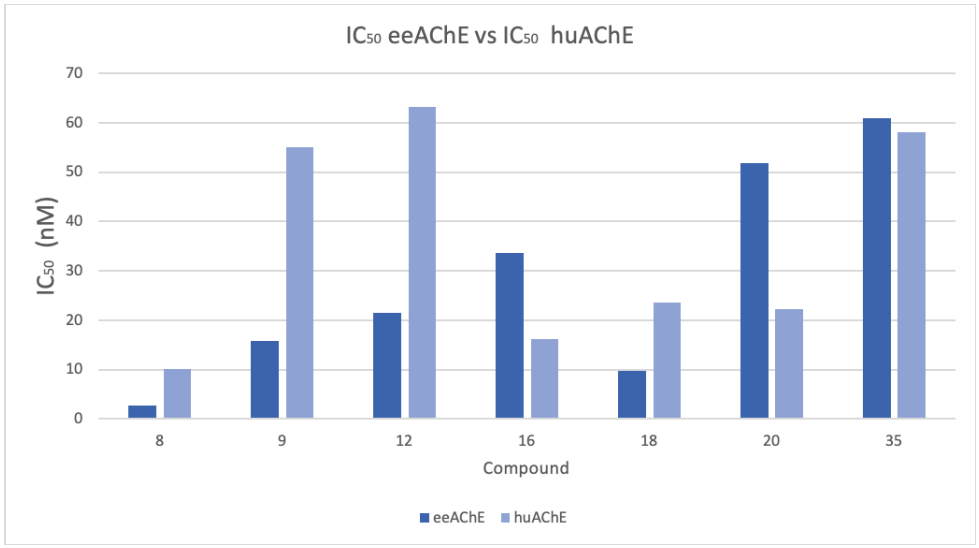

Figure 35. Correlation between $IC_{50(eeAChE)}$ and $IC_{50(huAChE)}$

C.5 Affinity of tacrine towards eeAChE vs. eqBChE

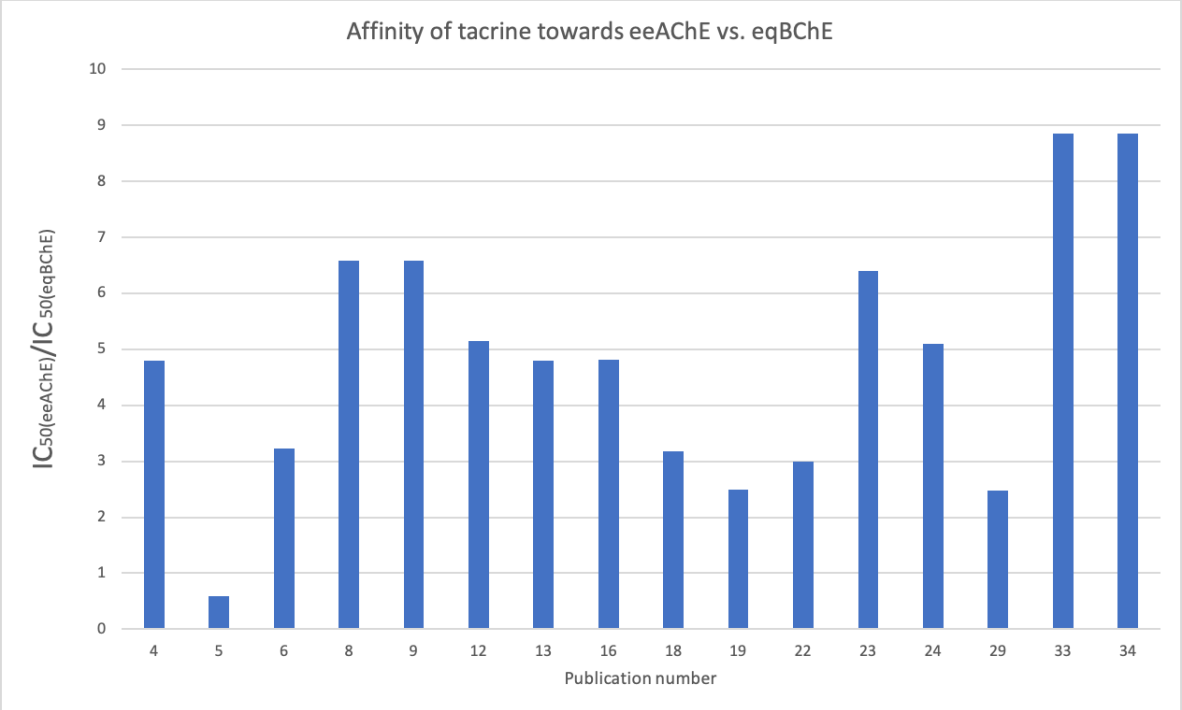

Figure 36. Correlation between $IC_{50(eeAChE)}$ and $IC_{50(eqBChE)}$ of tacrine

D Molecular modeling

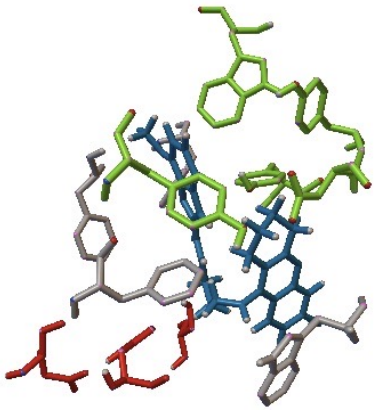

No. 1: -10.5

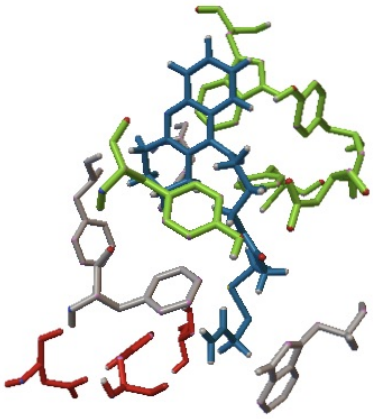

No. 2: -8.2

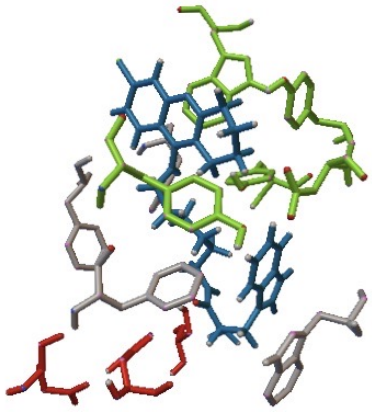

No. 3: -10.6

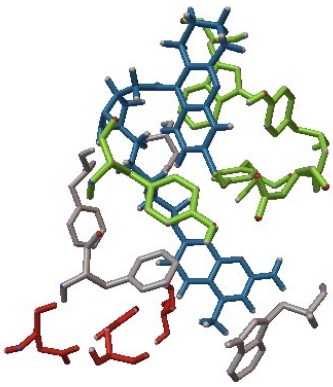

No. 4: -10.7

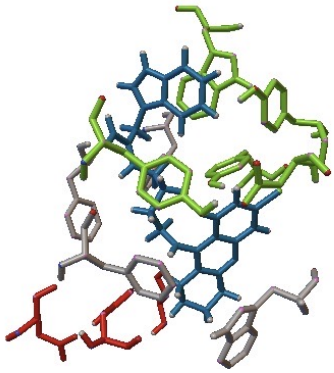

No. 5: -11.0

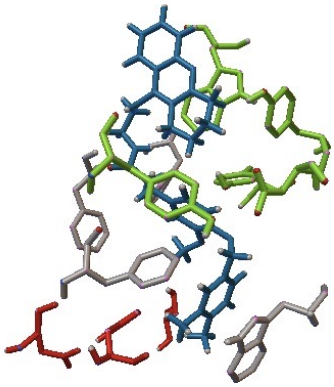

No. 6: -11.4

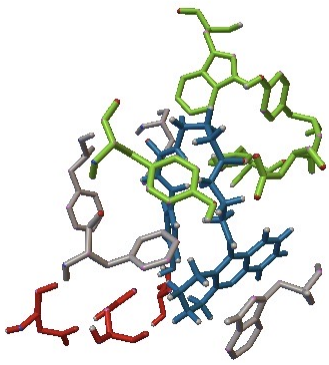

No. 7: -10.8

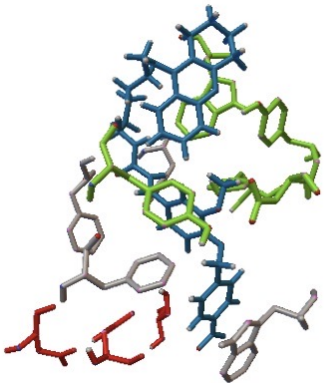

No. 8: -9.4

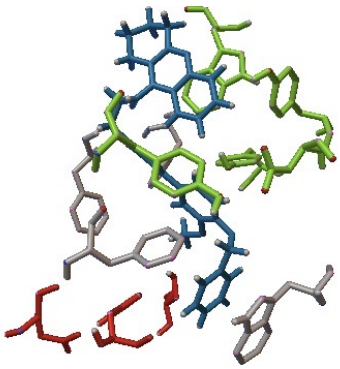

No. 9: -11.5

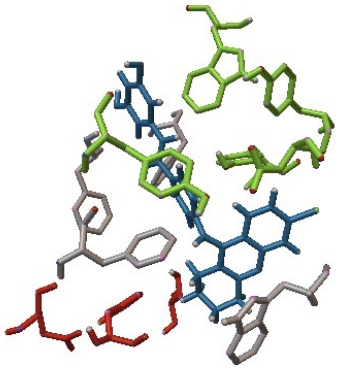

No. 10: -12.7

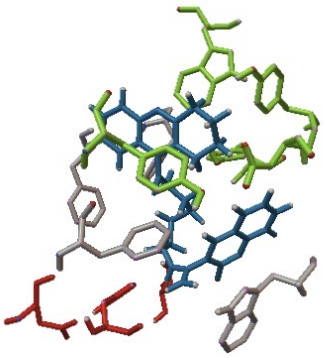

No. 11: -10.5

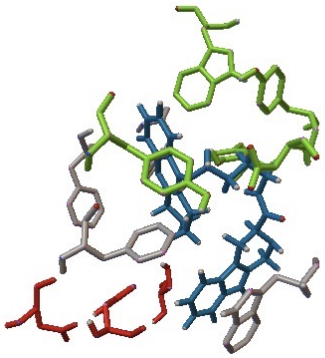

No. 12: -11.6

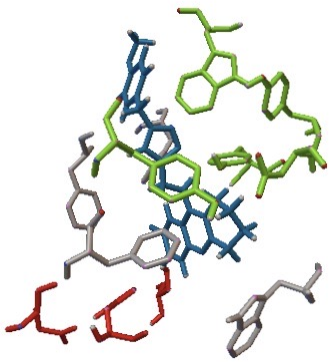

No. 13: -10.2

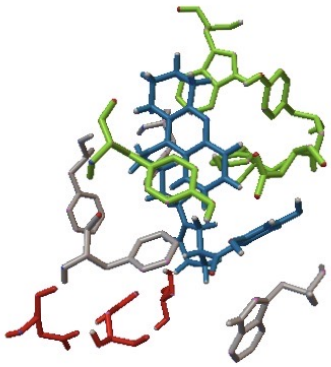

No. 14: -11.2

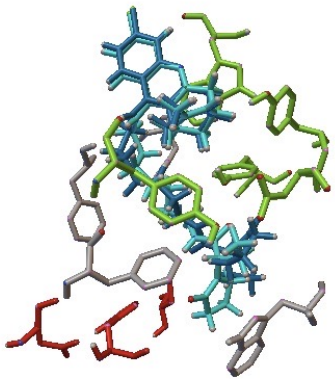

No. 15: -9.9

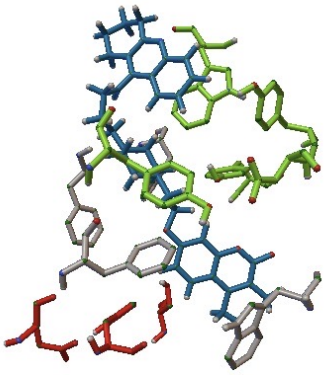

No. 16: -11.0

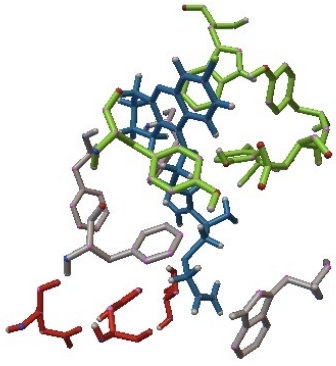

No. 17: -8.4

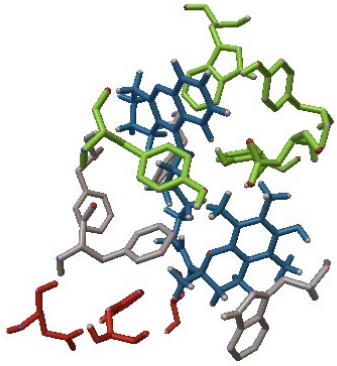

No. 18: -12.3

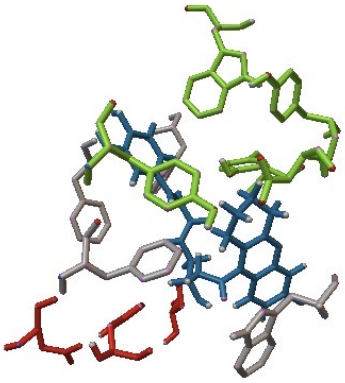

No. 19: -10.7

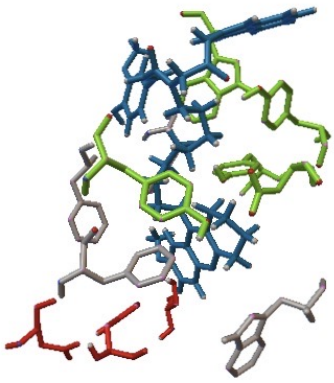

No. 20: -9.9

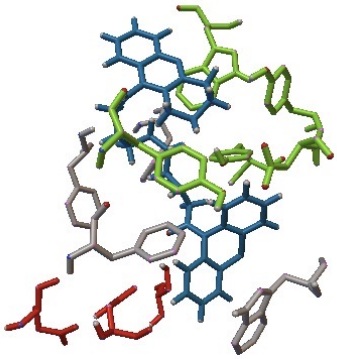

No. 21: -11.0

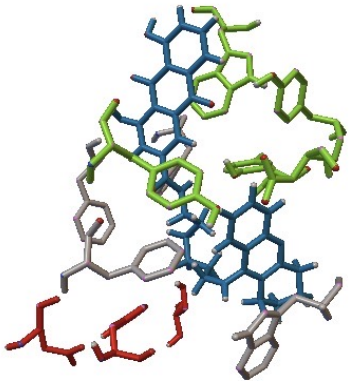

No. 22: -11.8

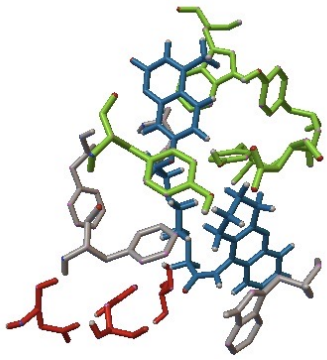

No. 23: -11.9

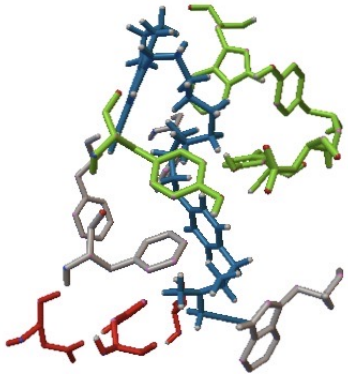

No. 24: -8.9

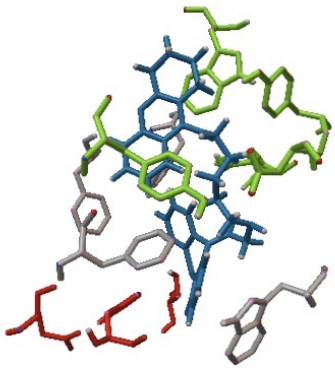

No. 25: -11.7

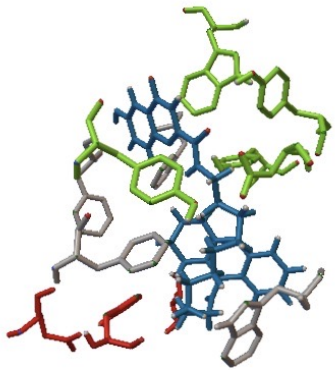

No. 27: -10.5

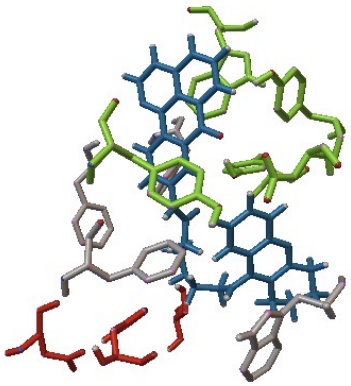

No. 28: -12.8

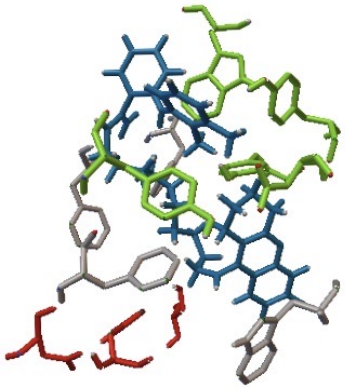

No. 29: -10.3

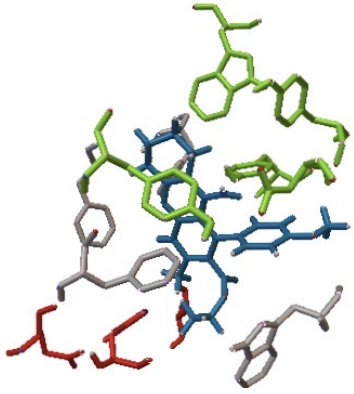

No. 30: -9.1

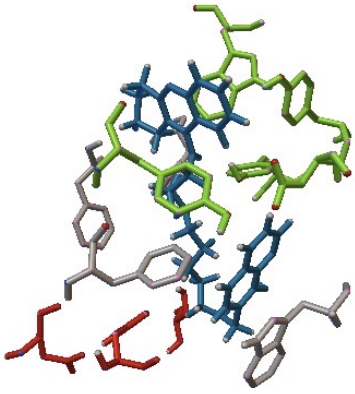

No. 31: -10.4

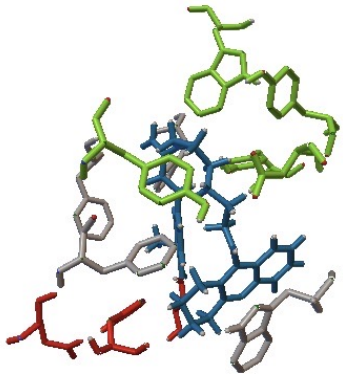

No. 33: -10.1

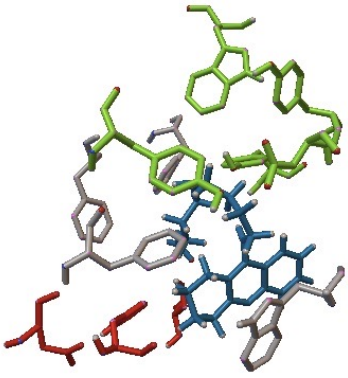

No. 34: -7.9

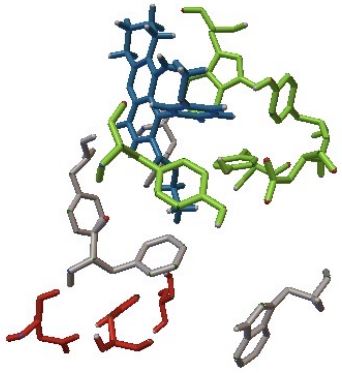

No. 35: -8.7

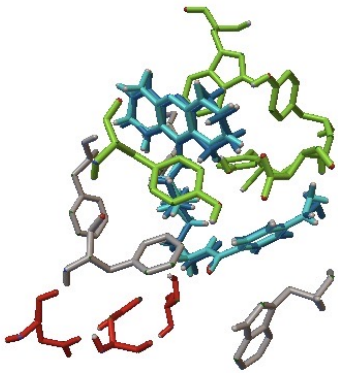

No. 36: -10.1

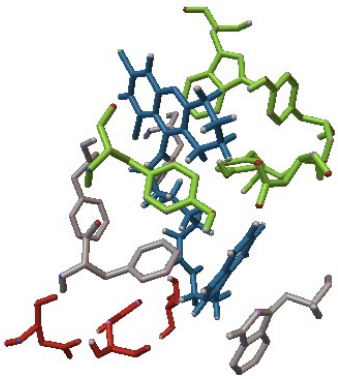

No. 37: -10.5

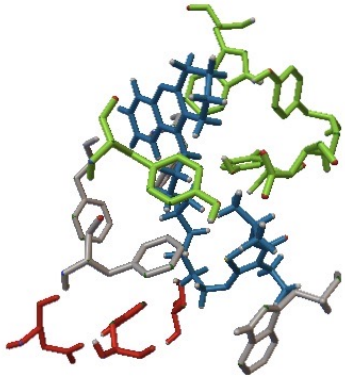

No. 38: -8.8

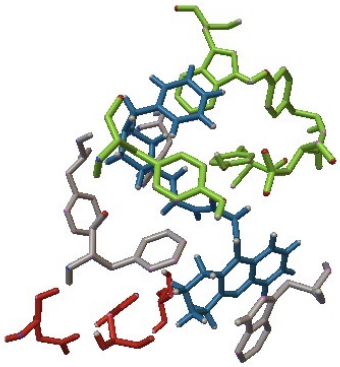

No. 39: -11.3

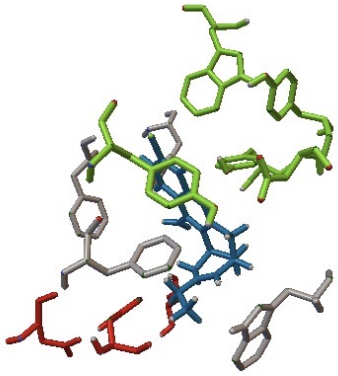

No. 40: -10.0

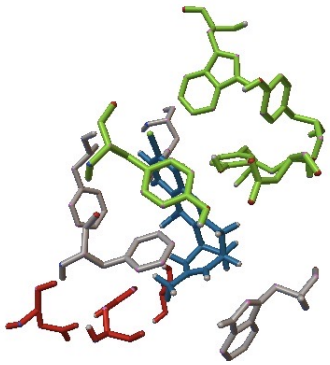

No. 41: -9.8

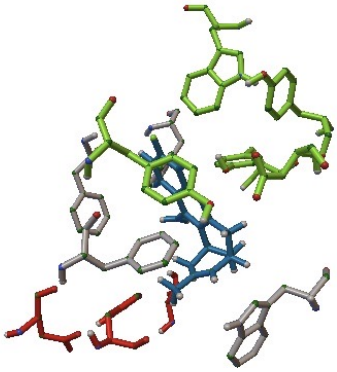

No. 42: -9.8

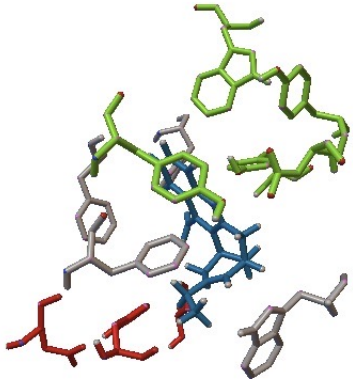

No. 43: -9.8

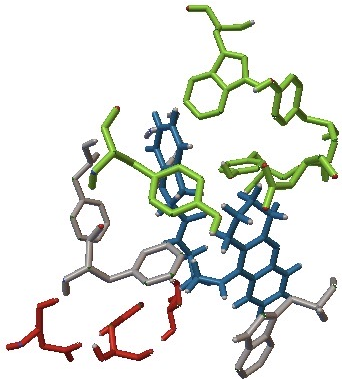

No. 44: -10.7

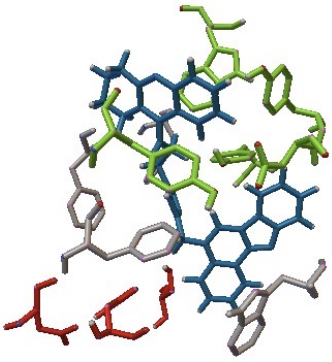

1a pose 1: -12.1

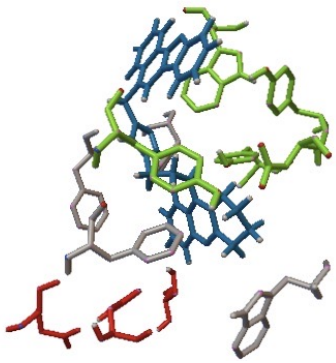

1a pose 2: -11.9

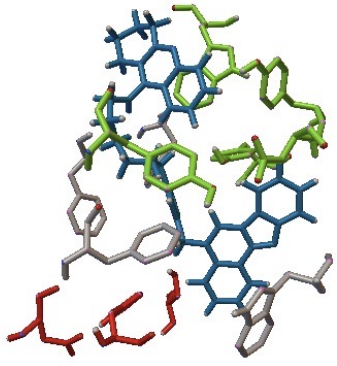

1b pose 1: -12.0

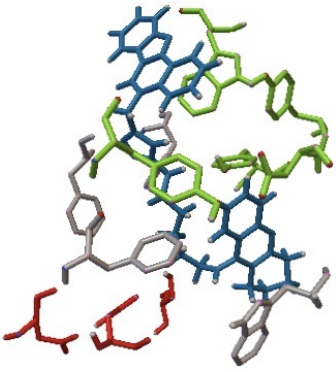

1b pose 2: -11.3

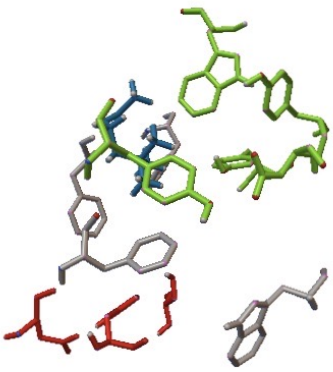

ACh pose 1: -4.3

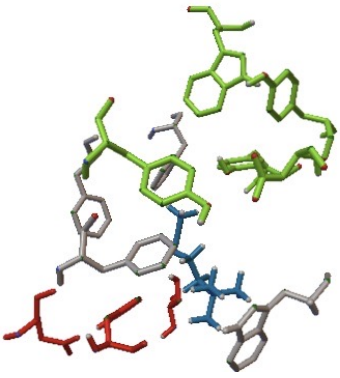

ACh pose 2 -4.3

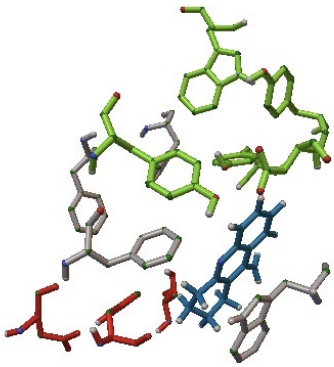

Tacrine: -8.1

Figure 37. Docking output, and their respective docking scores, of molecule 1-44, 1a, 1b, ACh and Tacrine. These are the poses assigned the highest score by 1-click-docking. The potential AD pharmasuticals and ACh are colored blue. The aminoacids at PAS and the catalytic triad are respectivly green and red.

Docking of molecule 15 and 36 gave two poses with identical docking scores. The two poses almost simultaneous and are depicted in different shades of blue.

E NMR spectra

E.1 Compound 10´

^{1}H-NMR (400 MHz, $CDCl_3$)

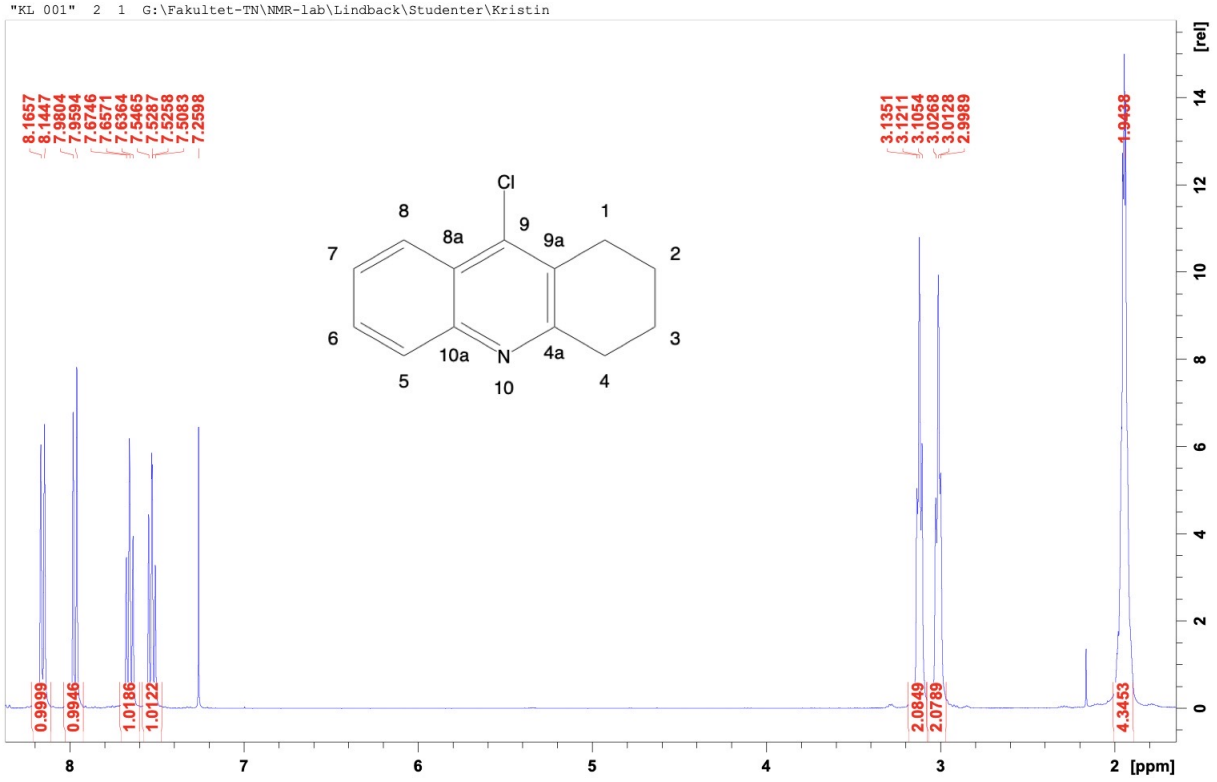

^{13}C-NMR (100 MHz, $CDCl_3$)

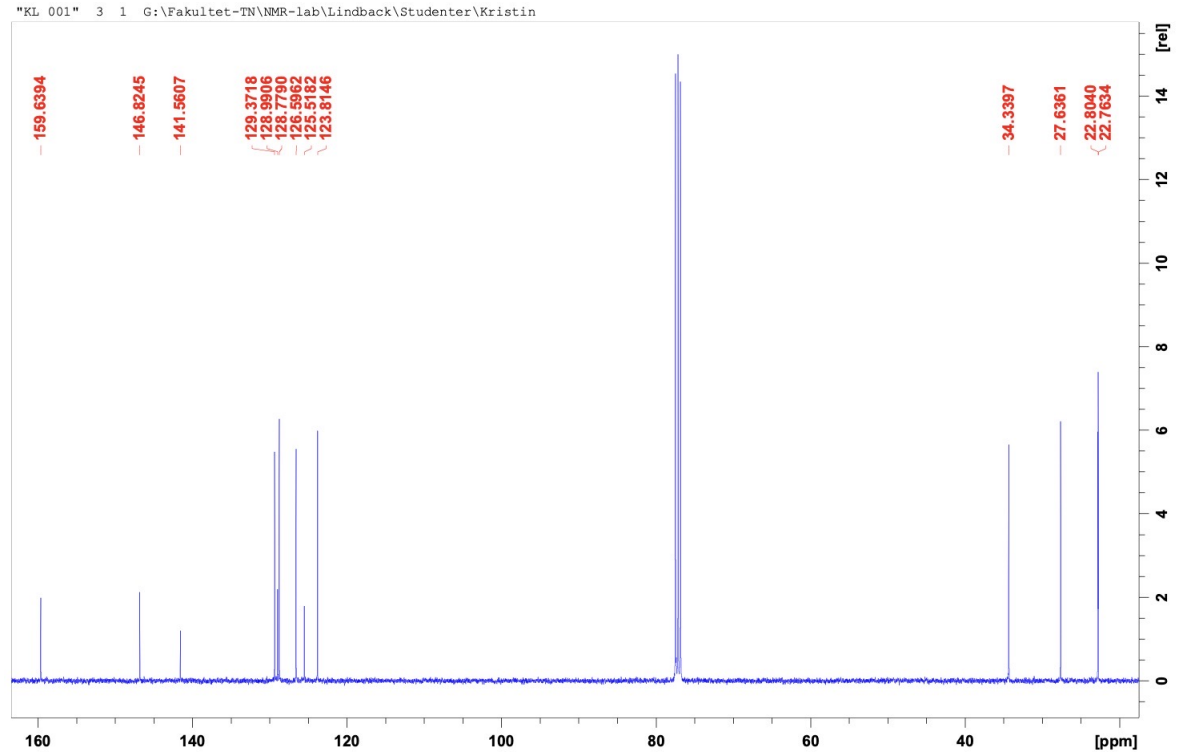

IR

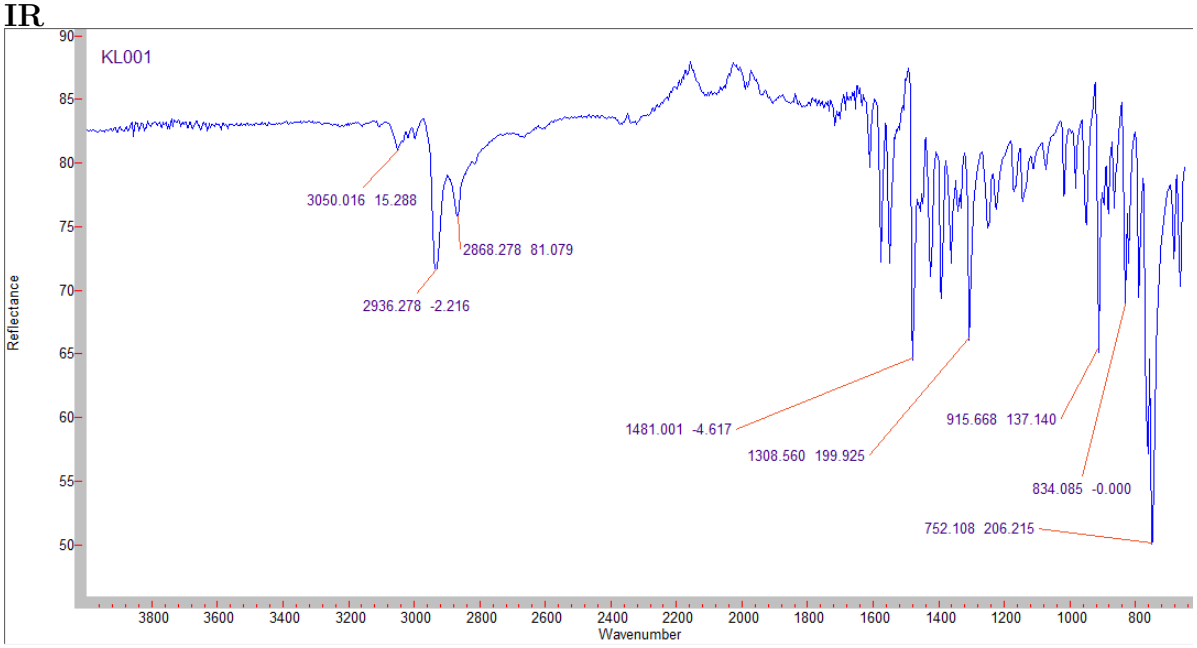

E.2 Compound 11´

^{1}H-NMR (400 MHz, $CDCl_3$)

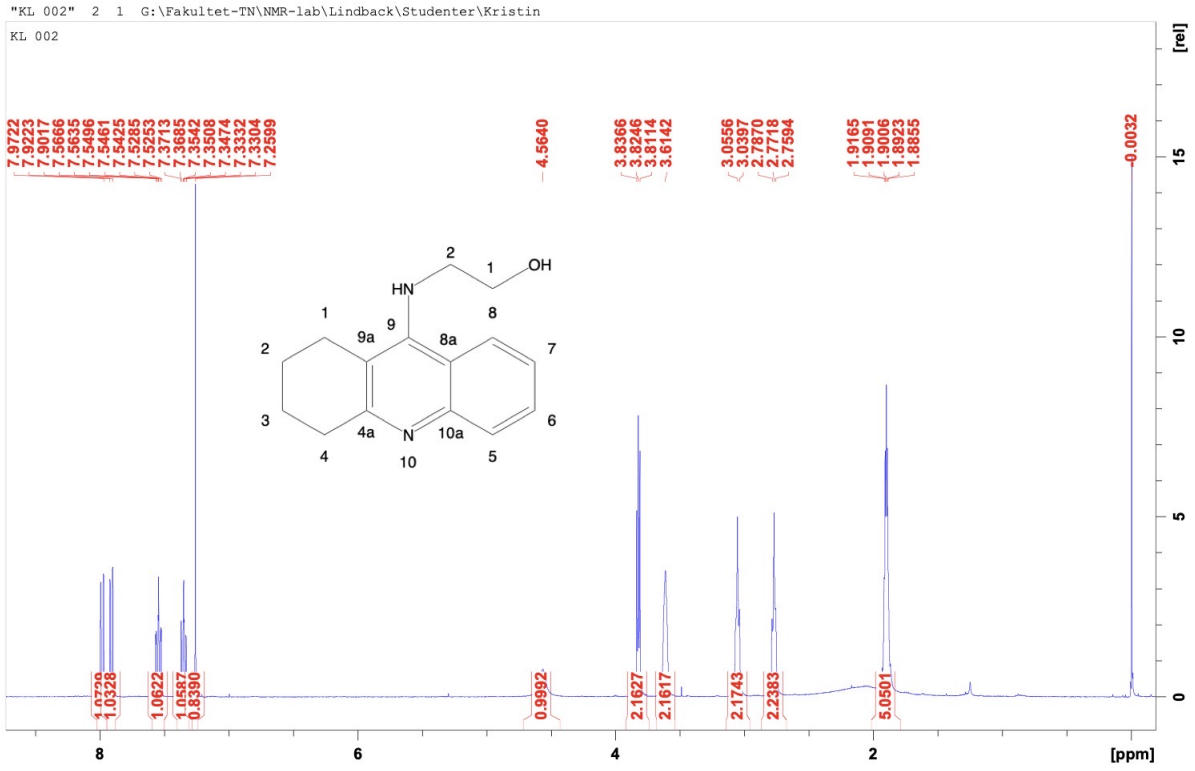

^{13}C-NMR (100 MHz, $CDCl_3$)

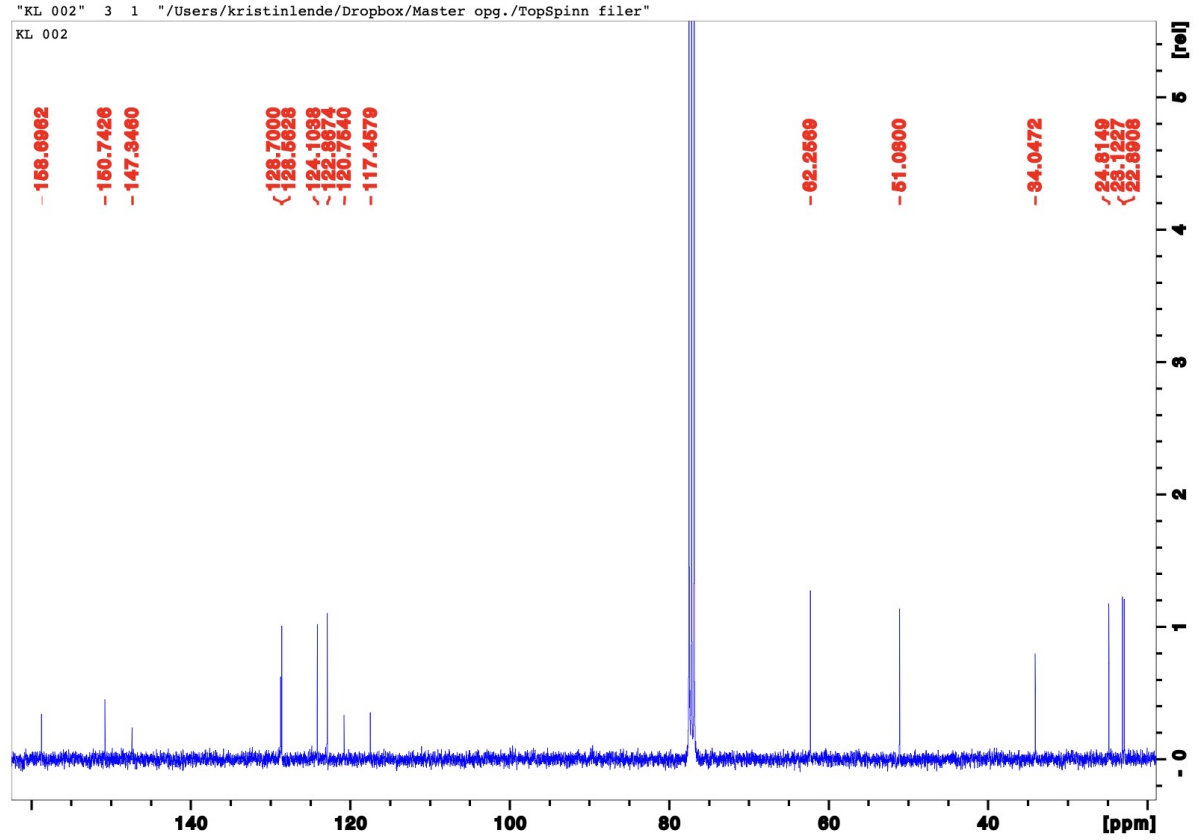

IR

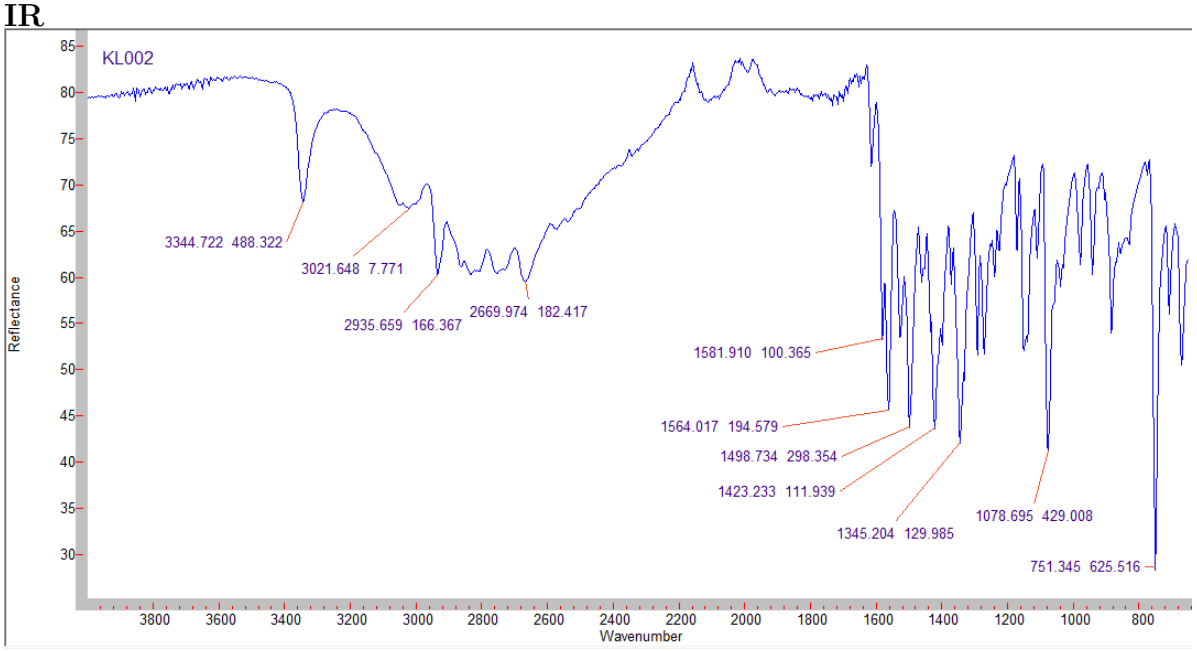

E.3 Compound 13´

^{1}H-NMR (400 MHz, $CDCl_3$)

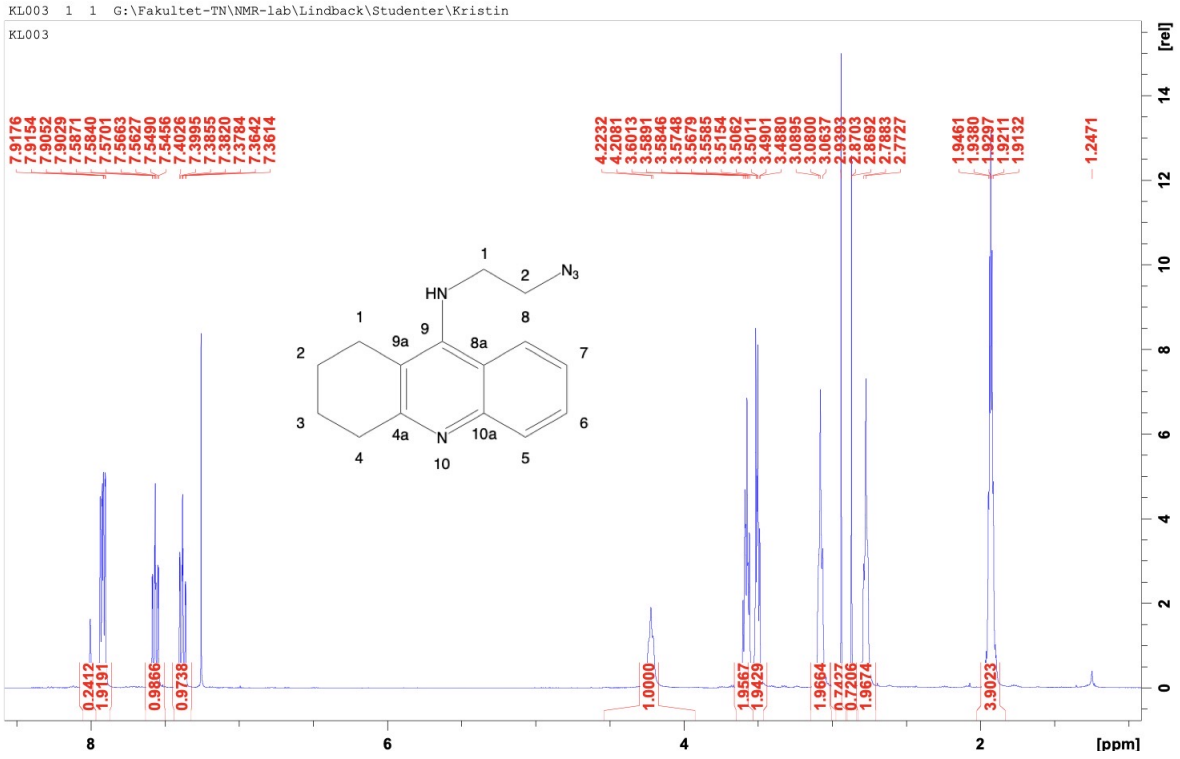

^{13}C-NMR (100 MHz, $CDCl_3$)

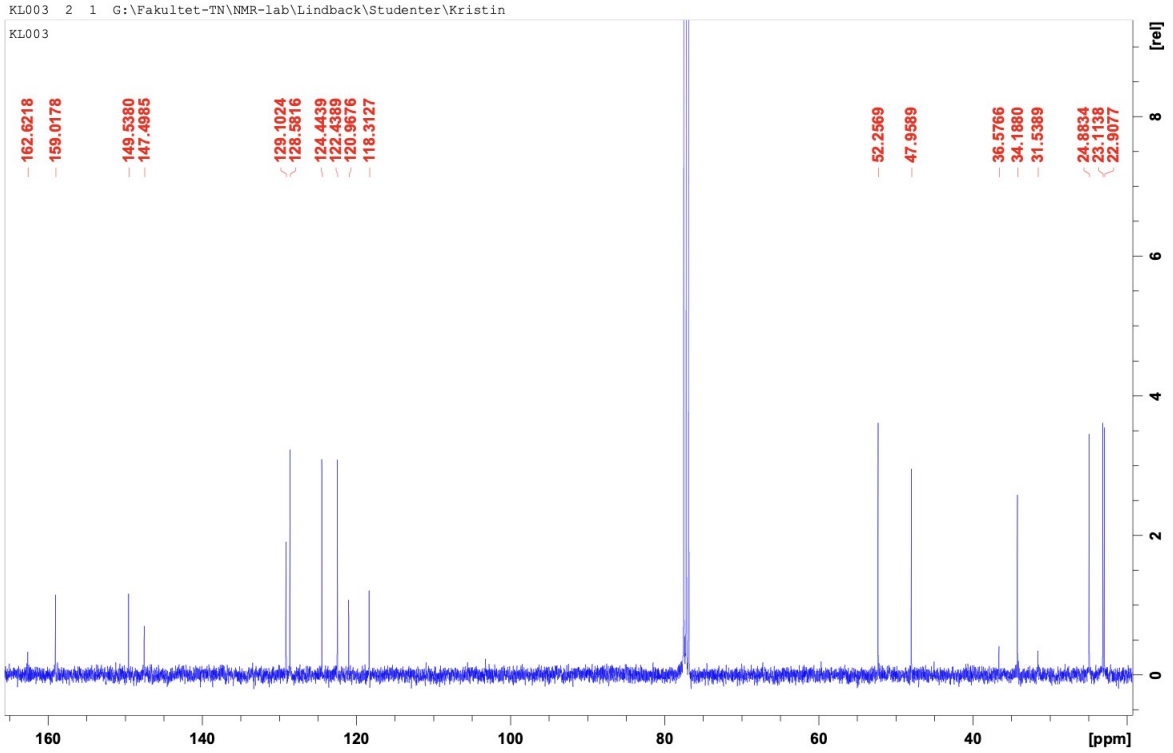

IR

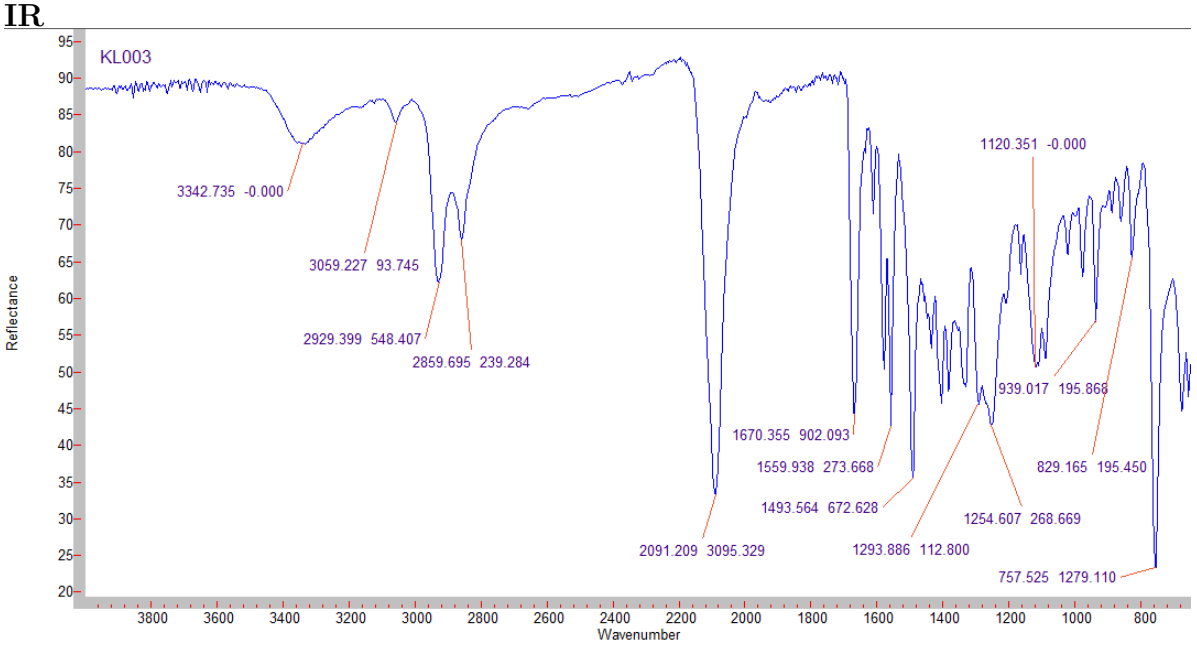

E.4 Compound 4´

^{1}H-NMR (400 MHz, $CDCl_3$)

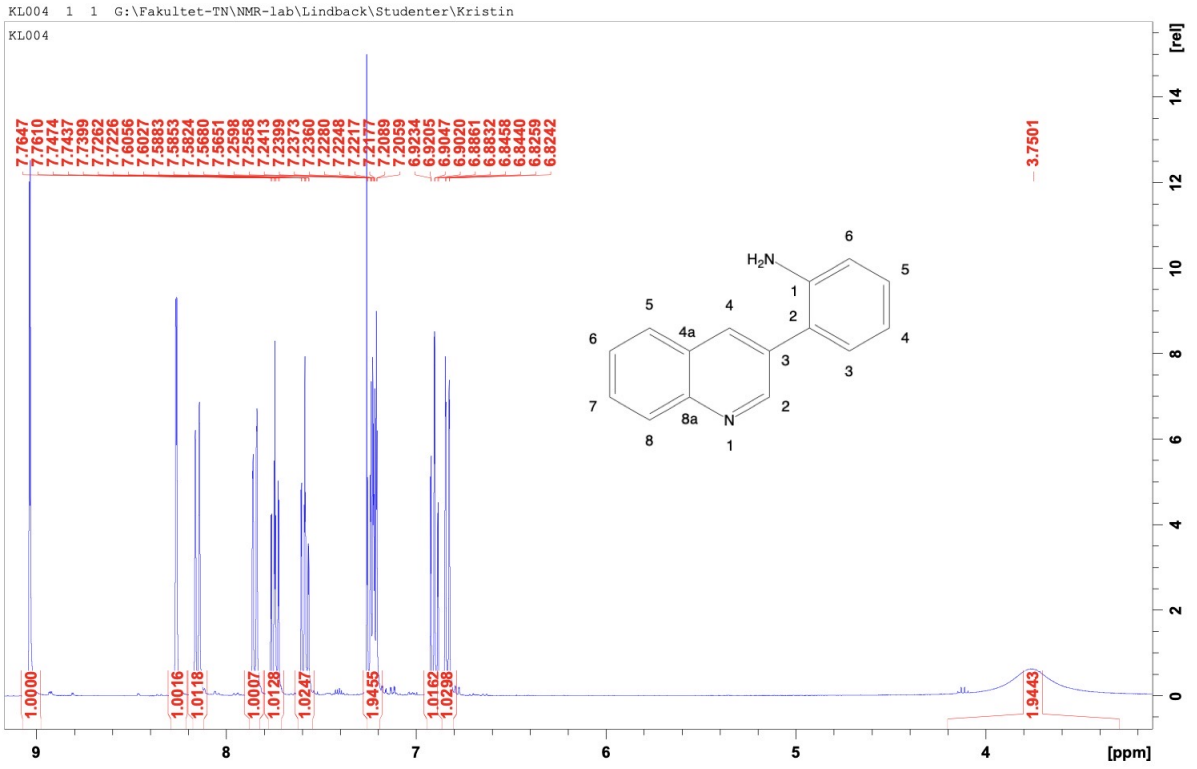

^{13}C-NMR (100 MHz, $CDCl_3$)

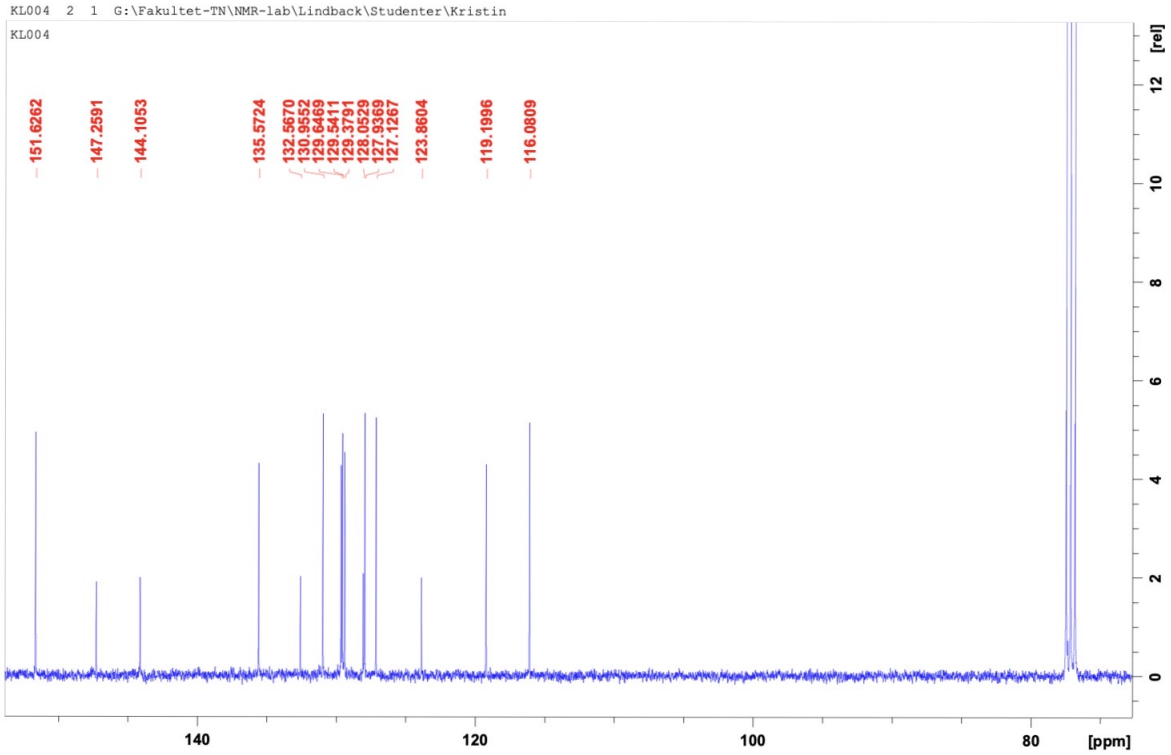

IR

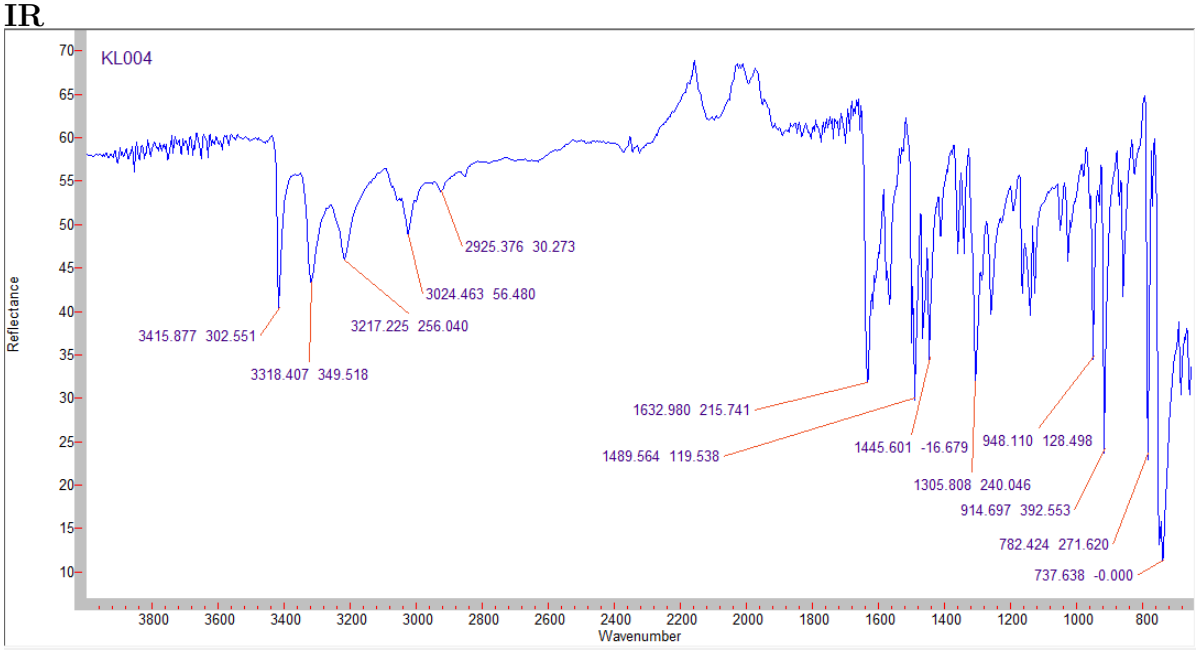

E.5 Compound 6´

^{1}H-NMR (400 MHz, $CDCl_3$)

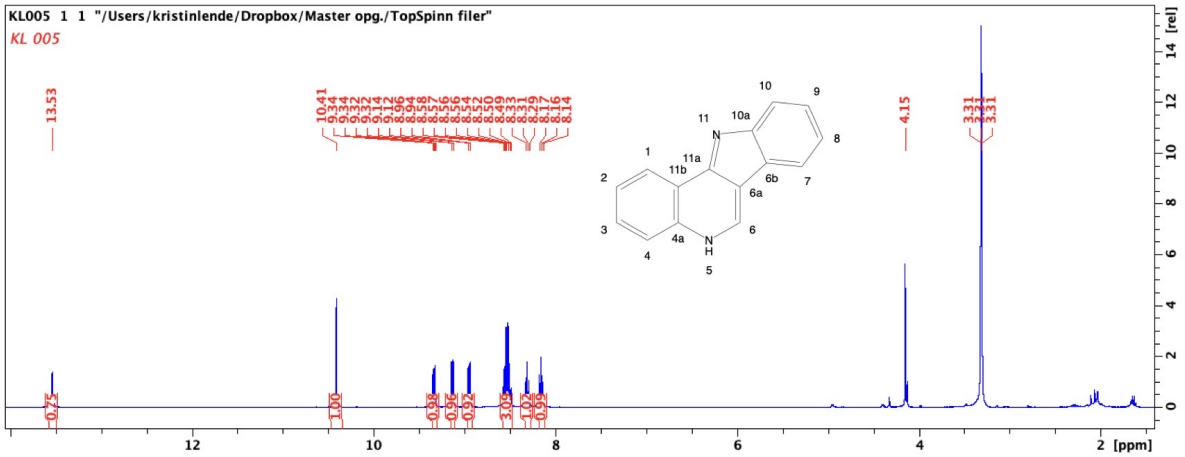

IR

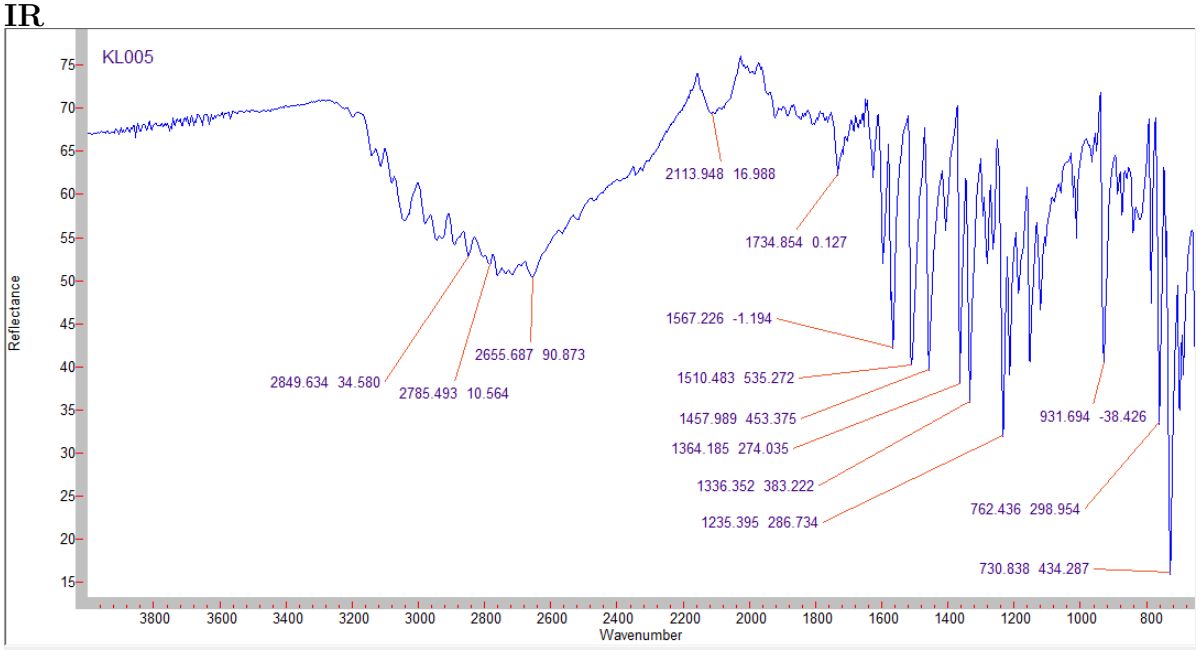

E.6 Compound 7´

Raw product ^{1}H-NMR (400 MHz, $CDCl_3$)

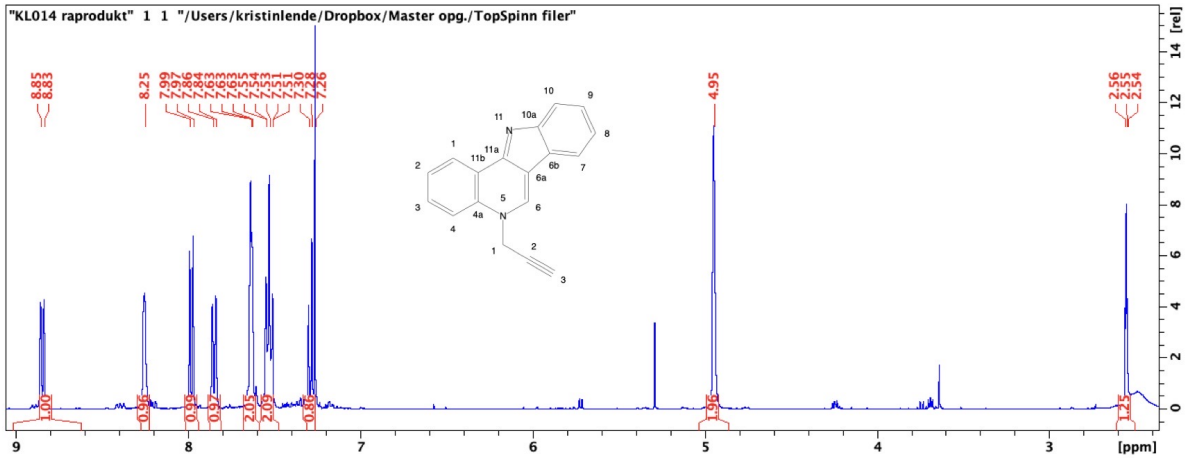

Raw product ^{13}C-NMR (100 MHz, $CDCl_3$)

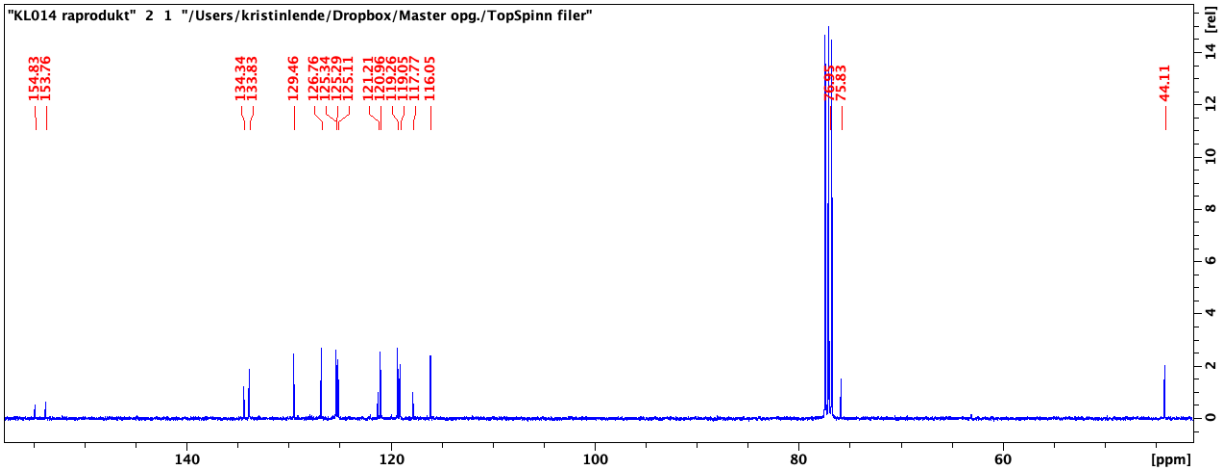

E.7 Compound 15´

^{1}H-NMR (400 MHz, $CDCl_3$)

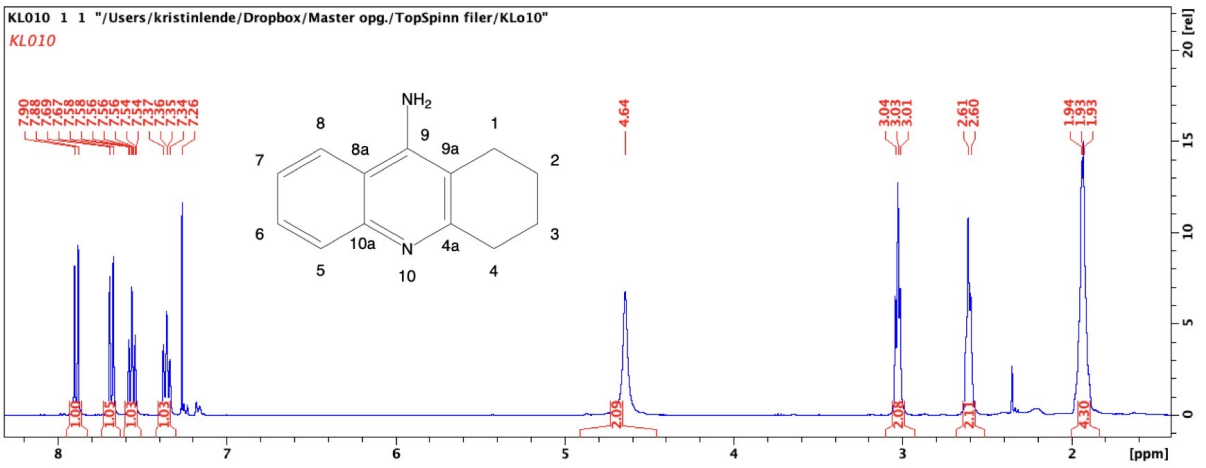

^{13}C-NMR (100 MHz, $CDCl_3$)

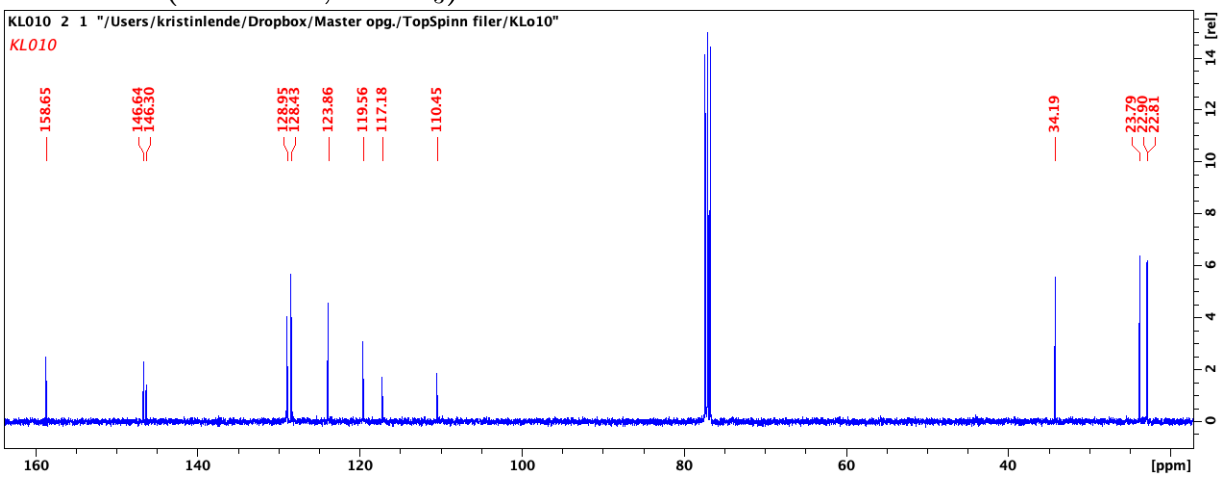

IR

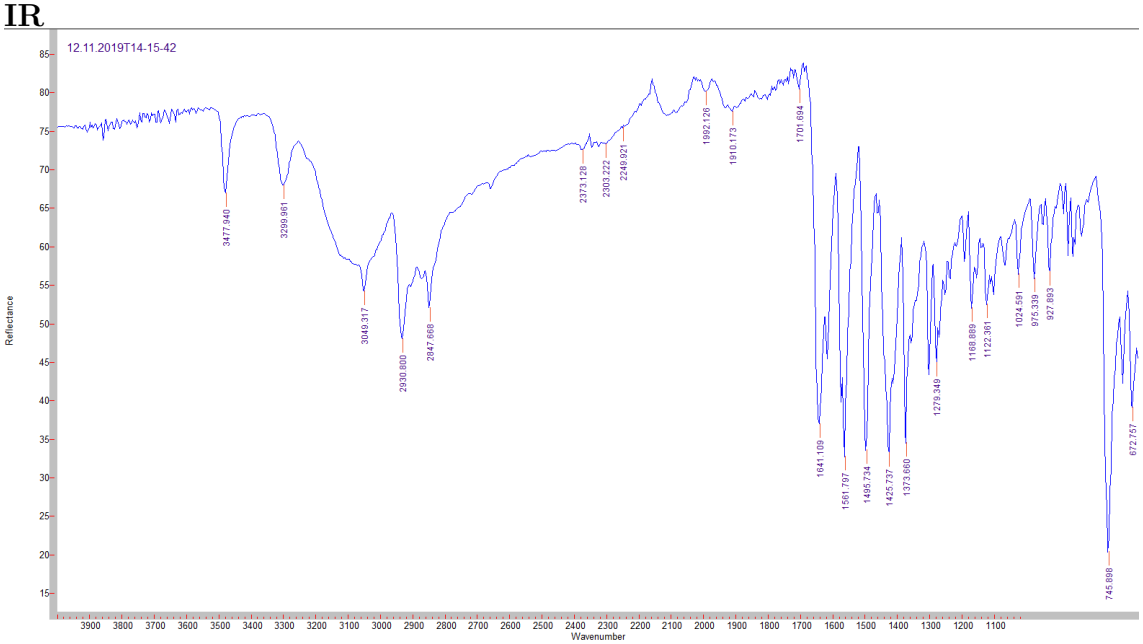
12.11.2019T14-15-42
Reflectance
Wavenumber
3477.940
3299.961
3049.317
2930.800
2847.668
2373.128
2303.222
2249.921
1992.126
1910.173
1701.694
1641.109
1561.797
1495.734
1425.737
1373.660
1279.349
1168.889
1122.361
1024.591
975.339
927.893
745.898
672.757

E.8 Compound 16´

^{1}H-NMR (400 MHz, $CDCl_3$)

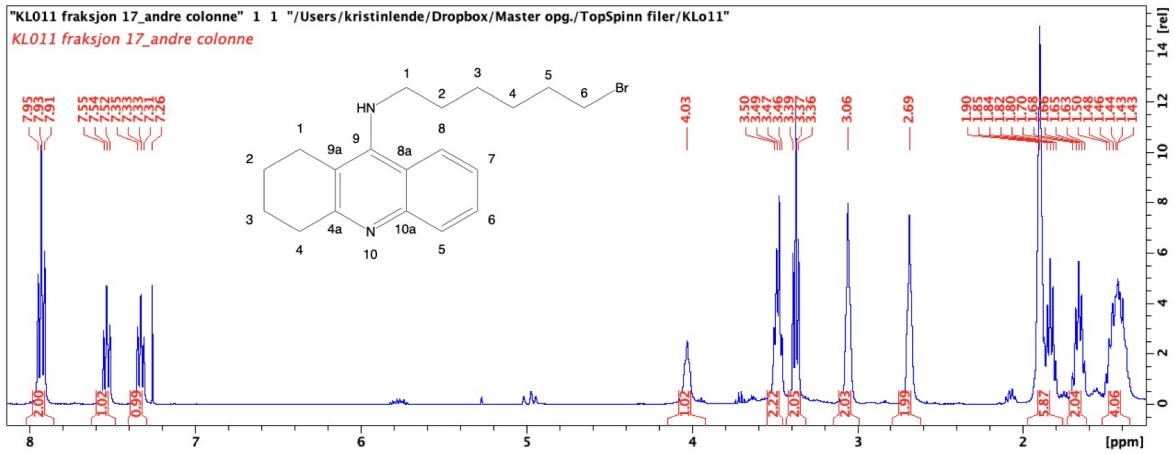

^{13}C-NMR (100 MHz, $CDCl_3$)

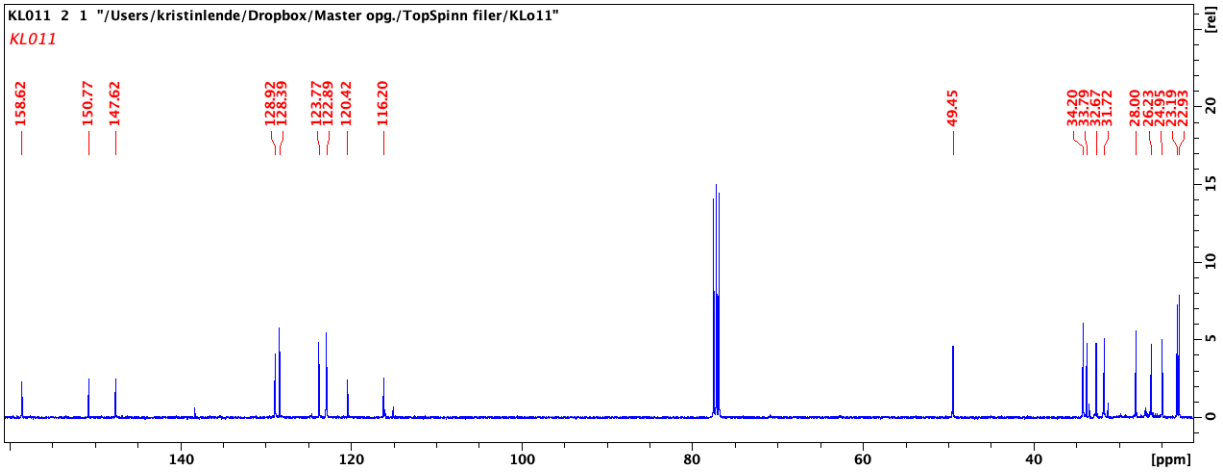

IR

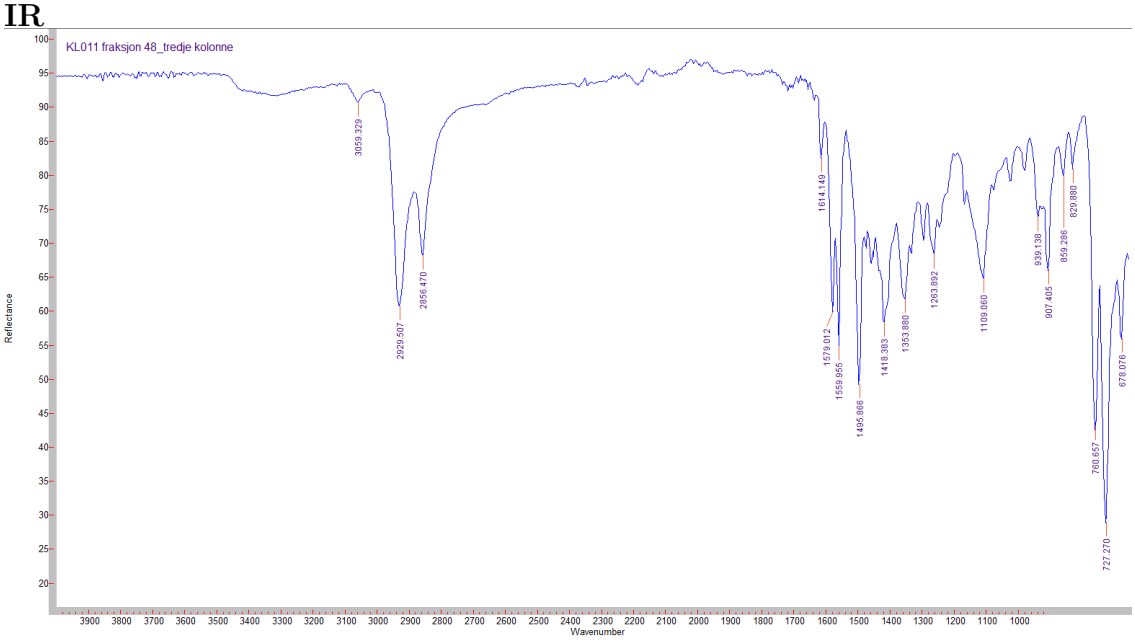
KL011 fraksjon 48_tredje kolonne
Reflectance
Wavenumber
3059.329
2929.507
2856.470
1614.149
1579.012
1559.955
1495.866
1418.383
1353.880
1263.992
1109.060
939.138
907.405
859.286
829.880
760.657
727.270
678.076

E.9 Compound 17´

^{1}H-NMR (400 MHz, $CDCl_3$)

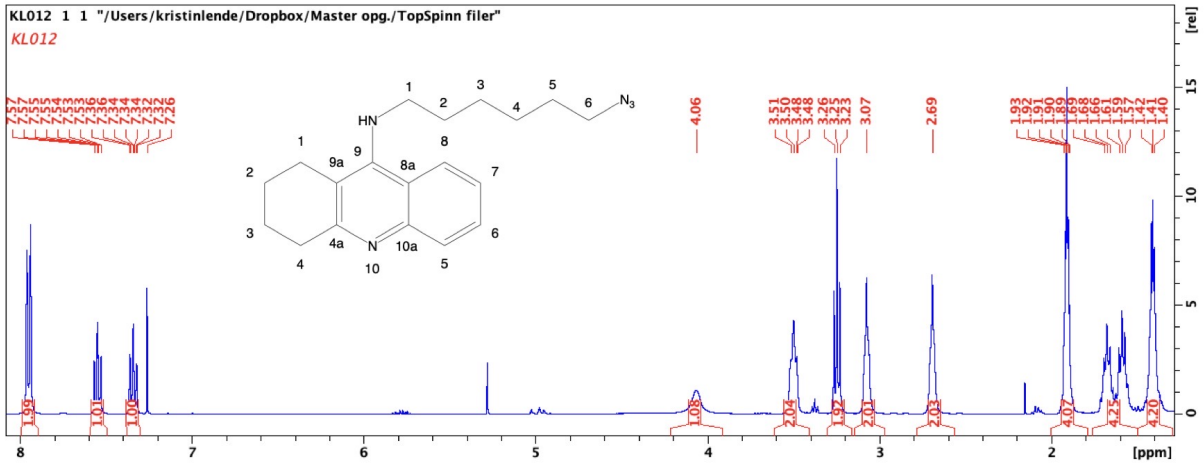

^{13}C-NMR (100 MHz, $CDCl_3$)

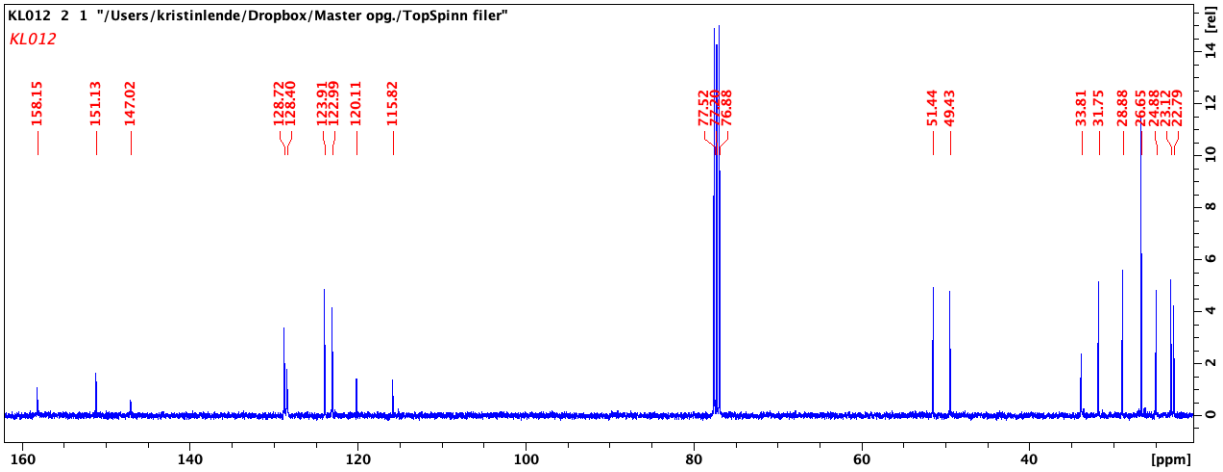

IR

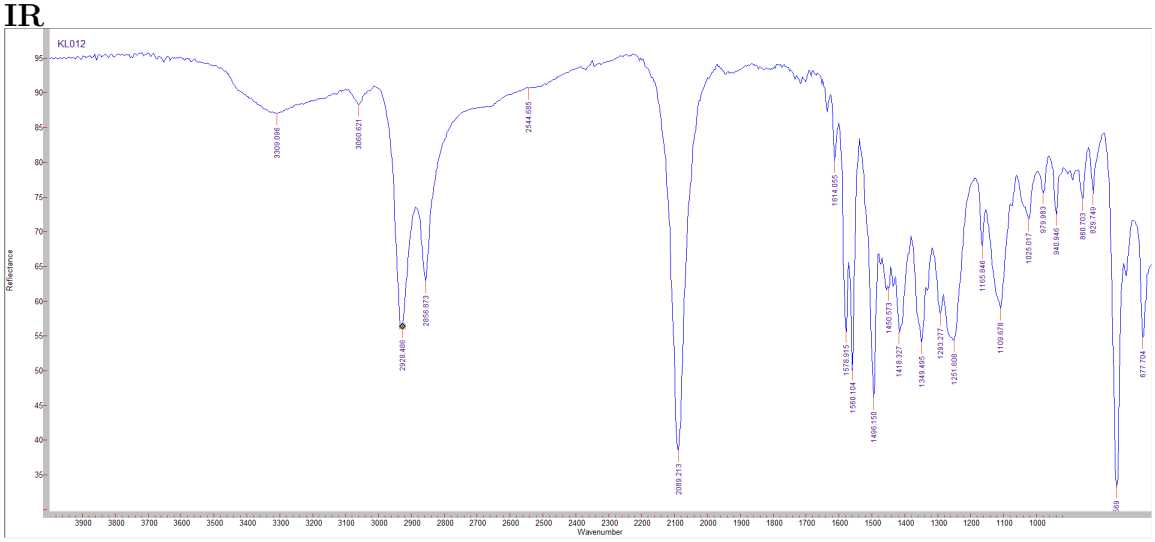
KL012
Reflectance
Wavenumber
3300.096
3060.621
2926.486
2859.873
2544.685
2089.213
1614.055
1578.915
1560.104
1496.150
1450.573
1418.327
1349.495
1293.277
1251.608
1165.846
1109.878
1026.017
979.983
940.946
860.703
828.749
677.704

E.10 Compound 1a´

^{1}H-NMR (400 MHz, $CDCl_3$)

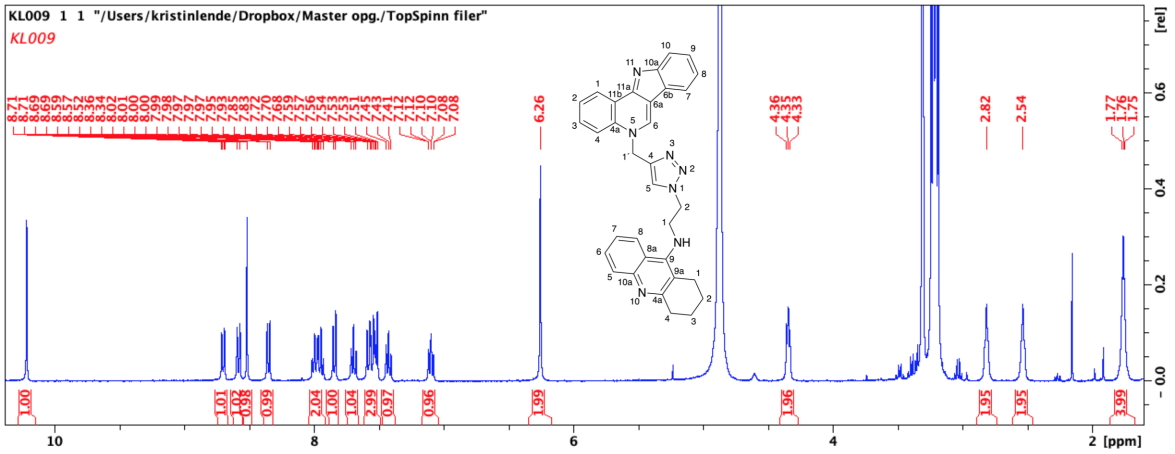

E.11 Compound 1b´

^{1}H-NMR (400 MHz, $CDCl_3$)

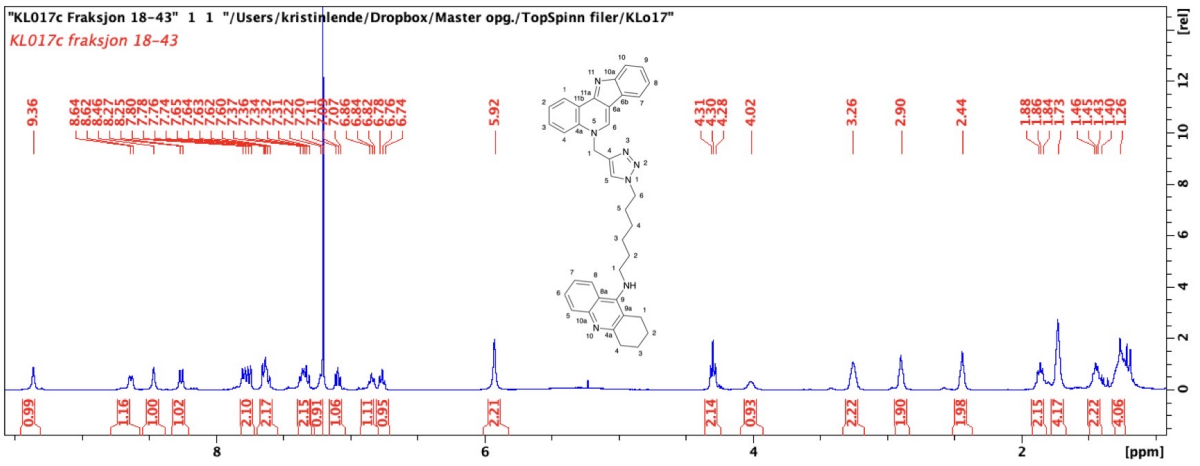

^{13}C-NMR (100 MHz, $CDCl_3$)

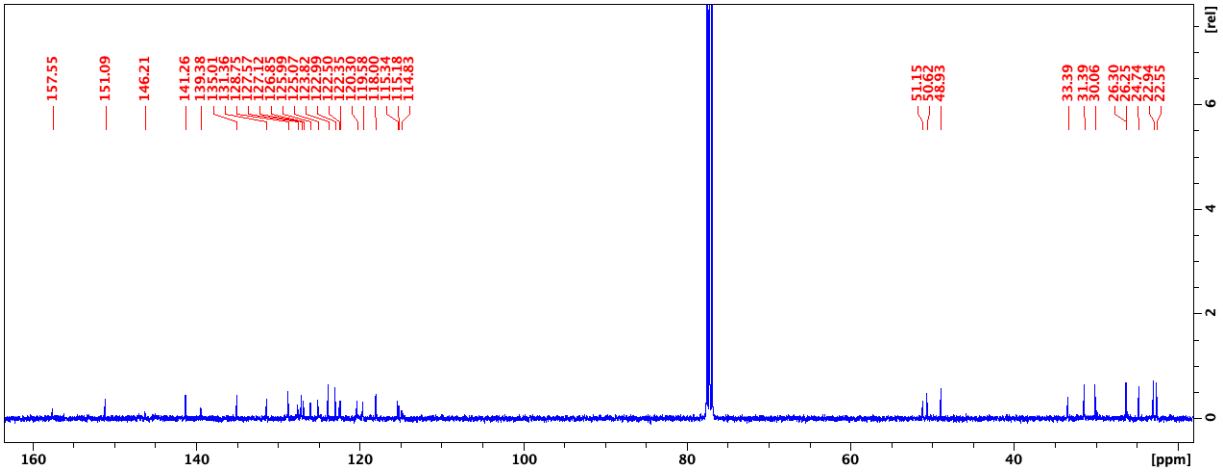

F Blast

The Amino acid sequence from human acetylcholinesterase, with GI number: 545225, was retrieved from the protein databank at **www.ncbi.nlm.nih.gov**. A search for matches among proteins of Torpedo Californica gave 57-59% similarity with acetylcholinesterase from Torpedo californica (figure 38).

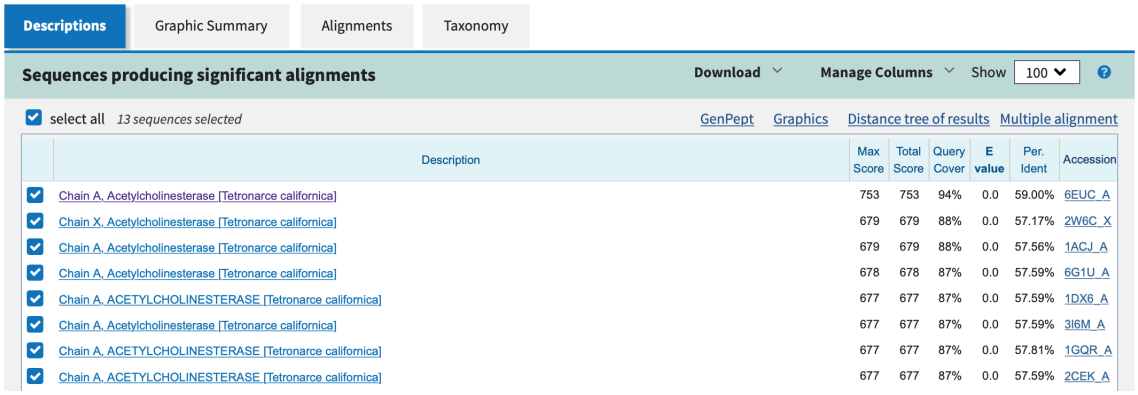

Figure 38. Output of search for similarities between hAChE and tcAChE.

Figure 39 displays the alignment of the amino acid sequence of given hAChE with the best matching tcAChE in the database of ncbi.

Chain A, Acetylcholinesterase [Tetronarce californica]

Sequence ID: 6EUC_A **Length:** 572 **Number of Matches:** 1

Range 1: 1 to 572 GenPept Graphics ▼ Next Match ▲ Previous Match

Score	Expect	Method	Identities	Positives	Gaps
753 bits(1943)	0.0	Compositional matrix adjust.	341/578(59%)	442/578(76%)	6/578(1%)

```
Query  37   AELLVTVRGGRLRGIRLKTPGGPVSAFLGIPFAEPPMGPRRFLPPEPKQPWSGVVDATTF  96
            +ELLV  + G++ G R+      +SAFLGIPFAEPP+G  RF  PEPK+PWSGV +A+T+
Sbjct  1    SELLVNTKSGKVMGTRVPVLSSHISAFLGIPFAEPPVGNMRFRRPEPKKPWSGVWNASTY  60

Query  97   QSVCYQYVDTLYPGFEGTEMWNPNRELSEDCLYLNVWTPYPRPTSPTPVLVWIYGGGFYS  156
             + C QYVD  +PGF G+EMWNPNRE+SEDCLYLN+W P PRP S T V+VWIYGGGFYS
Sbjct  61   PNNCQQYVDEQFPGFSGSEMWNPNREMSEDCLYLNIWVPSPRPKSTT-VMVWIYGGGFYS  119

Query  157  GASSLDVYDGRFLVQAERTVLVSMNYRVGAFGFLALPGSREAPGNVGLLDQRLALQWVQE  216
            G+S+LDVY+G++L   E  VLVS++YRVGAFGFLAL GS+EAPGNVGLLDQR+ALQWV +
Sbjct  120  GSSTLDVYNGKYLAYTEEVVLVSLSYRVGAFGFLALHGSQEAPGNVGLLDQRMALQWVHD  179

Query  217  NVAAFGGDPTSVTLFGESAGAASVGMHLLSPPSRGLFHRAVLQSGAPNGPWATVGMGEAR  276
            N+  FGGDP +VT+FGESAG ASVGMH+LSP SR LF RA+LQSG+PN PWA+V + E R
Sbjct  180  NIQFFGGDPKTVTIFGESAGGASVGMHILSPGSRDLFRRAILQSGSPNCPWASVSVAEGR  239

Query  277  RRATQLAHLVGCPPGGTGGNDTELVACLRTRPAQVLVNHEWHVLPQESVFRFSFVPVVDG  336
            RRA +L   + C       +D EL+ CLR +  Q L++ EW+VLP +S+FRFSFVPV+DG
Sbjct  240  RRAVELGRNLNC----NLNSDEELIHCLREKKPQELIDVEWNVLPFDSIFRFSFVPVIDG  295

Query  337  DFLSDTPEALINAGDFHGLQVLVGVVKDEGSYFLVYGAPGFSKDNESLISRAEFLAGVRV  396
            +F   + E+++N+G+F   Q+L+GV KDEGS+FL+YGAPGFSKD+ES ISR +F++GV++
Sbjct  296  EFFPTSLESMLNSGNFKKTQILLGVNKDEGSFFLLYGAPGFSKDSESKISREDFMSGVKL  355

Query  397  GVPQVSDLAAEAVVLHYTDWLHPEDPARLREALSDVVGDHNVVCPVAQLAGRLAAQGARV  456
             VP  +DL  +AV L YTDW+   +  + R+ L D+VGDHNV+CP+    G
Sbjct  356  SVPHANDLGLDAVTLQYTDWMDDNNGIKNRDGLDDIVGDHNVICPLMHFVNKYTKFGNGT  415

Query  457  YAYVFEHRASTLSWPLWMGVPHGYEIEFIFGIPLDPSRNYTAEEKIFAQRLMRYWANFAR  516
            Y Y F HRAS L WP WMGV HGYEIEF+FG+PL    NYTAEE+  ++R+M YWA FA+
Sbjct  416  YLYFFNHRASNLVWPEWMGVIHGYEIEFVFGLPLVKELNYTAEEEALSRRIMHYWATFAK  475

Query  517  TGDPNEPRDPKAPQWPPYTAGAQQYVSLDLRPLEVRRGLRAQACAFWNRFLPKLLSATDT  576
            TG+PNEP   ++ +WP +T   Q+++ L+  P++V + LR Q C FWN+FLPKLL+AT+T
Sbjct  476  TGNPNEPHSQES-KWPLFTTKEQKFIDLNTEPMKVHQRLRVQMCVFWNQFLPKLLNATET  534

Query  577  LDEAERQWKAEFHRWSSYMVHWKNQFDHYSKQDRCSDL  614
            +DEAERQWK EFHRWSSYM+HWKNQFDHYS+ + C++L
Sbjct  535  IDEAERQWKTEFHRWSSYMMHWKNQFDHYSRHESCAEL  572
```

Figure 39. Alignment of the amino acid sequence of given hAChE with the best matching tcAChE.

G Nitrous acid protonation

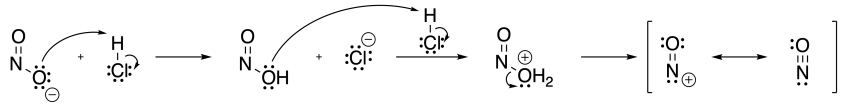

Figure 40. Nitrus acid may protonate and form nitrosonium ion through the mechanism illustrated.[53]